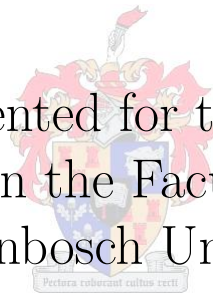


Oriented 123-TQFTs via String-Nets and State-Sums

Gerrit Goosen

Dissertation presented for the degree of Doctor
of Philosophy in the Faculty of Science at
Stellenbosch University



Supervised by Dr Bruce Bartlett
March 2018

Declaration

By submitting this thesis electronically, I declare that the entirety of the work contained therein is my own, original work, that I am the sole author thereof (save to the extent otherwise stated), that reproduction and publication thereof by Stellenbosch University will not infringe any third party rights and that I have not previously in its entirety or in part submitted it for obtaining any qualification.

Abstract

In a series of papers Bartlett, Douglas, Schommer-Pries, and Vicary discovered a finite generators-and-relations presentation of the oriented bordism bicategory. This simplifies the task of finding oriented once-extended topological quantum field theories (123-TQFTs). We combine this result with the theory of string-nets, specifically Kirillov's generalization of the theory to surfaces with boundary, and construct an oriented 123-TQFT based on string-nets. Previously, string-nets were only understood at the level of surfaces - in particular, it was not known how to assign linear maps to cobordisms which changed the topology of the surface. We also reformulate the extended Turaev-Viro theory developed by Balsam and Kirillov into the bicategorical generators-and-relations formalism, and use this to prove that the string-net and Turaev-Viro 123-TQFTs are equivalent.

Opsomming

In 'n reeks artikels het Bartlett, Douglas, Schommer-Pries, en Vicary 'n eindige voortbringer-en-verwantskap voorstelling van die geörienteerde kobordisme bikategorie ontdek. Hierdie voorstelling vergemaklik die taak om geörienteerde eenmaaluitgebreide topologiese kwantumveldtoerëe (123-TKVT_e) op te spoor. Ons kombineer hierdie resultaat met die teorie van string-nette, veral Kirillov se veralgemening van die teorie na begrensde oppervlakke, om sodoende 'n geörienteerde 123-TKVT gebaseer op string-nette te konstrueer. Voorheen was die teorie slegs verstaan vir oppervlakke - byvoorbeeld, dit was nie bekend hoe om 'n lineêre transformasie te assosieer met 'n kobordisme wat die topologie van die onderlinge ruimte verander nie. Ons herformuleer ook die uitgebreide Turaev-Viro teorie ontwikkel deur Balsam en Kirillov binne die bikategorieese voorbringer-en-verwantskap raamwerk, en gebruik dit om te bewys dat die string-net en Turaev-Viro 123-TKVT_e ekwivalent is.

Dedication

To Andrea, Kaitlyn, and my parents, Danie and Antoinette.

Acknowledgments

1 Pet 4:11. *If anyone serves, they should serve in the strength that God supplies, so that in all things God may be glorified through Christ Jesus, to whom belongs the glory and dominion forever and ever. Amen.*

My deepest thanks and appreciation are reserved for my friend and mentor, Dr Bruce Bartlett. Bruce, without your friendship, advice, helpful insights and conversations too numerous to count, this thesis would never have been possible. I will never forget all the long hours we spent doing calculations together, and I am sure that we shall spend many more such hours together in the future!

To my beloved wife, Andrea. It goes without saying that, had I not met you near the start of my PhD, I would be nowhere near the man I am today. Your constant love and support saw me through the difficult times where the calculations just didn't seem to come together. For every kiss, for every hug, for every word of encouragement, I thank you and I love you.

To my little Kaitlyn. Your precious laughter helped me to work harder, just so I come home a little sooner to hear it again. I look forward to explaining TQFT to you when you get older!

To my parents, I owe a debt greater than I could ever hope to repay. What can one say that would even begin to honour a lifetime of love, support, wisdom, encouragement, and joy? I don't know what else to say except thank you. May the Lord give me grace to love my children the way you loved me.

The work done in this thesis was partially supported by the National Research Foundation. My sincere thanks go to the NRF for making this thesis possible.

SOLI DEO GLORIA

Contents

1	Introduction	1
1.1	Results	2
2	Preliminaries	4
2.1	Monoidal Categories	4
2.1.1	Basics	4
2.1.2	Graphical Calculus	9
2.1.3	Useful Lemmas and Conventions	16
2.2	Bicategories	22
2.3	PLCW Complexes	24
3	123-TQFTs via generators and relations	30
4	String-nets	38
4.1	Basics	38
4.2	Evaluation	41
4.3	Equivalence	44
5	The string-net 123-TQFT	48
5.1	String-nets and the Drinfel'd center	48
5.2	Generators	55
5.3	Relations	65
6	Extended Turaev-Viro Theory	70
6.1	Preliminaries	70
6.1.1	Extended Surfaces	70
6.1.2	The State Space	72
6.1.3	Extended 3-manifolds	76
6.2	The Invariant	78
6.3	Properties of the Invariant	91
6.4	TV = String-Nets	96

7	The Turaev-Viro 123-TQFT	101
7.1	Generators	101
7.1.1	Nu and its dagger.	105
7.1.2	Mu and its dagger.	107
7.1.3	Eta and its dagger.	115
7.1.4	Epsilon and its dagger	126
7.2	Relations	133

Chapter 1

Introduction

Given two manifolds M and M' , are they homeomorphic? This is one of the oldest and most enduring questions in topology. One of the most successful techniques for answering this question is the computation of invariants. One of the most well-known invariants of 3-manifolds were defined by Turaev and Viro in their 1992 paper [30]. In the same paper, the authors also showed that these invariants can be extended to a 3-dimensional topological quantum field theory (TQFT). The notion of a TQFT was fully axiomatized by Atiyah in 1990:

Definition 1. An n -dimensional TQFT is a symmetric monoidal functor

$$Z : \mathbf{Cob}_n \rightarrow \mathbf{Vect}_{\mathbb{C}}$$

where the objects of \mathbf{Cob}_n are closed $(n - 1)$ -manifolds and the morphisms are cobordisms between them.

At a minimum, every TQFT yields a numerical invariant of a closed 3-manifold by viewing it as a cobordism from \emptyset to \emptyset . However, TQFTs have a far richer structure than merely computing numerical invariants. Indeed, they are currently an active topic of research in their own right; in particular, Lurie's paper [22] has led to a renewed interest in studying TQFTs extended to manifolds of codimension greater than 1. A 3-dimensional TQFT which has been extended once is called a 123-TQFT (or simply an extended TQFT).

In their 2010 paper [2] Balsam and Kirillov described how the invariants of Turaev and Viro may be reformulated as an extended TQFT. Their theory takes as input a fixed spherical fusion category \mathcal{A} and assigns the Drinfel'd center $Z(\mathcal{A})$ to S^1 . They did not consider manifolds with corners directly, preferring to work with 3-manifolds with framed embedded tubes, which are

closely related.

Akin to Atiyah's axioms, the data of an extended TQFT may also be described categorically (*bicategorically*, to be precise):

Definition 2. An oriented 123-TQFT is a symmetric monoidal pseudofunctor

$$Z : \mathbf{Bord}_{123}^{\text{or}} \rightarrow \mathbf{Prof}_{\mathbb{C}}.$$

where $\mathbf{Bord}_{123}^{\text{or}}$ is a bicategory whose objects are closed 1-manifolds, 1-morphisms are cobordisms between the objects, and 2-morphisms are cobordisms between the 1-morphisms.

In a series of papers [6, 7, 8, 9] by Bartlett, Douglas, Schommer-Pries, and Vicary, the authors discovered (among other things) a finite generators-and-relations presentation $\mathbf{F}(\mathcal{O})$ ¹ of $\mathbf{Bord}_{123}^{\text{or}}$.

Remark 3. At the time of writing, the paper [6] containing the proof of the equivalence $\mathbf{F}(\mathcal{O}) \simeq \mathbf{Bord}_{123}^{\text{or}}$ is still unpublished. However, note that [9] shows that representations of $\mathbf{F}(\mathcal{O})$ correspond to modular categories, and modular categories in turn are known [1, 29] to give rise to 3d-TQFTs.

The presentation simplifies the task of describing an extended TQFT, as one merely needs to specify the data assigned to the generators, and then check that all the relevant relations are satisfied. Indeed, this presentation is the key ingredient in our results.

1.1 Results

The first main result of this thesis is the construction of an oriented 123-TQFT based on string-nets. String-nets first appeared in the physics literature by Levin and Wen [21] as a physical mechanism for dealing with topological phases of matter. Our work principally relies on Kirillov's more mathematical description [18] and generalization of the theory to surfaces with boundary. Taking as input a fixed spherical fusion category \mathcal{A} , we prove:

Theorem 4. *String-nets have the structure of an oriented 123-TQFT, such that $Z_{SN}^{123}(S^1) = Z(\mathcal{A})$.*

¹This idea is analogous to taking the free group on a collection of generators, subject to certain relations.

Our second main result is a reformulation of Balsam and Kirillov's extension of Turaev-Viro theory into the bicategorical generators-and-relations framework. It is known that string-nets are equivalent to the 2-dimensional part of Turaev-Viro theory - in particular, Kirillov showed in [18] that this correspondence also holds for surfaces with boundary. Our third main result compares Turaev-Viro theory and string-nets as extended TQFTs.

Theorem 5. *We have an equivalence of oriented 123-TQFTs,*

$$Z_{SN}^{123}(S^1) \simeq Z_{TV}^{123}.$$

Chapter 2

Preliminaries

In this chapter we establish the common notions and notational conventions which we shall use throughout the thesis.

2.1 Monoidal Categories

We shall take for granted the basic definitions and lemmas of introductory category theory. A standard reference for readers unfamiliar with these facts is the book by MacLane [23].

2.1.1 Basics

Definition 6. A category \mathcal{C} is called *monoidal*¹ if it is equipped with the following data:

1. A bifunctor $\otimes : \mathcal{C} \times \mathcal{C} \rightarrow \mathcal{C}$. For objects $U, V \in \mathcal{C}$, we abuse the notation and write their image as $U \otimes V := \otimes(U, V)$. We call this bifunctor the *tensor product*.
2. For objects $U, V, W \in \mathcal{C}$, a natural isomorphism

$$\alpha_{U,V,W} : (U \otimes V) \otimes W \rightarrow U \otimes (V \otimes W)$$

called the *associator*.

3. An object $1 \in \mathcal{C}$, called the *unit* and, for any object $V \in \mathcal{C}$, natural isomorphisms

$$\lambda_V : 1 \otimes V \rightarrow V$$

¹They are also called *tensor* categories.

and

$$\rho_V : V \otimes 1 \rightarrow V$$

called the *left* and *right unitor* respectively.

These structure maps are required to satisfy the *triangle* and *pentagon* coherence equations - see [23].

Definition 7. A monoidal category \mathcal{C} is called *strict* if its associator α and left and right unitors λ and ρ are identity maps.

The following theorem allows us to treat monoidal categories as though they were strict.

Theorem 8. [23] *Every monoidal category is equivalent to a strict monoidal category.*

We make extensive use of this theorem. In particular, we omit the morphisms α , λ , and ρ in the graphical calculus we define in Section 2.1.2. An equivalent approach would have been to use non-strict monoidal categories, but simply suppress the associators and unitors in the notation, making use of MacLane’s well-known coherence theorem (See [23]).

Example 9. A basic example of a monoidal category is $\mathbf{Vect}_{\mathbb{C}}$, the category of finite-dimensional complex vector spaces. The tensor product is simply the usual vector space tensor product, and the unit object is the ground field \mathbb{C} .

Definition 10. A monoidal category \mathcal{C} is called *right rigid* if for every object $X \in \mathcal{C}$ there exists an object X^* , called the *right dual* of X , together with maps

$$\begin{aligned} \text{coev}_X : 1 &\rightarrow X \otimes X^* \\ \text{ev}_X : X^* \otimes X &\rightarrow 1 \end{aligned}$$

satisfying the so-called snake relations:

$$\begin{aligned} X &\xrightarrow{\text{coev}_X \otimes \text{id}_X} X \otimes X^* \otimes X \xrightarrow{\text{id}_X \otimes \text{ev}_X} X = \text{id}_X \\ X^* &\xrightarrow{\text{id}_{X^*} \otimes \text{coev}_X} X^* \otimes X \otimes X^* \xrightarrow{\text{ev}_X \otimes \text{id}_{X^*}} X^* = \text{id}_{X^*}. \end{aligned}$$

These maps are called² the *coevaluation* and *evaluation* maps respectively. There is an analogous definition for *left rigid* monoidal categories, where each

²After we have discussed the graphical calculus, we shall also call these maps the “cap” and “cup” respectively.

object has a *left dual* $*X$ together with suitable coevaluation and evaluation maps:

$$\begin{aligned} \text{coev}^X : 1 &\rightarrow *X \otimes X \\ \text{ev}^X : X \otimes *X &\rightarrow 1 \end{aligned}$$

satisfying analogous snake relations. Monoidal categories which are both left rigid and right rigid are simply called rigid. Note that, in a rigid category, an object's right dual and left dual are not necessarily isomorphic. Moreover, Definition 10 merely asserts that right duals exist, not that a specific right dual has been chosen (for each X). For a right rigid category \mathcal{C} , if we do choose a right dual X^* for each X , the operation of sending an object to its dual can be extended to a contravariant functor, which we denote

$$* : \mathcal{C} \rightarrow \mathcal{C}.$$

Definition 11. A pivotal category is a right rigid monoidal category \mathcal{C} equipped with a monoidal natural isomorphism

$$\Phi : \text{id}_{\mathcal{C}} \rightarrow **.$$

In a pivotal category, a right dual X^* can be used as a left dual as well. Indeed, we set

$$\begin{aligned} 1 \xrightarrow{\text{coev}^X} X^* \otimes X &:= 1 \xrightarrow{\text{coev}_{X^*}} X^* \otimes (X^*)^* \xrightarrow{\text{id}_{X^*} \otimes \Phi_X^{-1}} X^* \otimes X \\ X \otimes X^* \xrightarrow{\text{ev}^X} 1 &:= X \otimes X^* \xrightarrow{\Phi_X \otimes \text{id}_{X^*}} (X^*)^* \otimes X^* \xrightarrow{\text{ev}_{X^*}} 1. \end{aligned}$$

It is easy to see that these maps will satisfy the required snake relations. Thus pivotal categories are automatically left rigid, and hence rigid. Since the left and right duals of X coincide, we call X^* a two-sided dual or, more simply, just *the* dual of X . A pivotal category is called *strict* if Φ is the identity. The following theorem allows us to treat pivotal categories as though they were strict.

Theorem 12. [4] *Every pivotal category is equivalent to a strict pivotal category.*

We make extensive use of this theorem throughout the thesis, as it greatly simplifies the graphical calculus we define in Section 2.1.2.

Definition 13. [3] A *spherical category* is a pivotal category \mathcal{C} satisfying the following extra condition: For any $X \in \mathcal{C}$ and any $f \in \text{Hom}(X, X)$, we have

$$\text{ev}^X \circ (f \otimes \text{id}_{X^*}) \circ \text{coev}_X = \text{ev}_X \circ (\text{id}_{X^*} \otimes f) \circ \text{coev}^X. \quad (2.1)$$

The expressions on the left- and right-hand side of Equation 2.1 above are known as the left and right *trace* of f respectively. In other words, a pivotal category is spherical if for every endomorphism f , its left and right traces are equal. In this case we may therefore simply speak of *the* trace of f , and we denote it by $\text{tr}(f)$.

The monoidal categories of interest to us shall have the property that their hom-sets are not merely sets, but vector spaces, and with composition bilinear. Such a category is called a *monoidal linear category*.³

Definition 14. A monoidal linear category \mathcal{C} is called *semisimple* if

- \mathcal{C} has finite biproducts (usually called direct sums),
- all idempotents in \mathcal{C} split,⁴
- there exists a set $\text{Irr}(\mathcal{A}) = \{X_i\}_{i \in I}$ of objects, called *simple objects*, such that $\text{Hom}(X_i, X_j) \cong \delta_{ij}\mathbb{C}$. Moreover, for any objects $V, W \in \mathcal{C}$, the natural composition map

$$\bigoplus_{i \in I} \text{Hom}(V, X_i) \otimes \text{Hom}(X_i, W) \rightarrow \text{Hom}(V, W) \quad (2.2)$$

is an isomorphism.

In a semisimple category, any object V can be written as a direct sum of the simple objects, where each simple object appears with the appropriate multiplicity. That is,

$$V \cong \bigoplus_{i \in I} n_i X_i$$

where $n_i \in \mathbb{N}$ counts the multiplicity of X_i .

³Technically, we are speaking of a monoidal category which is enriched over $\text{Vect}_{\mathbb{C}}$. In our case, the hom-spaces will always be finite-dimensional. See [16] for more details about enriched categories.

⁴An idempotent $p : A \rightarrow A$ is said to *split* if there exists an object B and maps $r : A \rightarrow B$ and $i : B \rightarrow A$ such that $p = i \circ r$ and $r \circ i = \text{id}_B$.

Remark 15. In the remainder of the thesis, we shall frequently abuse the notation and write i for both the simple object X_i as well as its index. We shall be careful to make sure that the precise meaning is clear from the context.

Definition 16. A *spherical fusion category* is a rigid semisimple linear spherical monoidal category, with only finitely many simple objects, and such that the monoidal unit 1 is simple.

Example 17. A basic example of a spherical fusion category is the category $\text{Vect}_{\mathbb{C}}[G]$ of complex G -graded vector spaces, where G is a finite group.

Spherical fusion categories are the basic algebraic ingredient for virtually all the TQFT calculations to follow. Throughout the thesis, \mathcal{A} shall always denote a spherical fusion category. For a detailed discussion of the properties of spherical fusion categories we refer the reader to [11].

Since $1 \in \mathcal{A}$ is simple, the maps $\text{ev}^V \circ \text{coev}_V$ and $\text{ev}_V \circ \text{coev}^V$ (which are equal since \mathcal{A} is spherical) simply amount to a complex number. This number is called the *dimension* of V , and we denote it by d_V . In accord with Remark 15, we write d_i for the dimension of the simple object X_i . We also define the number

$$\mathcal{D} = \sqrt{\sum_{i \in \text{Irr}(\mathcal{A})} d_i^2} \quad (2.3)$$

called the *dimension* of \mathcal{A} . It is known [12] that simple objects have nonzero real dimension,⁵ which implies that $\mathcal{D} \neq 0$.

Definition 18. A monoidal category \mathcal{C} is called *braided* if it is equipped with a natural isomorphism

$$B_{X,Y} : X \otimes Y \rightarrow Y \otimes X \quad (2.4)$$

called the *braiding*, such that the hexagon equations hold - see [23] for details.

In the case where \mathcal{C} is semisimple, we write $B_{i,j}$ for the braiding of two simple objects X_i and X_j .

Definition 19. A spherical fusion category is *modular* if it is braided and the braiding satisfies the following non-degeneracy condition: The matrix S defined by

$$S_{ij} = \text{tr}(B_{j,i} \circ B_{i,j}) \quad (2.5)$$

is invertible.

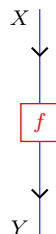
⁵For a diagrammatic proof of this fact, see [5].

2.1.2 Graphical Calculus

Throughout the thesis, we make frequent use of the so-called tangle diagram calculus for depicting morphisms in our categories. Tangle diagrams have their roots in the paper of Roger Penrose [25], who used them to describe tensor products of linear operators. Eventually, it was realised that these diagrams had applications in more general situations. Through the papers of Joyal and Street [13] [14] [15], tangle diagrams made their way into monoidal category theory as an indispensable tool for depicting morphisms (and equations between them).

Though this graphical calculus is routinely used by experts (see for example the standard references [29] and [1]) a systematic treatment of the theory only appeared in 2010 in Selinger’s survey article [28]. In an attempt to make the thesis as self-contained as possible, as well as to establish notational conventions, we include a brief introduction of the basic idea. However, most of the technical details will be omitted. For a more thorough treatment, we refer the reader to Selinger’s paper.

Let \mathcal{C} be a category. We depict a given morphism $f \in \text{Hom}_{\mathcal{C}}(X, Y)$ as follows:



Note that we think of the diagram as running “from top to bottom”. Thus the source object X labels the top wire, and the target object Y labels the bottom wire. The rectangular coupon (i.e. the box) is labelled by the morphism f itself.

Composition in \mathcal{C} is depicted by vertically stacking the relevant morphisms. Let $f \in \text{Hom}_{\mathcal{C}}(X, Y)$ and $g \in \text{Hom}_{\mathcal{C}}(Y, Z)$. Then we set

$$\begin{array}{ccc}
 \begin{array}{c} X \\ \downarrow \\ \boxed{f} \\ \downarrow \\ Y \\ \downarrow \\ \boxed{g} \\ \downarrow \\ Z \end{array} & = & \begin{array}{c} X \\ \downarrow \\ \boxed{g \circ f} \\ \downarrow \\ Z \end{array}
 \end{array} \tag{2.6}$$

A wire with no coupons is considered to depict the identity.

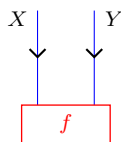
$$\begin{array}{ccc}
 \begin{array}{c} X \\ \downarrow \\ X \end{array} & = & \begin{array}{c} X \\ \downarrow \\ \boxed{\text{id}_X} \\ \downarrow \\ X \end{array}
 \end{array} \tag{2.7}$$

Monoidal Structure

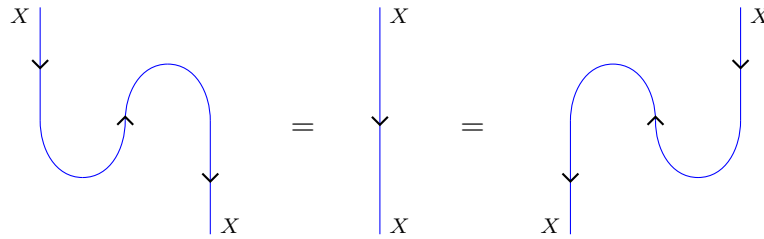
Tensor product is depicted by stacking the relevant diagrams horizontally. Thus, for $f \in \text{Hom}_{\mathcal{C}}(X, Y)$ and $g \in \text{Hom}_{\mathcal{C}}(X', Y')$, we have

$$\begin{array}{ccc}
 \begin{array}{cc} X & X' \\ \downarrow & \downarrow \\ \boxed{f} & \boxed{g} \\ \downarrow & \downarrow \\ Y & Y' \end{array} & = & \begin{array}{c} X \otimes Y \\ \downarrow \\ \boxed{f \otimes g} \\ \downarrow \\ X' \otimes Y' \end{array}
 \end{array} \tag{2.8}$$

A string labeled by the monoidal unit 1 will be left blank. So, for example, the diagram below depicts a morphism $f \in \text{Hom}_{\mathcal{C}}(X \otimes Y, 1)$.



Using the above convention, the snake relations have the following diagrammatic form:



We may use the maps above to define isomorphisms:

$$\text{Hom}_{\mathcal{C}}(X, Y) \rightarrow \text{Hom}_{\mathcal{C}}(1, Y \otimes X^*)$$

given by

(2.10)

and

$$\text{Hom}_{\mathcal{C}}(X, Y) \rightarrow \text{Hom}_{\mathcal{C}}(X \otimes Y^*, 1)$$

given by

(2.11)

These isomorphisms are known colloquially as the “yanking moves”. In the figures above, the strings are yanked to the right (of f). There are analogous versions of these isomorphisms yanking the string to the left. The yanking moves are used in various computations throughout the thesis.

Spherical Structure

In tangle diagram notation, the sphericity condition is given as follows:

$$\begin{array}{ccc}
 \boxed{\text{coev}_X} & & \boxed{\text{coev}^X} \\
 \downarrow \quad \uparrow & = & \downarrow \quad \uparrow \\
 X \quad X & & X \quad X \\
 \uparrow \quad \downarrow & & \uparrow \quad \downarrow \\
 \boxed{\text{ev}^X} & & \boxed{\text{ev}_X}
 \end{array}$$

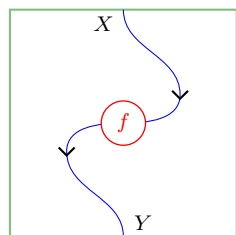
Making use of our graphical conventions, we may write this more simply as

$$\begin{array}{ccc}
 \text{X} \downarrow & & \uparrow \text{X} \\
 \circlearrowleft & = & \circlearrowright \\
 \uparrow \text{X} & & \text{X} \downarrow
 \end{array}$$

Recall that in a spherical fusion category, the diagrams above both represent the dimension $d_X \in \mathbb{C}$.

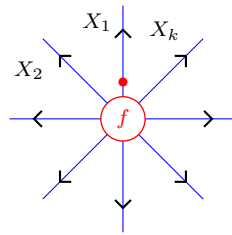
Circular Coupons

Following Balsam and Kirillov, we allow circular coupons, in addition to rectangular coupons, in our diagrams. This serves the purpose of making the diagrammatic notation much more intuitive. Since circular coupons lack a well-defined top and bottom (unlike rectangular coupons), it seems at first that they are not a suitable choice for representing morphisms in tangle diagrams. In the diagram below, for example, it is not clear to which hom-space f belongs.

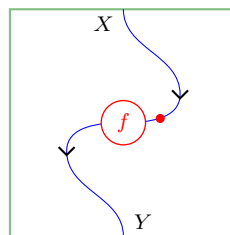

(2.12)

We thus declare that each circular coupon represent a morphism which has source equal to the monoidal unit 1 and that, moreover, each circular coupon comes equipped with a distinguished *initial half-edge*. Graphically, we indicate the initial half-edge by endowing it with a small red dot near the coupon.

With these amendments, the ambiguity is removed. If the edges incident to some coupon labeled by f are labeled by X_1, \dots, X_k , starting with the initial half-edge and then moving counterclockwise, we declare that $f \in \text{Hom}_{\mathcal{A}}(1, X_1 \otimes \dots \otimes X_k)$.

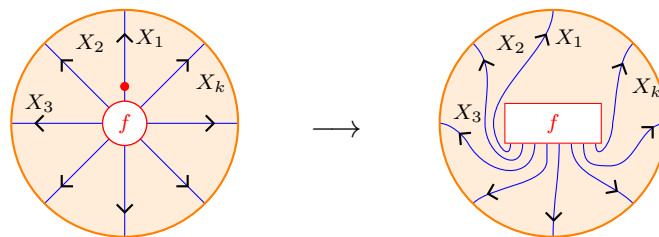


In Diagram 2.12, if the top edge is the initial half-edge (see Diagram 2.13 below) then clearly $f \in \text{Hom}_{\mathcal{A}}(1, X^* \otimes Y)$.



(2.13)

It is easy to see that the circular coupon notation is equivalent to the standard rectangular coupon notation via the following correspondence:



(2.14)

It can be shown that, up to a canonical isomorphism, a circular coupon is independent of the choice of initial half-edge. Indeed, consider the following equation:

(2.15)

The orange shaded areas represent neighbourhoods around a coupon within their respective tangle diagrams. Outside of these neighbourhoods the two tangle diagrams are identical, that is, they represent the same morphism. The equal sign means that the two tangle diagrams are equal. The coupon labels satisfy the equation:

(2.16)

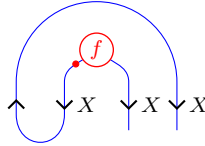
In other words, we may rotate the choice of initial half-edge for a coupon counterclockwise provided we also change the coupon label according to the equation above. This process may be iterated, with $f^{(2)} = (f^{(1)})^{(1)}$, and so on. Lastly, we note that $f^{(k)} = f$ since \mathcal{A} is pivotal.⁶

In their papers, Balsam and Kirillov do not make use of initial half-edges, considering the labels $f, f^{(1)}, f^{(2)}, \dots, f^{(k-1)}$ to be, for all practical purposes, equivalent. While this does not lead to problems in the vast majority of situations, ambiguities may nevertheless occur, as the following discussion⁷ shows.

Let $X \in \mathcal{A}$ be a self-dual simple object, let $f \in \text{Hom}_{\mathcal{A}}(1, X \otimes X)$, and suppose that the yanking move isomorphisms have been applied twice, as shown below.

⁶See [1, Section 5.3] for details.

⁷The discussion given here mirrors the style of [31, Section 4.5].



Since $\text{Hom}_{\mathcal{A}}(1, X \otimes X) \cong \text{Hom}_{\mathcal{A}}(X^*, X) \cong \mathbb{C}$, the morphism above is a scalar multiple of f .

$$\text{Diagram} = \nu_X \text{Diagram} \quad (2.17)$$

The scalar ν_X is called the *Frobenius-Schur indicator*. If we “pull the wires straight” on the diagram on the left above, which is precisely the sort of natural topological move we would like to be able to use, we notice that the equation could be rewritten as

$$\text{Diagram} = \nu_X \text{Diagram} \quad (2.18)$$

Clearly, if the red dots were not present, we would be tempted to conclude that $\nu_X = 1$, which does not hold in general.

In summary: It does not really matter which half-edge is chosen to be initial, so long as that choice remains consistent throughout the given computation. Being careful to do this, we shall omit the red dots from our diagrams whenever doing so does not lead to confusion.

2.1.3 Useful Lemmas and Conventions

Let \mathcal{A} be a spherical fusion category. Since we shall be using circular coupons (almost exclusively) in our tangle diagrams, we define a functor $\mathcal{A}^{\boxtimes n} \rightarrow \text{Vect}_{\mathbb{C}}$ by

$$\langle V_1, \dots, V_n \rangle := \text{Hom}_{\mathcal{A}}(1, V_1 \otimes \dots \otimes V_n). \quad (2.19)$$

The yanking moves give an isomorphism:

$$\langle V_1, \dots, V_n \rangle \cong \langle V_2, \dots, V_n, V_1 \rangle \quad (2.20)$$

Indeed, this corresponds precisely to the operation of rotating the choice of initial half-edge, i.e. $f \mapsto f^{(1)}$. There is a natural composition map:

$$\langle V_1, \dots, V_n, X^* \rangle \otimes \langle X, W_1, \dots, W_m \rangle \rightarrow \langle V_1, \dots, V_n, W_1, \dots, W_m \rangle \quad (2.21)$$

given by:

$$\begin{array}{ccc} \begin{array}{c} \boxed{\varphi} \\ \downarrow \dots \downarrow \uparrow \\ V_1 \quad V_n \quad X \end{array} & \begin{array}{c} \boxed{\psi} \\ \downarrow \dots \downarrow \\ X \quad W_1 \quad W_m \end{array} & \xrightarrow{\circ_X} \begin{array}{c} \boxed{\varphi} \quad \boxed{\psi} \\ \downarrow \dots \downarrow \quad \downarrow \dots \downarrow \\ V_1 \quad V_n \quad X \quad W_1 \quad W_m \end{array} \end{array} \quad (2.22)$$

We may write down an equivalent version of Equation 2.2 in terms of the above composition:

$$\bigoplus_i \langle V_1, \dots, V_n, X_i^* \rangle \otimes \langle X_i, W_1, \dots, W_m \rangle \xrightarrow{\cong} \langle V_1, \dots, V_n, W_1, \dots, W_m \rangle \quad (2.23)$$

Note that multiple applications of the composition 2.22 also gives a non-degenerate pairing

$$\langle V_1, \dots, V_n \rangle \otimes \langle V_n^*, \dots, V_1^* \rangle \rightarrow \mathbb{C} \quad (2.24)$$

We denote this by $\varphi \otimes \psi \mapsto (\varphi, \psi)$. Since the pairing is nondegenerate, we have an isomorphism

$$\langle V_1, \dots, V_n \rangle^* \cong \langle V_n^*, \dots, V_1^* \rangle. \quad (2.25)$$

Remark 20. We make use of the following summation convention: If a diagram contains a pair of circular coupons, one with outgoing wires labelled V_1, \dots, V_n (proceeding counterclockwise, with the V_1 half-edge initial) and the other with outgoing wires labelled V_n^*, \dots, V_1^* (proceeding counterclockwise, with the V_n^* half-edge initial), and where the coupons are labelled by pairs of letters φ, φ^* (or ψ, ψ^* , and so on), this indicates summation over the dual bases:

(2.26)

On the right-hand side of the diagram above we are summing⁸ over α , and $\varphi_\alpha \in \langle V_1, \dots, V_n \rangle$ and $\varphi^\alpha \in \langle V_n^*, \dots, V_1^* \rangle$ are dual bases⁹ with respect to the pairing 2.24.

The following two lemmas are used repeatedly throughout the thesis. We name them to make referencing them more intuitive. We omit the proofs, referring the reader to [2].

Lemma 21 (The Resolution Lemma).

(2.27)

Lemma 22 (The Fusion Lemma.). *If the subgraphs A, B are not connected, then*

(2.28)

In the fusion lemma above, we mean that A and B are tangle diagrams with no incoming or outgoing wires other than V_1, \dots, V_n , however, a version of the fusion lemma also holds if one (but not both) of either A or B does have other outgoing wires.

⁸This is the Einstein summation convention.

⁹That is, $(\varphi_\alpha, \varphi^\beta) = \delta_\alpha^\beta$.

The Drinfel'd Center

The following notion is ubiquitous throughout the thesis. The reader may wish to consult [24] for more details.

Definition 23. Let \mathcal{A} be a spherical fusion category. The *Drinfel'd center* of \mathcal{A} , denoted $Z(\mathcal{A})$, is a monoidal category whose

- objects are pairs (Y, Φ_Y) of an object $Y \in \mathcal{A}$ and a natural isomorphism

$$\Phi_Y : Y \otimes - \rightarrow - \otimes Y \quad (2.29)$$

called the *half-braiding*, which is compatible with the tensor product; and whose

- morphisms from (Y, Φ_Y) to $(Y', \Phi_{Y'})$ are morphisms in \mathcal{A} from Y to Y' which commute with the half-braiding.

The monoidal structure on $Z(\mathcal{A})$ is given by

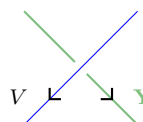
$$(Y, \Phi_Y) \otimes (Y', \Phi_{Y'}) = (Y \otimes Y', (\Phi_Y \otimes \text{id}) \circ (\text{id} \otimes \Phi_{Y'})). \quad (2.30)$$

We shall employ the convention of writing a bold green letter when referring to elements of $Z(\mathcal{A})$:

$$\mathbf{Y} := (Y, \Phi_Y).$$

Remark 24. There is an obvious forgetful functor $F : Z(\mathcal{A}) \rightarrow \mathcal{A}$ given by $\mathbf{Y} \mapsto Y$. Using F , we follow Balsam and Kirillov and extend the graphical calculus to include wires labeled by elements in $Z(\mathcal{A})$ - such wires will be drawn in green. For brevity we shall frequently choose to write \mathbf{Y} instead of $F(\mathbf{Y})$, where $\mathbf{Y} \in Z(\mathcal{A})$, in our equations and diagrams.

We denote the half-braiding $\Phi_Y(V) : Y \otimes V \rightarrow V \otimes Y$ diagrammatically by



$$(2.31)$$

The following theorem, proved by Muger [24], is critical for establishing a connection between Turaev-Viro and Reshetikhin-Turaev theory.

Theorem 25. *Let \mathcal{A} be a spherical fusion category. Then $Z(\mathcal{A})$ is modular; in particular, it is semisimple with finitely many simple objects, it is braided and has a pivotal structure which coincides with the pivotal structure on \mathcal{A} .*

Lemma 26. [2, Lemma 2.2] Let $\mathbf{Y}, \mathbf{Z} \in Z(\mathcal{A})$. Define the operator

$$P : \text{Hom}_{\mathcal{A}}(Y, Z) \rightarrow \text{Hom}_{\mathcal{A}}(Y, Z)$$

by the formula:

$$P(\psi) = \frac{1}{\mathcal{D}^2} \sum_{i \in \text{Irr}(\mathcal{A})} d_i \text{ (diagram) } \quad (2.32)$$

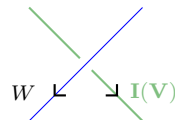
Then P is a projector onto the subspace $\text{Hom}_{Z(\mathcal{A})}(\mathbf{Y}, \mathbf{Z}) \subset \text{Hom}_{\mathcal{A}}(Y, Z)$.

Finally, we shall also need the following theorem.

Theorem 27. [2, Thm 2.3] Let $F : Z(\mathcal{A}) \rightarrow \mathcal{A}$ be the forgetful functor and let $I : \mathcal{A} \rightarrow Z(\mathcal{A})$, called the induction functor, be the (left) adjoint of F . Then, for $V \in \mathcal{A}$, one has

$$I(V) = \bigoplus_{r \in \text{Irr}(\mathcal{A})} X_r \otimes V \otimes X_r^* \quad (2.33)$$

with the half-braiding



given by

$$\sum_{j,k} \sqrt{d_j} \sqrt{d_k} \text{ (diagram) } \quad (2.34)$$

where

$$p_j : \bigoplus_{r \in \text{Irr}(\mathcal{A})} X_r \otimes V \otimes X_r^* \rightarrow X_j \otimes V \otimes X_j^*$$

and

$$i_k : X_k \otimes V \otimes X_k^* \rightarrow \bigoplus_{r \in \text{Irr}(\mathcal{A})} X_r \otimes V \otimes X_r^*$$

are the natural projection and injection maps associated to the direct sum.

Recall that the injection and projection maps satisfy the following properties:

$$\begin{array}{c}
 \begin{array}{c}
 k \downarrow \quad \downarrow V \quad \uparrow k \\
 \boxed{i_k} \\
 \downarrow \text{I(V)} \\
 \boxed{p_j} \\
 j \downarrow \quad \downarrow V \quad \uparrow j
 \end{array}
 = \delta_{j,k} \begin{array}{c}
 j \downarrow \quad \downarrow V \quad \uparrow j
 \end{array}
 \end{array} \quad (2.35)$$

and

$$\sum_{k \in \text{Irr}(\mathcal{A})} \begin{array}{c}
 \downarrow \text{I(V)} \\
 \boxed{p_k} \\
 k \downarrow \quad \downarrow V \quad \uparrow k \\
 \boxed{i_k} \\
 \downarrow \text{I(V)}
 \end{array}
 = \downarrow \text{I(V)} . \quad (2.36)$$

2.2 Bicategories

In this section we review bicategories very briefly. The 123-TQFTs we define in this thesis have bicategories as their source and target. For a slightly more thorough introduction to bicategories, see [20].

Definition 28. A *bicategory* consists of the following data:

- A collection of objects x, y, z, \dots , also called *0-cells*;
- For each pair of 0-cells x, y , a category $B(x, y)$, whose objects are called morphisms, or *1-cells*, and whose morphisms are called 2-morphisms or *2-cells*;
- For each 0-cell x , a distinguished 1-cell $1_x \in B(x, x)$ called the *identity morphism* or identity 1-cell at x ;
- For each triple of 0-cells x, y, z , a functor $\circ : B(y, z) \times B(x, y) \rightarrow B(x, z)$ called *horizontal composition*;
- For each pair of 0-cells x, y, z , natural isomorphisms called *unitors*

$$\text{id}_{B(x,y)} \circ \text{const}_{1_x} \cong \text{id}_{B(x,y)} \cong \text{const}_{1_y} \circ \text{id}_{B(x,y)} : B(x, y) \rightarrow B(x, y); \quad (2.37)$$

- For each quadruple of 0-cells w, x, y, z , a natural isomorphism called the *associator* between the two functors from $B(y, z) \times B(x, y) \times B(w, x)$ to $B(w, z)$ built out of \circ such that the associators satisfy the pentagon equation and the unitors satisfy the triangle equations.

We review the two most important examples of bicategories we shall need.

Example 29. There is a bicategory, denoted $\mathbf{Prof}_{\mathbb{C}}$, defined as follows:

- Objects in $\mathbf{Prof}_{\mathbb{C}}$ are linear categories (i.e. $\mathbf{Vect}_{\mathbb{C}}$ -enriched);
- Morphisms in $\mathbf{Prof}_{\mathbb{C}}$ are $\mathbf{Vect}_{\mathbb{C}}$ -valued profunctors.¹⁰ Recall that a profunctor $F : \mathcal{C} \dashrightarrow \mathcal{D}$ is defined as an ordinary functor $F : \mathcal{D}^{op} \boxtimes \mathcal{C} \rightarrow \mathbf{Vect}_{\mathbb{C}}$.¹¹ For two profunctors $F : \mathcal{C} \dashrightarrow \mathcal{D}$ and $G : \mathcal{D} \dashrightarrow \mathcal{E}$, the composite

$$G \circ F : \mathcal{E}^{op} \boxtimes \mathcal{C} \rightarrow \mathbf{Vect}_{\mathbb{C}}$$

¹⁰We shall simply call them profunctors from now on, with values in $\mathbf{Vect}_{\mathbb{C}}$ being understood.

¹¹Here \boxtimes is Deligne's tensor product - see [10].

is defined by

$$(G \circ F)(e, c) := \bigoplus_{d \in \mathcal{D}} (G(e, d) \otimes F(d, c)) / \sim \quad (2.38)$$

where \sim is the equivalence relation generated by the relation $(g \cdot x, f) \sim (g, x \cdot f)$ for all $g \in G(e, d)$, $f \in F(d', c)$, and $x \in \text{Hom}_{\mathcal{D}}(d, d')$.

- The 2-morphisms in $\mathbf{Prof}_{\mathbb{C}}$ are called “maps of profunctors”. These are simply natural transformations between the associated $\mathbf{Vect}_{\mathbb{C}}$ -valued ordinary functors.

It can be shown that with the above choices, all the required relations will be satisfied. Lastly, note that $\mathbf{Prof}_{\mathbb{C}}$ also has a monoidal structure given by the enriched tensor product. The objects of $\mathcal{C} \boxtimes \mathcal{D}$ consist of pairs of objects $(c, d) \in \mathcal{C} \times \mathcal{D}$, and the morphism vector spaces are given by $\text{Hom}_{\mathcal{C} \boxtimes \mathcal{D}}((c, d), (c', d')) = \text{Hom}_{\mathcal{C}}(c, c') \otimes_k \text{Hom}_{\mathcal{D}}(d, d')$.

Example 30. There is a bicategory, denoted $\mathbf{Bord}_{123}^{\text{or}}$, defined as follows:

- The objects in $\mathbf{Bord}_{123}^{\text{or}}$ are closed oriented 1-manifolds, i.e. disjoint unions of a finite (possibly zero) number of circles.

$$\bigcirc \quad \bigcirc \quad \bigcirc \quad \cdots \quad \bigcirc \quad (2.39)$$

- The 1-morphisms in $\mathbf{Bord}_{123}^{\text{or}}$ are compact oriented 2-dimensional cobordisms between the objects. For instance, the picture below is a 1-morphism from one copy of S^1 to two copies of S^1 .

$$\begin{array}{c} \text{---} \\ \cup \\ \cup \\ \cup \\ \text{---} \end{array} \quad (2.40)$$

Composition works by gluing the manifolds together in the obvious way.

- The 2-morphisms in $\mathbf{Bord}_{123}^{\text{or}}$ are 3-manifolds with corners which are cobordisms between the 1-morphisms. For example, the 3-manifold realizing the 2-morphism

$$\begin{array}{ccc} \begin{array}{c} \text{---} \\ | \\ | \\ | \\ \text{---} \end{array} & \begin{array}{c} \text{---} \\ | \\ | \\ | \\ \text{---} \end{array} & \Rightarrow & \begin{array}{c} \text{---} \\ \cup \\ \cup \\ \cup \\ \text{---} \end{array} \end{array} \quad (2.41)$$

may be visualized as the “fusing together” of the two cylinders over time.

At each level, $\mathbf{Bord}_{123}^{\text{or}}$ is also equipped with a monoidal structure, which is simply given by disjoint union. This definition is only a sketch; for all the technical details, see [27, Section 3.1.2].

2.3 PLCW Complexes

Piecewise-linear CW complexes, or PLCW complexes, are a kind of cellular decomposition of a manifold introduced by Kirillov [17]. They are less general than CW complexes, but more amenable to computations than triangulations. In particular, an analog of the Pachner moves exists for PLCW complexes. We discuss these so-called *elementary moves* below - See Definition 34. Balsam and Kirillov [2] made use of PLCW complexes to rewrite the definition of the Turaev-Viro invariant in PLCW complex terms. For the convenience of the reader, we recall the theory here, following very closely the style of [2]. We shall omit proofs - the full technical details may be found in Kirillov’s paper.

We shall take for granted certain basic notions from piecewise-linear topology, such as the definition of a triangulation, a piecewise-linear manifold, and so on. A standard reference for piecewise-linear topology is the book by Rourke and Sanderson [26].

Remark 31. In what follows, the word “manifold” denotes a compact, oriented, piecewise-linear (PL) manifold. Likewise, the words “map” and “homeomorphism” refer to PL maps and homeomorphisms. Note that in dimensions two and three, the category of PL manifolds is equivalent to the category of topological manifolds.

We make frequent use of the following standard notions:

- $B^n = [-1, 1]^n$ denotes the (closed) n -dimensional PL ball.
- $S^n = B^{n+1}^\bullet$ denotes the n -sphere.
- Δ^n denotes the standard n -simplex.
- A bullet “•” above a topological space denotes its boundary.
- A circle “o” above a topological space denotes its interior.

The basic idea is that a PLCW complex consists of a finite collection of cells, glued together using attaching maps which satisfy various conditions.¹² The

¹²See the full inductive definition of a PLCW complex in [17].

kind of cells used in PLCW complexes are called regular cells, and we define them below.

Definition 32. [17, Defn 3.3] A *regular n -cell* $C \subset \mathbb{R}^N$ is the image of a map

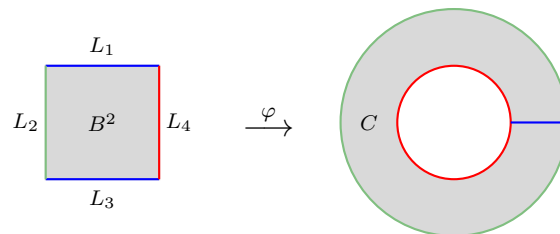
$$\varphi : B^n \rightarrow C$$

such that $\varphi|_{\overset{\circ}{B}^n}$ is injective. The map φ is called a *characteristic map* for C . For a regular cell C , we define

1. its interior $\overset{\circ}{C} := \varphi\left(\overset{\circ}{B}^n\right)$, and
2. its boundary $\overset{\bullet}{C} := \varphi\left(\overset{\bullet}{B}^n\right)$.

The main point in making use of regular cells instead of simplices to construct a PLCW complex is that the characteristic maps are permitted to identify codimension-1 cells on $\overset{\bullet}{B}^n$. They may not, however, identify boundary points arbitrarily, as is the case for CW complexes. For example, the standard CW complex structure on S^2 , consisting of a single 2-cell attached to a single 0-cell, is not possible here.

Example 33. The figure below depicts an example of a regular 2-cell C .



Here φ maps both L_1 and L_3 onto the short horizontal line segment, L_4 onto the inner loop, and L_2 onto the outer loop.

Finally, we may define a PLCW complex. As we mentioned previously, we shall not give the full inductive definition found in [17]. Instead, we follow the simpler description given in [2].

Definition 34. [2, Defn 3.1] A PLCW decomposition of a 2- or 3-dimensional PL manifold M (possibly with boundary) is a cellular decomposition which can be obtained from a triangulation from any of the following three moves $M1$, $M2$, $M3$, and their inverses (if M is 2-dimensional then only $M1$, $M2$ and their inverses).

- **M1 (removing a vertex):** Let v be a vertex (i.e. a regular 0-cell) which has a neighbourhood whose intersection with the 2-skeleton is homeomorphic to the “open book” shown below with $k \geq 1$ leaves; moreover, assume that all leaves in the figure are distinct 2-cells and the two 1-cells are also distinct (i.e. not two ends of the same edge). Then move M1 removes the vertex v and replaces the two 1-cells adjacent to it with a single 1-cell.

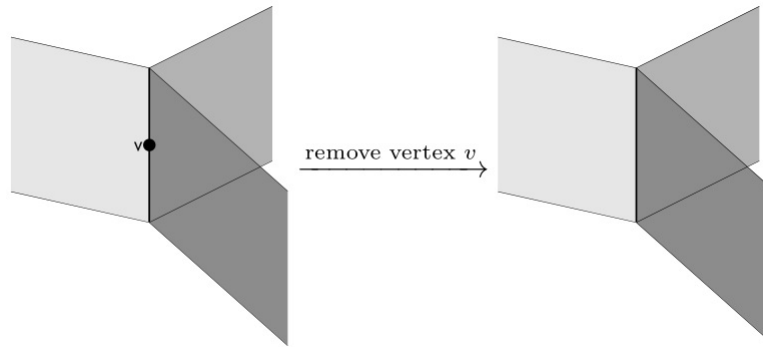


Figure 2.1: Move M1. Image taken from [2, pg. 11].

- **M2 (removing an edge):** Let e be a regular 1-cell which is adjacent to exactly two distinct 2-cells c_1 and c_2 as shown in the figure below. Then the move M2 removes e and replaces the cells c_1, c_2 with a single cell c .

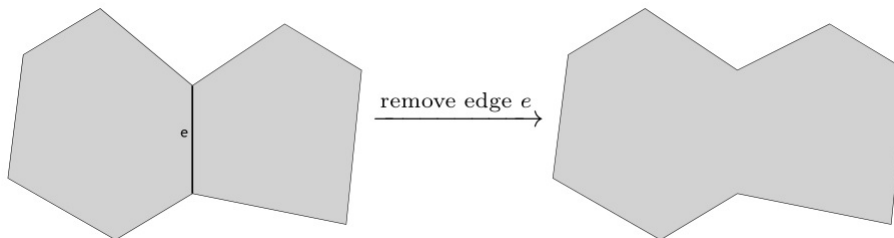


Figure 2.2: Move M2. Image taken from [2, pg. 11].

- **M3 (removing a 3-cell):** Let c be a regular 2-cell which is adjacent to exactly two distinct 3-cells F_1 and F_2 as shown in the figure below. Then the move M3 removes c and replaces the cells F_1, F_2 with a single cell F .

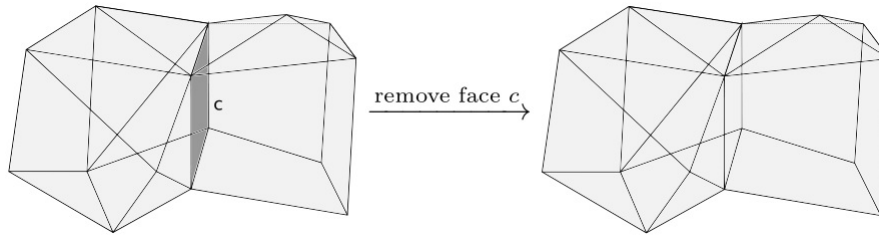


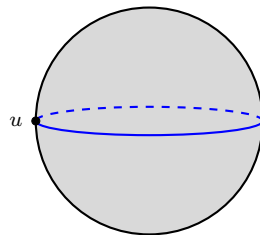
Figure 2.3: Move M3. Image taken from [2, pg. 12].

If M is an oriented 3-manifold (possibly with boundary) and X a PLCW decomposition of M , then we shall frequently write \mathcal{M} for the pair (M, X) , and call \mathcal{M} a *combinatorial manifold* - again following the terminology of Balsam and Kirillov. For 2-dimensional manifolds, we use the term *combinatorial surface*.

Example 35. The circle S^1 admits a PLCW decomposition consisting of a single 0-cell and a single 1-cell via the following sequence of moves, beginning with the triangle.

$$\begin{array}{c} \bullet \\ \circ \\ \bullet \\ \bullet \end{array} \xrightarrow{\text{remove } w} \begin{array}{c} \bullet \\ \circ \\ \bullet \end{array} \xrightarrow{\text{remove } v} \begin{array}{c} \bullet \\ \circ \end{array} \quad (2.42)$$

Similarly, starting with the surface of a tetrahedron, we may obtain the following PLCW decomposition of S^2 .



This PLCW decomposition has one 0-cell, one 1-cell, and two 2-cells. Lastly, we may also obtain a PLCW decomposition of the closed 3-ball consisting of one 0-cell, one 1-cell, two 2-cells, and one 3-cell. This is done by starting with the solid tetrahedron and eliminating vertices and edges, similarly to the case for S^2 .

The following theorem shows that the moves $M1 - M3$ play a role for PLCW decompositions similar to the role that the Pachner moves play for triangulations.

Theorem 36. [2, Thm 3.4] *Let M be a PL 2- or 3-manifold with boundary, and let X be a PLCW decomposition of ∂M . Then*

- (1) X can be extended to a PLCW decomposition Y of M which agree with X on ∂M .
- (2) Any two PLCW decompositions Y_1 and Y_2 of M which agree with X on ∂M can be obtained from each other by a finite sequence of moves $M1, M2, M3$ and their inverses (if M is 2-dimensional, only $M1, M2$ and their inverses are required).

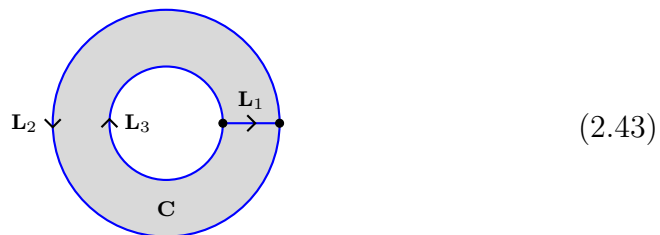
Oriented Cells

Thus far, we have not discussed orientations of cells. Let M be an oriented n -dimensional manifold with boundary and let X be a PLCW decomposition of M . Then any n -cell C in X inherits an orientation from the orientation on M in the obvious way. Notationally, we shall indicate an oriented cell using boldface.

Definition 37. Let \mathbf{C} be an oriented n -cell in X . We define $\partial\mathbf{C}$, called the *boundary* of \mathbf{C} , to be the collection of all oriented $(n - 1)$ -cells on \mathbf{C} , counted with correct multiplicity, and where the orientation on these $(n - 1)$ -cells is the induced orientation coming from the orientation on \mathbf{C} .

When we say that $(n - 1)$ -cells on the boundary of \mathbf{C} are counted “with the correct multiplicity” we mean that an unoriented $(n - 1)$ -cell L may appear twice as the boundary of \mathbf{C} is circumnavigated. If this happens, then each separate occurrence sees L with a different orientation.

Example 38. Consider the following PLCW decomposition of $M = S^1 \times [0, 1] \subset \mathbb{R}^2$. Here M is equipped with the standard counterclockwise orientation.



Here \mathbf{C} is the only 2-cell, and it is likewise oriented counterclockwise. Circumnavigating its boundary, we see that

$$\partial\mathbf{C} = \{\mathbf{L}_1, \mathbf{L}_2, \mathbf{L}_3, \overline{\mathbf{L}}_1\}.$$

The bar indicates that $\overline{\mathbf{L}}_1$ and \mathbf{L}_1 have the opposite orientation. The orientations of the 1-cells are shown as arrows in the diagram.

Lemma 39. [17, Lemma 9.4] *Let M be an oriented PL n -manifold with boundary and X a PLCW decomposition of M . Then*

$$\bigcup_{\mathbf{C}} \partial\mathbf{C} = \left(\bigcup_{\mathbf{D}} \mathbf{D} \right) \cup \left(\bigcup_{F} \mathbf{F} \cup \overline{\mathbf{F}} \right)$$

where

- \mathbf{C} runs over all n -cells of X , each taken with orientation induced by the orientation of X
- \mathbf{D} runs over all $(n - 1)$ -cells such that $\mathbf{D} \subset \partial X$, each taken with orientation induced by the orientation of ∂X
- F runs over all (unoriented) $(n - 1)$ -cells such that $\text{Int}(F) \subset \text{Int}(X)$, and \mathbf{F} and $\overline{\mathbf{F}}$ are the two possible orientations of F .

Chapter 3

123-TQFTs via generators and relations

As discussed in the introduction, the generators-and-relations description of 123-TQFTs, discovered by Bartlett, Douglas, Schommer-Pries, and Vicary [6, 7, 8, 9] is one of the main ingredients of this thesis, and is used in each of the remaining chapters. Thus, in an attempt to make this thesis as self-contained as possible (as well as to establish notational conventions), we review their construction briefly here.

Firstly, we recall the definition of an oriented 123-TQFT.

Definition 40. An oriented 123-TQFT is a symmetric monoidal pseudo-functor

$$Z : \mathbf{Bord}_{123}^{\text{or}} \rightarrow \mathbf{Prof}_{\mathbb{C}}. \quad (3.1)$$

Since $\mathbf{Bord}_{123}^{\text{or}}$ is very complicated, finding symmetric monoidal pseudofunctors out of it is a difficult problem. An analogous situation arises in group theory when trying to find homomorphisms out of some complicated group G . In that setting, the problem is greatly simplified if one can find a presentation for G . The problem is then reduced to defining the homomorphism on the generators and checking that the relations are satisfied. This suggests the naive question: Can one make sense of the notion of a presentation for $\mathbf{Bord}_{123}^{\text{or}}$? The answer turns out to be yes.

Definition 41. [27] A *presentation* \mathcal{G} for a bicategory consists of the following finite collection of data:

- a collection of generating objects;

- a collection of generating 1-morphisms, whose sources and targets are composites of generating objects;
- a collection of generating 2-morphisms, whose sources and targets are composites of generating 1-morphisms;
- a collection of relations, which are equations between composites of the generating 2-morphisms.

Finally, we take the *free quasistrict symmetric monoidal bicategory presented by \mathcal{G}* . That means that we adjoin, at each level, all possible composites that can be formed with the above data using the monoidal bicategory structure. We denote this resulting bicategory by $\mathbf{F}(\mathcal{G})$.

The following definition is taken directly from [8].

Definition 42. [8, Definitions 3,4, and 7] The *anomaly-free modular presentation \mathcal{O}* is the presentation with the following generators and relations:

- Generating object:

$$\circ \tag{3.2}$$

- Generating 1-morphisms:

$$\begin{array}{c} \text{cup} \quad \text{cap} \quad \text{cup} \quad \text{cap} \end{array} \tag{3.3}$$

- Invertible generating 2-morphisms:

$$\begin{array}{cc} \begin{array}{c} \text{cup} \\ \text{cup} \end{array} \xrightleftharpoons[\alpha^{-1}]{\alpha} \begin{array}{c} \text{cup} \\ \text{cap} \end{array} & \begin{array}{c} \text{cup} \\ \text{cap} \end{array} \xrightleftharpoons[\rho^{-1}]{\rho} \text{cylinder} \xrightleftharpoons[\lambda]{\lambda^{-1}} \begin{array}{c} \text{cup} \\ \text{cup} \end{array} \end{array} \tag{3.4}$$

$$\begin{array}{cc} \text{cup} \xrightleftharpoons[\beta^{-1}]{\beta} \begin{array}{c} \text{cup} \\ \text{cap} \end{array} & \text{cylinder} \xrightleftharpoons[\theta^{-1}]{\theta} \text{cylinder} \end{array} \tag{3.5}$$

Noninvertible generating 2-morphisms:

$$\begin{array}{cc} \text{cylinder} \text{cylinder} \xrightleftharpoons[\eta^\dagger]{\eta} \text{X} & \begin{array}{c} \text{cup} \\ \text{cap} \end{array} \xrightleftharpoons[\epsilon^\dagger]{\epsilon} \text{cylinder} \end{array} \tag{3.6}$$

$$\begin{array}{cc} \square \xrightleftharpoons[\nu^\dagger]{\nu} \text{cap} & \begin{array}{c} \text{cup} \\ \text{cap} \end{array} \xrightleftharpoons[\mu^\dagger]{\mu} \text{cylinder} \end{array} \tag{3.7}$$

The relations are as follows:

- (Inverses) Each of the invertible generating 2-morphisms ω satisfies $\omega \circ \omega^{-1} = \text{id}$ and $\omega^{-1} \circ \omega = \text{id}$.
- (Monoidal) The generators in (3.4) obey the pentagon and unit equations:

(3.8)

(3.9)

- (Balanced) The data (3.4) and (3.5) forms a braided monoidal object equipped with a compatible twist:

(3.10)

(3.11)

$$\boxed{\ominus} \xrightarrow{\theta} \ominus = \text{id} \quad (3.12)$$

Note that the second hexagon axiom is redundant in the presence of a twist

- (Rigidity) Write ϕ_l for the following composite (‘left Frobeniusator’):

$$\phi_l := \begin{array}{c} \text{---} \\ \text{---} \\ \text{---} \end{array} \xrightarrow{\eta} \begin{array}{c} \text{---} \\ \text{---} \\ \text{---} \end{array} \xrightarrow{\alpha} \begin{array}{c} \text{---} \\ \text{---} \\ \text{---} \end{array} \xrightarrow{\epsilon} \begin{array}{c} \text{---} \\ \text{---} \\ \text{---} \end{array} \quad (3.13)$$

The left rigidity relation says that ϕ_l is invertible, with the following explicit inverse:

$$\phi_l^{-1} = \begin{array}{c} \text{---} \\ \text{---} \\ \text{---} \end{array} \xrightarrow{\epsilon^\dagger} \begin{array}{c} \text{---} \\ \text{---} \\ \text{---} \end{array} \xrightarrow{\alpha^{-1}} \begin{array}{c} \text{---} \\ \text{---} \\ \text{---} \end{array} \xrightarrow{\eta^\dagger} \begin{array}{c} \text{---} \\ \text{---} \\ \text{---} \end{array} \quad (3.14)$$

Similarly, write ϕ_r for ϕ_l rotated about the z -axis (‘right Frobeniusator’):

$$\phi_r := \begin{array}{c} \text{---} \\ \text{---} \\ \text{---} \end{array} \xrightarrow{\eta} \begin{array}{c} \text{---} \\ \text{---} \\ \text{---} \end{array} \xrightarrow{\alpha^{-1}} \begin{array}{c} \text{---} \\ \text{---} \\ \text{---} \end{array} \xrightarrow{\epsilon} \begin{array}{c} \text{---} \\ \text{---} \\ \text{---} \end{array} \quad (3.15)$$

The right rigidity relation says that ϕ_r is invertible, with the following explicit inverse:

$$\phi_r^{-1} = \begin{array}{c} \text{---} \\ \text{---} \\ \text{---} \end{array} \xrightarrow{\epsilon^\dagger} \begin{array}{c} \text{---} \\ \text{---} \\ \text{---} \end{array} \xrightarrow{\alpha} \begin{array}{c} \text{---} \\ \text{---} \\ \text{---} \end{array} \xrightarrow{\eta^\dagger} \begin{array}{c} \text{---} \\ \text{---} \\ \text{---} \end{array} \quad (3.16)$$

- (Ribbon) The twist satisfies the following equation:

$$\begin{array}{c} \text{---} \\ \text{---} \\ \text{---} \end{array} \xrightarrow{\theta} \begin{array}{c} \text{---} \\ \text{---} \\ \text{---} \end{array} = \begin{array}{c} \text{---} \\ \text{---} \\ \text{---} \end{array} \xrightarrow{\theta} \begin{array}{c} \text{---} \\ \text{---} \\ \text{---} \end{array} \quad (3.17)$$

- (Biadjoint) The data (3.6) expresses $\begin{array}{c} \text{---} \\ \text{---} \\ \text{---} \end{array}$ as the biadjoint of $\begin{array}{c} \text{---} \\ \text{---} \\ \text{---} \end{array}$, while (3.7) expresses $\begin{array}{c} \text{---} \\ \text{---} \\ \text{---} \end{array}$ as the biadjoint of $\begin{array}{c} \text{---} \\ \text{---} \\ \text{---} \end{array}$. That is, the following equations hold, along with daggers and rotations about the x -axis:

$$\begin{array}{c} \text{---} \\ \text{---} \\ \text{---} \end{array} \xrightarrow{\nu} \begin{array}{c} \text{---} \\ \text{---} \\ \text{---} \end{array} \xrightarrow{\mu} \begin{array}{c} \text{---} \\ \text{---} \\ \text{---} \end{array} = \text{id} \quad (3.18)$$

$$\begin{array}{c} \text{cylinder} \end{array} \xrightarrow{\eta} \begin{array}{c} \text{cylinder with green box} \end{array} \xrightarrow{\epsilon} \begin{array}{c} \text{cylinder} \end{array} = \text{id} \quad (3.19)$$

These are 8 equations in total.

- (Pivotality) The following equation holds, together with its rotation about the z -axis:

$$\begin{array}{c} \text{circle} \end{array} \xrightarrow{\epsilon^\dagger} \begin{array}{c} \text{circle with green box} \end{array} \xrightarrow{\mu^\dagger} \begin{array}{c} \text{cylinder with green box} \end{array} \xrightarrow{\mu} \begin{array}{c} \text{circle with green box} \end{array} \xrightarrow{\epsilon} \begin{array}{c} \text{circle} \end{array} = \text{id} \quad (3.20)$$

- (Modularity) The following equation holds, together with its rotation about the z -axis:

$$\begin{array}{c} \text{cylinder} \end{array} \begin{array}{l} \xrightarrow{\epsilon^\dagger} \begin{array}{c} \text{cylinder with green box} \end{array} \xrightarrow{\theta, \theta^{-1}} \begin{array}{c} \text{cylinder with green box} \end{array} \xrightarrow{\epsilon} \begin{array}{c} \text{cylinder} \end{array} \\ \xrightarrow{\mu^\dagger} \begin{array}{c} \text{circle} \end{array} \xrightarrow{\mu} \begin{array}{c} \text{cylinder} \end{array} \end{array} \quad (3.21)$$

- (Anomaly-freeness) The following equation holds:

$$\begin{array}{c} \text{circle} \end{array} \xrightarrow{\epsilon^\dagger} \begin{array}{c} \text{circle with green box} \end{array} \xrightarrow{\theta} \begin{array}{c} \text{circle with green box} \end{array} \xrightarrow{\epsilon} \begin{array}{c} \text{circle} \end{array} = \begin{array}{c} \text{circle} \end{array} \xrightarrow{\text{id}} \begin{array}{c} \text{circle} \end{array} \quad (3.22)$$

Theorem 43. [8, Corollary 1.2] *There is a symmetric monoidal equivalence $\mathbf{Bord}_{123}^{\text{or}} \simeq \mathbf{F}(\mathcal{O})$ between the oriented 3-dimensional bordism bicategory and the bicategory generated by the anomaly-free modular presentation \mathcal{O} .*

Remark 44. It is worth emphasizing that, despite what their notation would suggest, the generators of $\mathbf{F}(\mathcal{O})$ are algebraic, not topological, entities. However, the equivalence in Theorem 43 allows us to treat them as though they were actual surfaces, bordisms, etc. With this in mind, it is worth stating what the implicit geometric realizations of the generators are:¹

- the generating object represents a circle;

¹The description of the geometric realizations given here is a shortened version of the discussion on page 6 of [8].

- the generating 1-morphisms represent the 2-dimensional bordisms naively suggested by the pictured surfaces;
- the invertible generating 2-morphisms represent the invertible 3-dimensional bordisms arising as mapping cylinders of diffeomorphisms of the suggested pictured surfaces;
- the generating 2-morphisms η^\dagger , ϵ , and μ^\dagger represent the bordism implementing the addition of a 2-handle, with η , ϵ^\dagger , and μ representing the corresponding time-reversed bordisms;
- the generating 2-morphisms ν represents the bordism implementing the addition of a 3-handle, with ν^\dagger the time reversed bordism of ν .

Using the above equivalence, oriented 123-TQFTs can, therefore, be found via symmetric monoidal pseudofunctors Z out of $\mathbf{F}(\mathcal{O})$. The following discussion shows how we may do this in practice.²

Let \mathcal{G} be a presentation of a bicategory, and denote by $\mathbf{Fun}(\mathbf{F}(\mathcal{G}), \mathbf{B})$ the symmetric monoidal bicategory of symmetric monoidal homomorphisms from $\mathbf{F}(\mathcal{G})$ to \mathbf{B} , symmetric monoidal transformations between them, and symmetric monoidal modifications between those, in the sense of [27].

Definition 45. [9, Defn 2.1] Given a symmetric monoidal bicategory \mathbf{B} and a presentation \mathcal{G} , denote by $\text{Rep}_{\mathbf{B}}(\mathcal{G})$ the bicategory of \mathcal{G} -structures in \mathbf{B} , defined as follows:

- an object is a strict symmetric monoidal functor $\mathbf{F}(\mathcal{G}) \rightarrow \mathbf{B}$;
- a 1-morphism is a strict symmetric monoidal natural transformation;
- a 2-morphism is a symmetric monoidal modification.

Obviously, the definition above is incredibly terse. For a more detailed description of $\text{Rep}_{\mathbf{B}}(\mathcal{G})$, we refer the reader to the discussion immediately following [9, Defn 2.1].

Theorem 46. [27, Theorems 2.78 and 2.96] *Given a presentation \mathcal{G} , there is a natural equivalence of bicategories*

$$\mathbf{Fun}(\mathbf{F}(\mathcal{G}), \mathbf{B}) \simeq \text{Rep}_{\mathbf{B}}(\mathcal{G}). \quad (3.23)$$

²There is much more which can be said regarding presentations of bicategories - for all the technical details we refer the reader to the PhD thesis of Chris Schommer-Pries [27].

Putting Theorem 43 and Theorem 46 together for the case where $\mathcal{G} = \mathcal{O}$ and $\mathbf{B} = \mathbf{Prof}_{\mathbb{C}}$, we observe that in order to give an oriented 123-TQFT Z , it suffices to give an \mathcal{O} -structure in $\mathbf{Prof}_{\mathbb{C}}$. This is the technique we shall use in this thesis. The following corollary describes the details of the required data.

Corollary 47. *To give an oriented 123-TQFT Z , it suffices to give the following data:*

- (objects) A $\mathbf{Vect}_{\mathbb{C}}$ -enriched category $Z(S^1)$;
- (1-morphisms) For any objects $A, B, C \in Z(S^1)$, vector spaces³

$$Z(\text{cap})_{B \boxtimes C}^A \quad Z(\text{cup})_C^{A \boxtimes B} \quad Z(\text{cap})^A \quad Z(\text{cup})_A$$

- (2-morphisms) A family of linear maps

$$\begin{array}{ccc} Z\left(\text{cap}\right) & \begin{array}{c} \xrightarrow{Z(\rho)} \\ \xleftarrow{Z(\rho^{-1})} \end{array} & Z\left(\text{cylinder}\right) & \begin{array}{c} \xrightarrow{Z(\lambda^{-1})} \\ \xleftarrow{Z(\lambda)} \end{array} & Z\left(\text{cup}\right) \\ \\ Z\left(\text{triple cap}\right) & \begin{array}{c} \xrightarrow{Z(\alpha)} \\ \xleftarrow{Z(\alpha^{-1})} \end{array} & Z\left(\text{triple cup}\right) \\ \\ Z\left(\text{cap}\right) & \begin{array}{c} \xrightarrow{Z(\beta)} \\ \xleftarrow{Z(\beta^{-1})} \end{array} & Z\left(\text{cup}\right) & \begin{array}{c} \xrightarrow{Z(\theta)} \\ \xleftarrow{Z(\theta^{-1})} \end{array} & Z\left(\text{cylinder}\right) \\ \\ Z\left(\text{cylinder}\right) & \begin{array}{c} \xrightarrow{Z(\eta)} \\ \xleftarrow{Z(\eta^\dagger)} \end{array} & Z\left(\text{cup}\right) & \begin{array}{c} \xrightarrow{Z(\epsilon)} \\ \xleftarrow{Z(\epsilon^\dagger)} \end{array} & Z\left(\text{cylinder}\right) \\ \\ Z\left(\text{square}\right) & \begin{array}{c} \xrightarrow{Z(\nu)} \\ \xleftarrow{Z(\nu^\dagger)} \end{array} & Z\left(\text{cap}\right) & \begin{array}{c} \xrightarrow{Z(\mu)} \\ \xleftarrow{Z(\mu^\dagger)} \end{array} & Z\left(\text{cylinder}\right) \end{array}$$

such that all the relations of Definition 42 are satisfied.

Remark 48. In the description of the 2-generator data above, we have omitted explicit mention of the objects of $Z(S^1)$ which would colour the boundary circles. This is simply to make the presentation less cluttered; naturally, the colours will be the same on both the source and target in each case.

³These spaces are required to be functorial in the boundary labels.

In addition to aiding us in the construction of oriented 123-TQFTs, Theorem 46 may also be used to check when two such TQFTs are equivalent; two oriented 123-TQFTs will be equivalent precisely when their \mathcal{O} -structures are equivalent in $\text{Rep}_{\mathbf{Prof}_C}(\mathcal{O})$. For our purposes in this thesis, we shall only require a special case of the general notion, which we record below.

Definition 49. Let Z and Z' be two oriented 123-TQFTs such that

$$Z(S^1) = \mathcal{A} = Z'(S^1).$$

Then Z is equivalent to Z' if for any objects $A, B, C \in \mathcal{A}$ there exists a family of isomorphisms

$$\begin{array}{ccc} Z(\text{pants})_{B \boxtimes C}^A \xrightarrow{\psi_{\text{pants}}} Z'(\text{pants})_{B \boxtimes C}^A & & Z(\text{copants})_C^{A \boxtimes B} \xrightarrow{\psi_{\text{copants}}} Z'(\text{copants})_C^{A \boxtimes B} \\ Z(\text{cup})^A \xrightarrow{\psi_{\text{cup}}} Z'(\text{cup})^A & & Z(\text{cap})_A \xrightarrow{\psi_{\text{cap}}} Z'(\text{cap})_A \end{array}$$

which commute with the actions of the generating 2-morphisms. More precisely, for any generating 2-morphism $\Sigma_s \xrightarrow{\kappa} \Sigma_t$, the diagram

$$\begin{array}{ccc} Z(\Sigma_s) & \xrightarrow{Z(\kappa)} & Z(\Sigma_t) \\ \textcircled{\otimes}_{\sigma} \psi_{\sigma} \downarrow & & \downarrow \textcircled{\otimes}_{\omega} \psi_{\omega} \\ Z'(\Sigma_s) & \xrightarrow{Z'(\kappa)} & Z'(\Sigma_t) \end{array} \quad (3.24)$$

must commute (for all compatible labelings of the boundary circles). Here σ and ω run over all the generating 1-morphisms in Σ_s and Σ_t respectively.

Chapter 4

String-nets

The notion of a string-net was first introduced in the physics literature by Levin and Wen [21] as a physical mechanism for dealing with topological phases of matter. In their model, the vector spaces assigned to surfaces arise as the ground-state of a certain Hamiltonian operator. The same model also appeared in Kitaev's work [19] on quantum computation. Kirillov [18] then described the model in more mathematical terms and showed that, at the level of surfaces (with boundary), the Kitaev-Levin-Wen model was equivalent to the Turaev-Viro¹ model. In this chapter we shall give a detailed review of Kirillov's description, as it is a key ingredient in chapter 5.

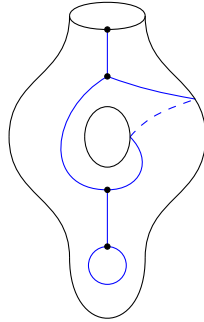
4.1 Basics

Let Σ be an oriented surface, where we allow Σ to be non-compact, have boundary, or have punctures. Let Γ be a finite unoriented graph which is embedded in Σ .² No two distinct vertices may overlap, and no edges are allowed to intersect, apart from at the vertices themselves. If Σ has a boundary, we permit Γ to have univalent³ vertices located on $\partial\Sigma$. The edges meeting such boundary vertices are the only edges permitted to touch $\partial\Sigma$, and they must do so transversely.

¹We describe the Turaev-Viro model in detail in Chapter 6.

²Topologically, this means that each edge of Γ , including the vertices at its endpoints, should be a compact 1-dimensional submanifold with boundary of Σ .

³A vertex is univalent if it has only one incident edge.



(4.1)

Figure 4.1: An example of an embedded graph Γ . Note that, in general, Γ need not be connected.

Next we label the vertices and edges of Γ with data coming from a fixed spherical fusion category \mathcal{A} . Denote the set of vertices of Γ by $V(\Gamma)$ and the set of oriented edges⁴ by $E(\Gamma)$.

Definition 50. A *labeling* of Γ is a triple (l, ϵ, φ) , where

- l assigns to each oriented edge $\mathbf{e} \in E(\Gamma)$ an object $l(\mathbf{e}) \in \mathcal{A}$, satisfying $l(\bar{\mathbf{e}}) = l(\mathbf{e})^*$, where $\bar{\mathbf{e}}$ represents the same underlying edge as \mathbf{e} , but with the opposite orientation;
- ϵ assigns to each interior vertex v a choice of *initial half-edge* ϵ_v incident to v ;
- φ assigns to each interior vertex v a morphism

$$\begin{aligned} \varphi_v &\in \text{Hom}_{\mathcal{A}}(1, l(\mathbf{e}_1) \otimes \cdots \otimes l(\mathbf{e}_n)) \\ &= \langle l(\mathbf{e}_1), \cdots, l(\mathbf{e}_n) \rangle \end{aligned}$$

where the edges incident to v are $\mathbf{e}_1, \cdots, \mathbf{e}_n$, taken in counterclockwise (using the orientation on Σ) order, each with an outgoing orientation, and with \mathbf{e}_1 the initial half-edge.

A labeling is called *simple* if each $l(\mathbf{e})$ is a simple object. Two labelings (l, ϵ, φ) and $(l', \epsilon', \varphi')$ are called *isomorphic* if there exists a family $f = \{f_{\mathbf{e}}\}$ of isomorphisms

$$f_{\mathbf{e}} : l(\mathbf{e}) \rightarrow l'(\mathbf{e})$$

such that

⁴Recall that an oriented edge is an edge plus a choice of orientation (i.e. direction) for that edge.

- f commutes with the operation of changing edge orientation, and
- for each internal vertex v we have, $f \circ \varphi_v = \varphi'_v$. That is,

$$\begin{array}{ccc}
 \begin{array}{c} \boxed{\varphi_V} \\ \downarrow l(\mathbf{e}_1) \quad \downarrow l(\mathbf{e}_n) \\ \boxed{f_{\mathbf{e}_1}} \cdots \boxed{f_{\mathbf{e}_n}} \\ \downarrow l'(\mathbf{e}_1) \quad \downarrow l'(\mathbf{e}_n) \end{array} & = & \begin{array}{c} \boxed{\varphi'_V} \\ \downarrow l'(\mathbf{e}_1) \quad \downarrow l'(\mathbf{e}_n) \end{array} \quad (4.2)
 \end{array}$$

Note that for an internal vertex v , the choice of initial half-edge ϵ_v and vertex label φ_v are linked. So, if two labelings have identical values on all oriented edges (so that $f_{\mathbf{e}} = \text{id}$ for each \mathbf{e}), then each vertex label (and hence each choice of initial half-edge) must also be identical. Later, in Equations 4.8, and 4.9, we shall see situations where the choice of initial half-edge is allowed to change.

We adopt the convention of indicating vertex labels graphically by means of circular coupons. We also indicate initial half-edges by means of a red dot near the relevant vertex.

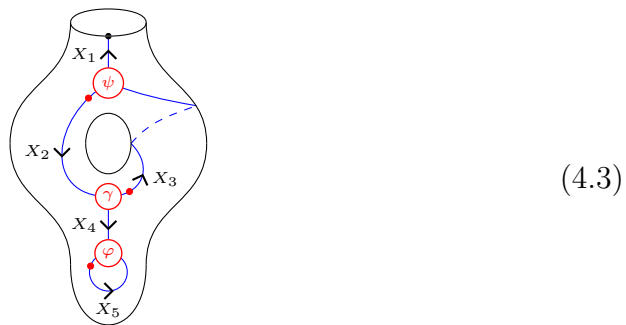


Figure 4.2: A labeling of the graph in Fig. 4.1. Here $\psi \in \langle X_2, X_3^*, X_1 \rangle$, $\gamma \in \langle X_3, X_2^*, X_4 \rangle$, and $\varphi \in \langle X_5, X_5^* \rangle$.

Remark 51. When we are dealing with a labeled graph, we shall usually abuse the notation somewhat and use the symbol Γ to refer to the graph together with its labeling data.

Every labeled graph Γ defines a collection of data associated to the boundary $\partial\Sigma$. We have

- a finite collection of points $B = \{b_1, \dots, b_n\} \subset \partial\Sigma$. These are the positions of the univalent vertices which lie on the boundary;
- a collection $\{V_b\}_{b \in B}$, where each $V_b \in \text{Obj}(\mathcal{C})$ is the label of the edge incident to the vertex at b , taken with an outgoing (i.e. “leaving” Σ) orientation.

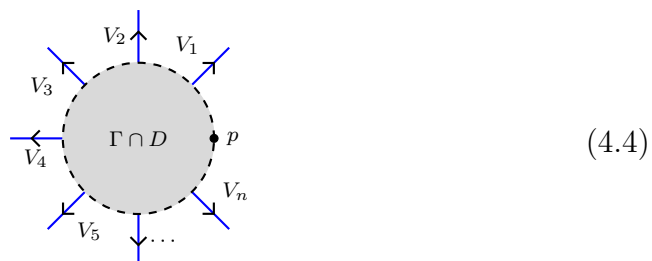
Definition 52. We call this data the *boundary value* of Γ , and denote it by $\mathbf{V} = (B, \{V_b\})$.

We denote by $\text{Graph}(\Sigma, \mathbf{V})$ the collection of all labeled graphs on Σ which have boundary value \mathbf{V} , and by $\text{VGraph}(\Sigma, \mathbf{V})$ the vector space of all formal finite linear combinations of labeled graphs on Σ having boundary value \mathbf{V} .

This definition, though very natural, has the drawback that $\text{VGraph}(\Sigma, \mathbf{V})$ is incredibly large. For instance, merely perturbing one of the edges by a small isotopy results in a completely different labeled graph. We may address this problem by means of an appropriate notion of equivalence between labeled graphs. In the next two sections we describe the notion of evaluating a labeled graph on the disk, and then use this to define the desired equivalence.

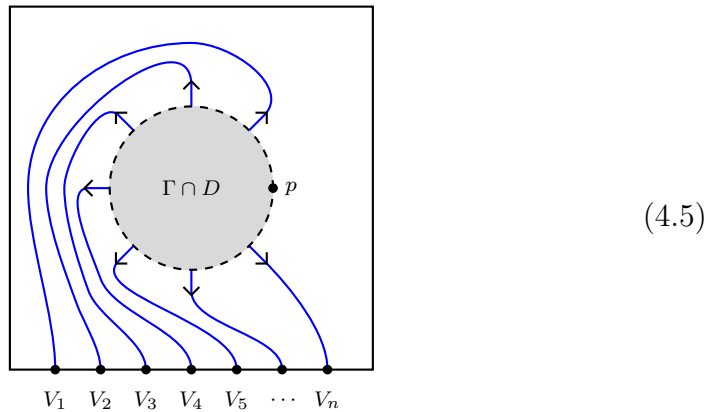
4.2 Evaluation

Let Σ be an oriented surface, as before. Let \mathbf{V} be a choice of boundary value for Σ and let $\Gamma \in \text{Graph}(\Sigma, \mathbf{V})$. An *embedded disk* is pair (D, p) , where $D \subset \Sigma$ is the image of the standard PL disk under some embedding, and $p \in \partial D$ is the image of the point $(1, 0)$ under the embedding. Finally, we impose the additional requirement that the edges of Γ intersect ∂D transversely, that no vertices of Γ lie on ∂D and that no edges of Γ pass through the point p . When no confusion can occur, we shall simply write D when referring to such a disk. The diagram below depicts the portion of Γ which lies in D .



The edges leaving D are labeled V_1, V_2, \dots, V_n , moving from p counterclockwise around ∂D .

Consider the following procedure: Place the contents of $\Gamma \cap D$ inside the unit square, scaling if necessary. Space n points evenly on the bottom edge of the square, and connect the edges leaving D with these points as depicted in the diagram below.



Note that the connecting paths are not permitted to intersect one another. It is immediate that this process results in a tangle diagram with circular coupons, denoted $\langle \Gamma \rangle_D$, in the sense of Section 2.1.2. Clearly, $\langle \Gamma \rangle_D$ is a graphical depiction of a morphism from 1 to $V_1 \otimes \dots \otimes V_n$. Finally, it is immediate that the mapping $\Gamma \mapsto \langle \Gamma \rangle_D$ can be extended linearly to $V\text{Graph}(\Sigma, \mathbf{V})$.

Definition 53. The morphism

$$\langle \Gamma \rangle_D \in \langle V_1, \dots, V_n \rangle \quad (4.6)$$

is called the *evaluation* of Γ in D .

We know that algebraic relations between morphisms in \mathcal{A} are mirrored in various graphical relations between their representative tangle diagrams. For instance, composition is depicted graphically by “merging” the coupons along the adjoining edge - see Equation 2.6. In the case of a labeled graph Γ , we can make sense of such graphical relations only *locally* - that is, in an embedded disk D . The following theorem lists some of the more common and important local relations satisfied by the evaluation.

Theorem 54. [18, Thm 2.3] *Let Γ, Γ' be labeled graphs on Σ and let $D \subset \Sigma$ be an embedded disk. Then the following holds:*

- If $\Gamma \cap D$ consists of a single vertex labeled by $\varphi \in \langle V_1, \dots, V_n \rangle$, then $\langle \Gamma \rangle_D = \varphi$. That is,

$$\text{Diagram} = \varphi \quad (4.7)$$

- If $\Gamma \cap D$ and $\Gamma' \cap D$ have the same underlying graph, and have isomorphic labelings, then $\langle \Gamma \rangle_D = \langle \Gamma' \rangle_D$.
- If $\Gamma \cap D$ and $\Gamma' \cap D$ differ only up to isotopy, then $\langle \Gamma \rangle_D = \langle \Gamma' \rangle_D$.
- Rotating the choice of initial half-edge gives the equality

$$\text{Diagram} = \text{Diagram} \quad (4.8)$$

where

$$\text{Diagram} = \text{Diagram} \quad (4.9)$$

- The following “merging moves” hold.

1. For vertices:

$$\text{Diagram} = \text{Diagram} \quad (4.10)$$

2. For edges:

$$\text{Diagram} = \text{Diagram} \quad (4.11)$$

where $Y = X_1 \otimes \cdots \otimes X_k$.

- Suppose $\varphi = a_1\varphi_1 + a_2\varphi_2$ holds inside $\langle V_1, \dots, V_n \rangle$. Then

$$(4.12)$$

- String-nets are linear with respect to direct sums. That is, if $Y = X_1 \oplus X_2$, then

$$(4.13)$$

Here φ_1 (resp. φ_2) is the composition of φ with the projector $X_1 \oplus X_2 \rightarrow X_1$ (resp. $X_1 \oplus X_2 \rightarrow X_2$), and similarly for ψ_1, ψ_2 .

4.3 Equivalence

Let Σ be an oriented surface, possibly with boundary, and let \mathbf{V} be a choice of boundary value.

Definition 55. Let $\Gamma = c_1\Gamma_1 + \cdots + c_n\Gamma_n \in \text{VGraph}(\Sigma, \mathbf{V})$, where each $\Gamma_i \in \text{Graph}(\Sigma, \mathbf{V})$, and let $D \subset \Sigma$ be any embedded disk. We say that Γ is a *null graph* if

$$\langle \Gamma \rangle_D = 0. \quad (4.14)$$

Definition 56. Let Σ be an oriented surface, possibly with boundary, and let \mathbf{V} be a choice of boundary condition. Then we define the *string-net space* as the quotient

$$H^{string}(\Sigma, \mathbf{V}) := \text{VGraph}(\Sigma, \mathbf{V}) / \text{Null}(\Sigma, \mathbf{V}) \quad (4.15)$$

where $\text{Null}(\Sigma, \mathbf{V})$ is the subspace spanned by null graphs (for all possible embedded disks $D \subset \Sigma$). Elements of $H^{\text{string}}(\Sigma, \mathbf{V})$ are called *string-nets*, and we denote⁵ the equivalence class of Γ by $\langle \Gamma \rangle$.

In other words, two labeled graphs are equivalent if one can be transformed into the other by making repeated local changes, for a multitude of different embedded disks, using the relations in Theorem 54.

Remark 57. When making local changes in practice, it is usually unnecessary to mention the particular embedded disk D (in which those local relations take place) explicitly. Therefore, for expediency, we omit mentioning it⁶ whenever no ambiguity may result.

Many local changes ultimately affect the string-net on a large scale. The following theorem makes this precise, by showing that some of the local relations have global analogs.

Theorem 58. [18, Thm 3.4] *Let $\Gamma, \Gamma' \in H^{\text{string}}(\Sigma, \mathbf{V})$. Then*

- *If Γ and Γ' are isotopic, then $\langle \Gamma \rangle = \langle \Gamma' \rangle$.*
- *If Γ and Γ' have the same underlying graph, and have isomorphic labelings, then $\langle \Gamma \rangle = \langle \Gamma' \rangle$.*
- *The map $\Gamma \mapsto \langle \Gamma \rangle$ respects linearity in vertex and edge colours, in the sense of Theorem 54.*
- *There is a natural isomorphism $H^{\text{string}}(\Sigma_1 \amalg \Sigma_2) \simeq H^{\text{string}}(\Sigma_1) \otimes H^{\text{string}}(\Sigma_2)$.*

Example 59. Let Γ be a string-net on S^2 . Then, it is easy to see that Γ may be moved via isotopy such that the entirety of Γ lay inside some embedded disk D . The graph $\Gamma \cap D$ has no incoming or outgoing edges, and hence $\langle \Gamma \rangle_D$ will simply be a scalar, so that Γ is equivalent to some scalar multiple⁷ of the empty string-net. Hence $H^{\text{string}}(S^2) \cong \mathbb{C}$.

⁵When no confusion can occur, we shall simply write Γ for the class $\langle \Gamma \rangle$, in keeping with Kirillov's conventions.

⁶See Corollary 60 for an example of how we shall routinely state and apply the local relations.

⁷This scalar is independent of the specific way in which Γ was moved into D . This is a consequence of the fact that \mathcal{A} is a *spherical* fusion category. Indeed, this is what motivated Barrett and Westbury to call such categories spherical in the first place - see [3].

The following corollaries illustrate some of the most useful consequences of the local relations.

Corollary 60. [18, Thm 3.4] *The following relations hold inside $H^{string}(\Sigma, \mathbf{V})$.*

$$\sum_{i \in Irr(\mathcal{A})} d_i \begin{array}{c} \begin{array}{c} \dots \\ \swarrow \quad \searrow \\ V_1 \quad \dots \quad V_n \\ \downarrow \\ \alpha^* \\ \downarrow^i \\ \alpha \\ \swarrow \quad \searrow \\ V_1 \quad \dots \quad V_n \end{array} \end{array} = \begin{array}{c} \downarrow \\ \dots \\ \downarrow \end{array} \begin{array}{c} V_1 \\ \dots \\ V_n \end{array} \quad (4.16)$$

$$\begin{array}{c} \circlearrowright \\ \downarrow^X \end{array} = d_X \quad (4.17)$$

$$\begin{array}{c} \bullet \\ \downarrow^i \end{array} = 0 \quad i \in Irr(\mathcal{A}), i \neq 1 \quad (4.18)$$

The shaded area in Equation 4.18 contains any subgraph such that the only edge crossing the boundary is the one labelled by i .

Corollary 61. [18, Corollary 3.5] *Let the unlabeled orange line be defined as follows:*

$$\begin{array}{c} | \\ \text{orange} \end{array} = \sum_{i \in Irr(\mathcal{A})} d_i \begin{array}{c} \downarrow^i \end{array} \quad (4.19)$$

Then the following relations hold:

$$(i) \quad \begin{array}{c} \circlearrowright \\ \text{orange} \end{array} = \mathcal{D}^2 \quad (4.20)$$

$$(ii) \quad \begin{array}{c} \begin{array}{c} \dots \\ \swarrow \quad \searrow \\ V_1 \quad \dots \quad V_n \\ \downarrow \\ \alpha^* \\ \downarrow \\ \alpha \\ \swarrow \quad \searrow \\ V_1 \quad \dots \quad V_n \end{array} \end{array} = \begin{array}{c} \downarrow \\ \dots \\ \downarrow \end{array} \begin{array}{c} V_1 \\ \dots \\ V_n \end{array} \quad (4.21)$$

Chapter 5

The string-net 123-TQFT

In this chapter we use Corollary 47 to define a generators-and-relations oriented 123-TQFT based on string-nets as described in Chapter 4. We take as input a fixed spherical fusion category \mathcal{A} , and denote our yet to be defined 123-TQFT by Z_{SN}^{123} . This construction is new.

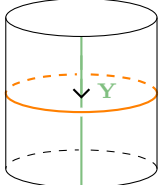
5.1 String-nets and the Drinfel'd center

Let N be a compact oriented surface whose boundary components $\{\partial N_a\}$ are indexed by some finite set A .

Definition 62. A *colouring* of (the boundary components of) N is a choice of object $\mathbf{Y}_a \in Z(\mathcal{A})$ for each $a \in A$. A colouring is called *simple* if each \mathbf{Y}_a is simple.

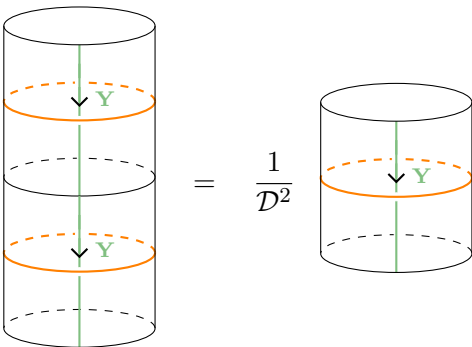
We wish to make precise the notion of a space of string-nets whose boundary values are determined by a colouring. We shall need the following definition.

Definition 63. Let $\mathbf{Y} \in Z(\mathcal{A})$. Then we define the string-net $P_{\mathbf{Y}}$ on $S^1 \times [0, 1]$ by

$$P_{\mathbf{Y}} = \frac{1}{\mathcal{D}^2} \text{ (Diagram) } \quad (5.1)$$


Here the unlabeled orange loop is the same as in Corollary 61 and the green string lies on the arc $\{(-1, 0)\} \times [0, 1]$. The half-braiding between the orange and green strings is the same as in Equation 2.31. Now $P_{\mathbf{Y}}$ is an idempotent,

in the following sense: If we glue $P_{\mathbf{Y}}$ to itself vertically in the obvious way and denote the resulting string-net by $P_{\mathbf{Y}}^2$, then it is easily computed that

$$P_{\mathbf{Y}}^2 = \left(\frac{1}{\mathcal{D}^2}\right)^2 \text{ (two cylinders)} = \frac{1}{\mathcal{D}^2} \text{ (one cylinder)} = P_{\mathbf{Y}}. \quad (5.2)$$


The idea is that one orange loop “slips” past the other via cloaking, and then disappears, producing a factor of \mathcal{D}^2 - see Corollary 61. Finally, we may define the desired string-net space.

Definition 64. Let $\{\mathbf{Y}_a\}$ be a colouring of N , and let $\{\psi_a\}$ be a family of parametrizations

$$\psi_a : S^1 \rightarrow \partial N_a$$

of the boundary components. Then we define $H^{string}(N, \{\psi_a\}, \{\mathbf{Y}_a\})$ to be the space of string-nets on N having the boundary value $(\{\psi_a(-1, 0)\}, \{\mathbf{Y}_a\})$ and which satisfy the additional property that $\Gamma \cdot P_{\mathbf{Y}_a} = \Gamma$ for each $a \in A$, where $\Gamma \cdot P_{\mathbf{Y}_a}$ indicates the operation of gluing¹ $P_{\mathbf{Y}_a}$ onto Γ at ∂N_a .

In other words, a string-net Γ in $H^{string}(N, \{\psi_a\}, \{\mathbf{Y}_a\})$ has a univalent, unlabeled vertex at each point $\psi_a(-1, 0) \in \partial N_a$. The edge incident to each point $\psi_a(-1, 0)$ has an outgoing (i.e. “leaving” the surface) orientation and is labeled by the colour \mathbf{Y}_a associated to ∂N_a . Finally, because gluing on the idempotent $P_{\mathbf{Y}_a}$ leaves Γ unchanged (for each $a \in A$), Γ behaves as though all of the boundary components have been cloaked.

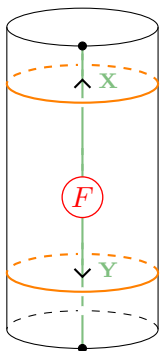
In the following example we investigate the string-net space of the 2-punctured sphere (i.e. the cylinder). This space will occur many times throughout the remainder of the thesis, and serves as a useful setting to exemplify several key techniques for manipulating string-nets.

¹Note that the parametrization is needed in order to make the gluing well-defined.

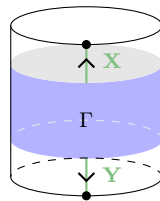
Lemma 65. *Let $N = S^1 \times [0, 1]$, let the boundary circles have the obvious parametrization, and let the top and bottom boundary circles be coloured by \mathbf{X} and \mathbf{Y} respectively. Then we have an isomorphism*

$$\Phi : \text{Hom}_{Z(\mathcal{A})}(1, \mathbf{X} \otimes \mathbf{Y}) \rightarrow H^{\text{string}}(N, \{\mathbf{X}, \mathbf{Y}\})$$

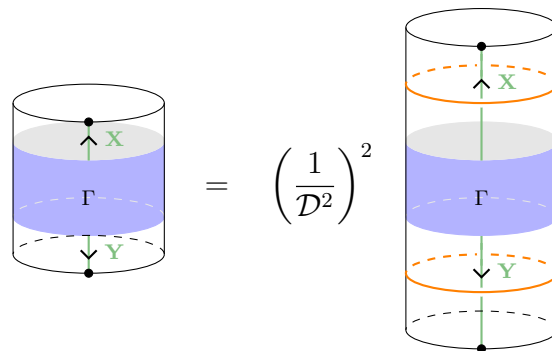
defined by

$$F \xrightarrow{\Phi} \left(\frac{1}{\mathcal{D}^2}\right)^2 \quad \text{(5.3)}$$


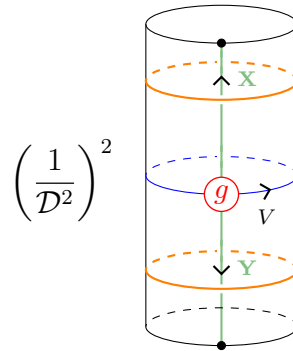
Proof. Firstly, we note that Φ is linear by Equation 4.12. Next we show that Φ is surjective, let $\Gamma \in H^{\text{string}}(N, \{\mathbf{X}, \mathbf{Y}\})$. We may assume without loss of generality that Γ consists of a single connected labeled graph.



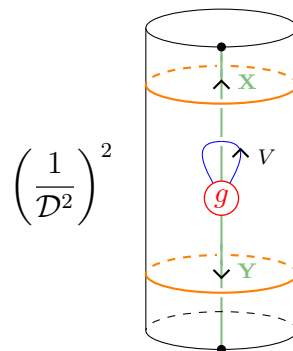
The wires labeled by \mathbf{X} and \mathbf{Y} intersect ∂N at $\{(-1, 0)\} \times \{1\}$ and $\{(-1, 0)\} \times \{0\}$ respectively. The property $\Gamma \cdot P_{\mathbf{X}} = \Gamma = \Gamma \cdot P_{\mathbf{Y}}$ yields the following:

$$= \left(\frac{1}{\mathcal{D}^2}\right)^2$$


Using isotopy, move all the vertices of Γ into an embedded disk D near the “center” of N and then repeatedly apply the vertex and edge merging moves (Equations 4.10 and 4.11) until Γ is in the following form.



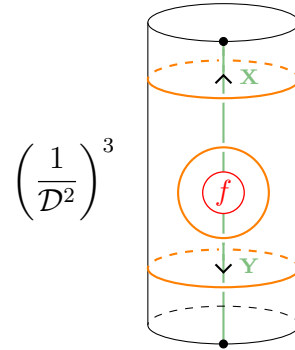
Next, since the top² boundary circle is cloaked, we may move the edge labeled by V past to obtain



We may then merge the little blue loop into the vertex labeled by g , yielding some new vertex label, say f . Lastly, we may “cloak” the vertex labeled by f with orange loop (weighted by $\frac{1}{\mathcal{D}^2}$). Adding such a loop to the string-net is possible since the boundary circles are cloaked.³

²We could equivalently have used the bottom boundary circle.

³We may simply drag the loop past the boundary circles, where it will eventually evaluate to \mathcal{D}^2 .



$$\left(\frac{1}{\mathcal{D}^2}\right)^3$$

Making use of Lemma 26, we observe that

$$\frac{1}{\mathcal{D}^2} \begin{array}{c} \uparrow \mathbf{X} \\ \circlearrowleft f \\ \downarrow \mathbf{Y} \end{array} = P(f) \in \text{Hom}_{Z(\mathcal{A})}(1, \mathbf{X} \otimes \mathbf{Y}).$$

Therefore, by definition, $\Phi(P(f)) = \Gamma$, so that Φ is surjective. Finally, to see that Φ is injective, we combine Theorem 7.3 in [18] with Example 8.6 in [2] to observe that the source and target spaces of Φ have the same (finite) dimension. \square

Remark 66. In many situations (indeed, in virtually all of our remaining calculations in this chapter) it shall be convenient for us to colour the top boundary circle of the cylinder by the dual \mathbf{X}^* . In this case, we have

$$H^{string}(N, \{\mathbf{X}^*, \mathbf{Y}\}) \cong \text{Hom}_{Z(\mathcal{A})}(1, \mathbf{X}^* \otimes \mathbf{Y}) \quad (5.4)$$

$$\cong \text{Hom}_{Z(\mathcal{A})}(\mathbf{X}, \mathbf{Y}) \quad (5.5)$$

where the final isomorphism is the familiar yanking move. Let $F \in \text{Hom}_{Z(\mathcal{A})}(1, \mathbf{X}^* \otimes \mathbf{Y})$, and let \widehat{F} denote the image of F under the yanking move above. Then we define

$$P_{\widehat{F}} = \Phi(F),$$

where Φ is the isomorphism given in the previous lemma. Note that, under this convention, the idempotent in Definition 63 satisfies

$$P_{\mathbf{Y}} = P_{1_{\mathbf{Y}}}.$$

The following corollary, which deals with the situation where the objects colouring the boundary components are simple, shall be particularly useful when we define the actions of the generating 2-morphisms.

Corollary 67. *Let $N = S^1 \times [0, 1]$, let \mathbf{X}^* and \mathbf{Y} be a simple colouring of the top and bottom boundary circle respectively, and let $f \in \text{Hom}_{\mathcal{A}}(1, \mathbf{X}^* \otimes \mathbf{Y})$. Then the following identity holds:*

The diagrammatic equation (5.6) consists of three parts. On the left is a cylinder with a vertical green line representing the identity 1. The top boundary circle is colored orange and labeled \mathbf{X}^* with a downward arrow. The bottom boundary circle is colored orange and labeled \mathbf{Y} with a downward arrow. A red circle containing the letter f is positioned in the middle of the cylinder, with a vertical green line passing through its center. In the middle is an equals sign followed by the fraction $\frac{\delta_{\mathbf{X}, \mathbf{Y}}}{d_{\mathbf{Y}}}$ multiplied by a green loop with an upward arrow and a red circle containing the letter f . On the right is another cylinder with a vertical green line representing the identity 1. The top boundary circle is colored orange and labeled \mathbf{X}^* with a downward arrow. The bottom boundary circle is colored orange and labeled \mathbf{Y} with a downward arrow. The entire diagrammatic equation is labeled (5.6) on the far right.

Proof. As in the proof of Lemma 65, cloak the vertex with a weighted orange loop. This projects f onto the subspace

$$\text{Hom}_{Z(\mathcal{A})}(1, \mathbf{X}^* \otimes \mathbf{Y}) \cong \text{Hom}_{Z(\mathcal{A})}(\mathbf{X}, \mathbf{Y}).$$

Since \mathbf{X} and \mathbf{Y} are simple, we have

$$\frac{1}{\mathcal{D}^2} \begin{array}{c} \downarrow \mathbf{X} \\ \circlearrowleft f \\ \downarrow \mathbf{Y} \end{array} = k \delta_{\mathbf{X}, \mathbf{Y}} \downarrow \mathbf{Y} \quad (5.7)$$

for some scalar k . Taking the trace of both sides of 5.7, we obtain

$$k = \frac{1}{\mathcal{D}^2} \frac{\delta_{\mathbf{X}, \mathbf{Y}}}{d_{\mathbf{Y}}} \begin{array}{c} \uparrow \mathbf{Y} \\ \circlearrowleft f \\ \downarrow \mathbf{Y} \end{array} = \frac{\delta_{\mathbf{X}, \mathbf{Y}}}{d_{\mathbf{Y}}} \begin{array}{c} \circlearrowleft f \\ \uparrow \mathbf{Y} \end{array}. \quad (5.8)$$

□

In the second equality above we use isotopy to expand the orange loop until the trace of f lies entirely inside it. After that, the orange loop evaluates to \mathcal{D}^2 . A similar result holds for the once-punctured sphere. Indeed, if \mathbf{Y} is simple and $f \in \text{Hom}_{\mathcal{A}}(1, \mathbf{Y})$ then we have

$$\begin{array}{c} \text{cup} \\ \downarrow \mathbf{Y} \\ \circlearrowleft f \\ \uparrow \mathbf{Y} \end{array} = \delta_{1, \mathbf{Y}} \circlearrowleft f \begin{array}{c} \text{cup} \\ \downarrow 1 \\ \circlearrowleft \text{id} \\ \uparrow \mathbf{Y} \end{array}. \quad (5.9)$$

Here the isolated vertex label f simply represents a scalar. We leave the proof of 5.9 as a simple exercise for the reader. Analogous techniques to those used for the 2-punctured sphere can be applied to the n -punctured sphere also, and doing so yields the following theorem.

Theorem 68. Let S_n^2 denote the 2-sphere with n boundary circles, let $\{\psi_a\}$ be a parametrization of the boundary circles, and let $\{\mathbf{Y}_a\}$ be a colouring of S_n^2 . Then we have an isomorphism

$$\mathrm{Hom}_{Z(\mathcal{A})}(1, \mathbf{Y}_1 \otimes \cdots \otimes \mathbf{Y}_n) \cong H^{string}(S_n^2, \{\psi_a\}, \{\mathbf{Y}_a\}). \quad (5.10)$$

defined by

$$F \longmapsto \left(\frac{1}{\mathcal{D}^2}\right)^n \quad \begin{array}{c} \text{Diagram: A semi-circular region with a red circle labeled } F \text{ at the top. Green arcs connect } F \text{ to } n \text{ boundary circles. Each boundary circle has a vertical line with a dot at the bottom and a dashed orange circle below it. Labels } \mathbf{Y}_1, \dots, \mathbf{Y}_n \text{ are placed near the boundary circles.} \end{array} \quad (5.11)$$

We end this section by noting that $H^{string}(N, \{\psi_a\}, \{\mathbf{Y}_a\})$ is natural with respect to diffeomorphisms of N . Indeed, if $f : N \rightarrow N'$ is such a diffeomorphism, then there exists a push-forward map

$$f_{\#} : H^{string}(N, \{\psi_a\}, \{\mathbf{Y}_a\}) \xrightarrow{\cong} H^{string}(N', \{\psi'_a\}, \{\mathbf{Y}_a\}) \quad (5.12)$$

where $\psi'_a = f \circ \psi_a$ for each a .

5.2 Generators

We are now ready to define the string-net generators-and-relations 123-TQFT. Firstly, we need a $\mathbf{Vect}_{\mathbb{C}}$ -enriched category assigned to S^1 . We choose this category to be the Drinfel'd center of \mathcal{A} .

$$\circlearrowleft \xrightarrow{Z_{SN}^{123}} Z(\mathcal{A}) \quad (5.13)$$

For objects $\mathbf{X}, \mathbf{Y}, \mathbf{Z} \in Z(\mathcal{A})$, we define

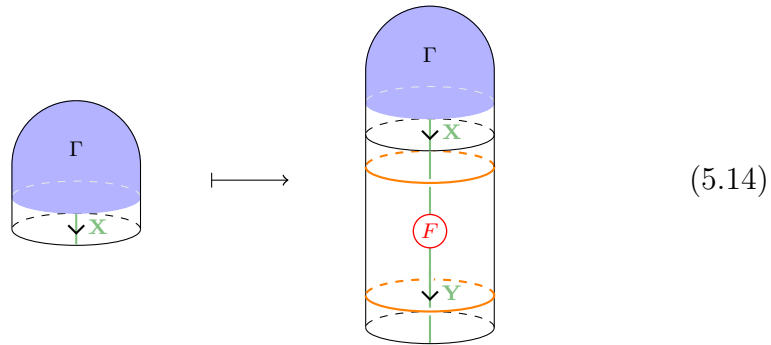
$$\begin{aligned} Z_{SN}^{123}(\ominus)^{\mathbf{X}} &:= H^{string}(\ominus, \mathbf{X}^*), \\ Z_{SN}^{123}(\odot)_{\mathbf{X}} &:= H^{string}(\odot, \mathbf{X}), \\ Z_{SN}^{123}(\bowtie)_{\mathbf{Y} \boxtimes \mathbf{Z}}^{\mathbf{X}} &:= H^{string}(\bowtie, \mathbf{X}^*, \mathbf{Y}, \mathbf{Z}), \\ Z_{SN}^{123}(\heartsuit)_{\mathbf{Z}}^{\mathbf{X} \boxtimes \mathbf{Y}} &:= H^{string}(\heartsuit, \mathbf{X}^*, \mathbf{Y}^*, \mathbf{Z}). \end{aligned}$$

It is easy to see that the assignment of vector spaces above is functorial⁴ in the colours of the boundary circles. We demonstrate this below using \ominus and $\omin�$ as examples.⁵

Given $\widehat{F} \in \text{Hom}_{Z(\mathcal{A})}(\mathbf{X}, \mathbf{Y})$ and $\Gamma \in Z_{SN}^{123}(\ominus)_{\mathbf{X}}$, we use isomorphism 5.4 to construct have a map

$$Z_{SN}^{123}(\ominus)_{\mathbf{X}} \rightarrow Z_{SN}^{123}(\ominus)_{\mathbf{Y}}$$

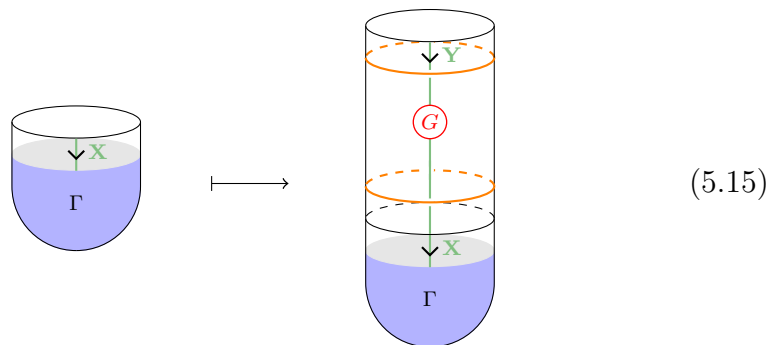
by gluing $P_{\widehat{F}}$ onto Γ in the obvious way. We write $\Gamma \mapsto \Gamma \cdot P_{\widehat{F}}$ and depict it graphically as



Similarly, given $\widehat{G} \in \text{Hom}_{Z(\mathcal{A})}(\mathbf{Y}, \mathbf{X})$ and $\Gamma \in Z_{SN}^{123}(\omin�)_{\mathbf{X}}$, we obtain a map

$$Z_{SN}^{123}(\omin�)_{\mathbf{X}} \rightarrow Z_{SN}^{123}(\omin�)_{\mathbf{Y}}$$

by gluing $P_{\widehat{G}}$ onto Γ , but “upside down” this time. That is, we glue the bottom part of $P_{\widehat{G}}$ onto Γ , instead of the top part like we did for \ominus . This time we write $\Gamma \mapsto P_{\widehat{G}} \cdot \Gamma$, and depict it graphically as



⁴Covariantly in the colours of the “bottom” boundary circles, and contravariantly in the colours of the “top” boundary circles.

⁵The argument is similar for $\omin�$ and $\omin�$.

Next we investigate the vector space assigned to a *composite* of the generating 1-morphisms. Let Σ be such a composite, with m top boundary circles and n bottom boundary circles, labelled by $\mathbf{X}_1, \dots, \mathbf{X}_m$ and $\mathbf{Y}_1, \dots, \mathbf{Y}_n$ respectively. Then, by Definition 2.38, we have

$$Z_{SN}^{123}(\Sigma)_{\mathbf{Y}_1 \boxtimes \dots \boxtimes \mathbf{Y}_n}^{\mathbf{X}_1 \boxtimes \dots \boxtimes \mathbf{X}_m} = \bigoplus_L \bigotimes_{\sigma} Z_{SN}^{123}(\sigma) / \sim \quad (5.16)$$

where the tensor product ranges over all 1-generators σ appearing in the decomposition of Σ , and the direct sum ranges over all possible labellings (with objects in $Z(\mathcal{A})$) of the internal boundary circles. Each generating profunctor $Z_{SN}^{123}(\sigma)$ is computed using the boundary conditions induced from L and the given boundary conditions on the top and bottom circles.

Unpacking Equation 5.16 we see that, in the string-net setting, the relation \sim has the following graphical description :

$$\left(\frac{1}{\mathcal{D}^2}\right)^2 \text{ [Left Diagram]} = \left(\frac{1}{\mathcal{D}^2}\right)^2 \text{ [Right Diagram]} \quad (5.17)$$

In the picture above, $F \in \text{Hom}_{Z(\mathcal{A})}(\mathbf{Y}_1, \mathbf{Y}_2)$, $\Gamma_1 \in Z_{SN}^{123}(\sigma_1)$, and $\Gamma_2 \in Z_{SN}^{123}(\sigma_2)$, where σ_1 and σ_2 are adjacent 1-generators in Σ .

In other words, the relation (in conjunction with 5.4) allows us to move string-net data from σ_1 “isotopically” through the internal boundary circle to σ_2 , as though σ_1 and σ_2 were actually glued together. If we let $\widehat{\Sigma}$ denote the surface obtained by gluing together all the generators in Σ along the internal boundary circles, the relation \sim therefore suggests that string-nets in $Z_{SN}^{123}(\Sigma)_{\mathbf{Y}_1 \boxtimes \dots \boxtimes \mathbf{Y}_n}^{\mathbf{X}_1 \boxtimes \dots \boxtimes \mathbf{X}_m}$ behave exactly like string-nets in $H^{string}(\widehat{\Sigma}, \{\mathbf{X}_1^*, \dots, \mathbf{X}_m^*, \mathbf{Y}_1, \dots, \mathbf{Y}_n\})$. In order to prove this, we shall need the following result.

Lemma 69 (The Lasso lemma). *Suppose that the string-net depicted on the left-hand side of the equation below, where $j \in \mathcal{A}$, occurs locally on an annular region of some surface. Then the following equality holds:*

$$\left(\text{Diagram: a vertical blue line with a downward arrow labeled } j \text{ between two curved lines} \right) = \left(\frac{1}{\mathcal{D}^2} \right)^2 \sum_{r,s} \sqrt{d_r} \sqrt{d_s} \left(\text{Diagram: a vertical blue line with a downward arrow labeled } j \text{ between two curved lines, containing a red circle } i_r \text{ with a rightward arrow } r \text{ and a red circle } p_s \text{ with a leftward arrow } s \text{, and an orange loop labeled } I(j) \text{ in the middle} \right) \quad (5.18)$$

Proof. Using the orange loop and the definition of the half-braiding on $\mathbf{I}(j)$ ⁶ the right-hand side of 5.18 becomes

$$\left(\frac{1}{\mathcal{D}^2} \right)^2 \sum_{k,r,s,l,m} d_k \sqrt{d_r} \sqrt{d_s} \sqrt{d_l} \sqrt{d_m} \left(\text{Diagram: a vertical blue line with a downward arrow labeled } j \text{ between two curved lines, containing a red circle } i_r \text{ with a rightward arrow } r \text{ and a red circle } p_s \text{ with a leftward arrow } s \text{, and an orange loop labeled } I(j) \text{ in the middle. The loop is further divided into segments labeled } k, l, m \text{ with arrows, and contains red circles } \alpha^* \text{ and } \alpha \text{ with arrows } j \text{ passing through them.} \right)$$

Next, using the properties of the injection and projection maps, we obtain

$$\left(\frac{1}{\mathcal{D}^2} \right)^2 \sum_{k,r,s} d_k d_r d_s \left(\text{Diagram: a vertical blue line with a downward arrow labeled } j \text{ between two curved lines, containing a red circle } \alpha^* \text{ with a rightward arrow } r \text{ and a red circle } \alpha \text{ with a leftward arrow } s \text{, and a blue loop labeled } k \text{ in the middle.} \right)$$

⁶For a reminder about the half-braiding and the injection and projection maps i_r and p_s , see Equations 2.34, 2.35, and 2.36.

The claim now follows immediately from the following fact:

$$\left(\frac{1}{\mathcal{D}^2}\right)^2 \sum_{k,r,s} d_k d_r d_s \begin{array}{c} \xrightarrow{r} \\ \alpha \quad \leftarrow \quad \alpha^* \\ \xleftarrow{s} \end{array} = 1$$

□

Finally, we are able to prove the following theorem.

Theorem 70. *Let Σ be a composite of the generating 1-morphisms of $\mathbf{F}(\mathcal{O})$, and let the top- and bottom boundary circles of Σ be labeled by $\mathbf{X}_1, \dots, \mathbf{X}_m$ and $\mathbf{Y}_1, \dots, \mathbf{Y}_n$ respectively. Let $\widehat{\Sigma}$ be the surface obtained by gluing the generators in Σ together along the internal boundary circles. Then we have an isomorphism*

$$Z_{SN}^{123}(\Sigma)_{\mathbf{Y}_1 \boxtimes \dots \boxtimes \mathbf{Y}_n}^{\mathbf{X}_1 \boxtimes \dots \boxtimes \mathbf{X}_m} \cong H^{string}(\widehat{\Sigma}, \{\mathbf{X}_1^*, \dots, \mathbf{X}_m^*, \mathbf{Y}_1, \dots, \mathbf{Y}_n\}). \quad (5.19)$$

Proof. Using Equation 5.16, we define a map

$$\Psi : \bigoplus_L \bigotimes_{\sigma} Z_{SN}^{123}(\sigma) / \sim \rightarrow H^{string}(\widehat{\Sigma}, \{\mathbf{X}_1^*, \dots, \mathbf{X}_m^*, \mathbf{Y}_1, \dots, \mathbf{Y}_n\}) \quad (5.20)$$

and demonstrate that it is an isomorphism. Fix a simple labeling L , and let $\bigotimes_{\sigma} \Gamma_{\sigma} \in \bigotimes_{\sigma} Z_{SN}^{123}(\sigma)$, where $\Gamma_{\sigma} \in Z_{SN}^{123}(\sigma)$ for each 1-generator appearing in the decomposition of Σ . Then we define $\Psi\left(\bigotimes_{\sigma} \Gamma_{\sigma}\right)$ to be the string-net on $\widehat{\Sigma}$ which looks like Γ_{σ} in each component σ , where the string-nets Γ_{σ} have been glued together along internal boundary circles in the obvious way.

We note immediately that Ψ is well-defined and one-to-one because elements are equivalent under \sim precisely when their images are equivalent under isotopy, as well as the usual string-net relations on each 1-generator σ . It remains therefore to show that Ψ is surjective.

Let $\Gamma \in H^{string}(\widehat{\Sigma}, \{\mathbf{X}_1^*, \dots, \mathbf{X}_m^*, \mathbf{Y}_1, \dots, \mathbf{Y}_n\})$. We may, without loss of generality, assume that

- (a) Γ is in general position⁷ with respect to the internal boundary circles (this can always be achieved via isotopy);
- (b) Γ consists of a single connected labeled graph;
- (c) and that there is only a single edge lying across each internal boundary circle. Indeed, if there were multiple edges, we may replace them with a single edge using Lemma 21. We denote by V_{ij} the label of edge lying between σ_i and σ_j . If there are two internal boundary circles between σ_i and σ_j (as in the case of ) , we denote the label of the edge traversing the second internal boundary circle by V'_{ij} .

Having made these assumptions, we apply the Lasso Lemma (Equation 5.18) in an annular neighbourhood of each internal boundary circle. For simplicity, let us assume that the orange loops created this way lie exactly on the boundary circles. We now make several observations:

- (1) We immediately have a colouring of each internal boundary circle. Indeed, the colour of the boundary circle between σ_i and σ_j is $\mathbf{I}(V_{ij})$ (if there is a second circle, its colour is $\mathbf{I}(V'_{ij})$).
- (2) Interposing⁸ the idempotent $P_{\mathbf{I}(V_{ij})}$ (or $\mathbf{I}(V'_{ij})$, when required) at the internal boundary circle between σ_i and σ_j leaves Γ unchanged.

Finally, writing Γ_σ for the part of Γ which lies on σ , we see from observation (2) above that $\bigotimes_{\sigma} \Gamma_\sigma$ determines an element of $Z_{SN}^{123}(\Sigma)_{\mathbf{Y}_1 \boxtimes \dots \boxtimes \mathbf{Y}_n}^{\mathbf{X}_1 \boxtimes \dots \boxtimes \mathbf{X}_m}$. It follows that Ψ is surjective. □

Next we define the actions of the generating 2-morphisms. Note that, by Lemma 5.3 of [9], it suffices to define these actions on spaces where boundary circles have been labeled by *simple* objects in $Z(\mathcal{A})$. We shall therefore make this assumption in the remainder of Chapter 5.

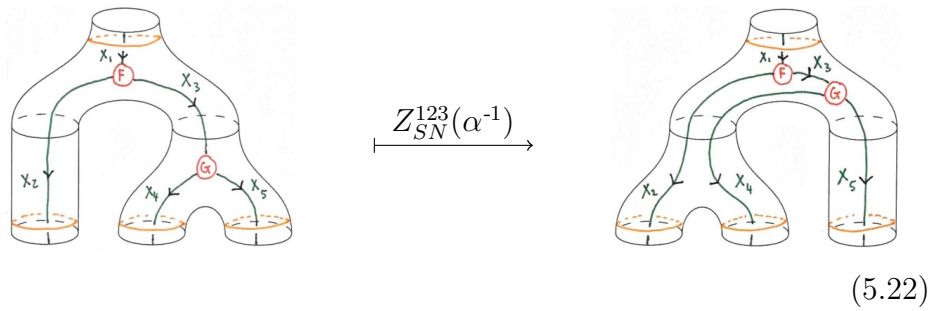
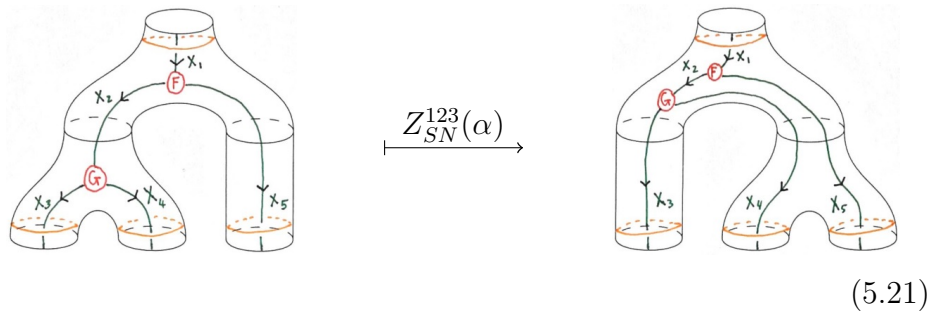
⁷Recall that this means that no vertices of Γ may lie on the internal boundary circles, and edges may only cross them transversely.

⁸Said more simply, adding an orange loop (weighted by $\frac{1}{D^2}$) near any internal boundary circle leaves Γ unchanged.

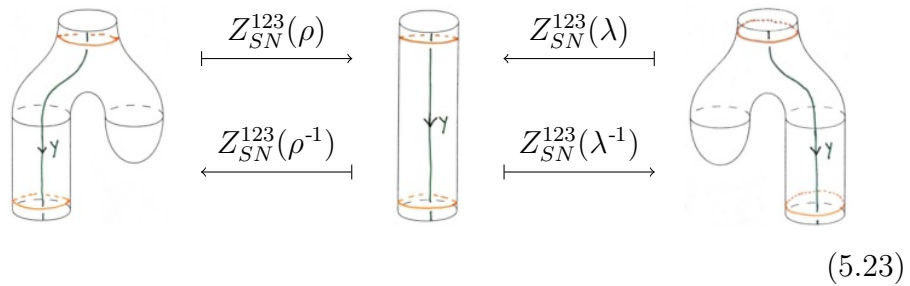
The Invertible 2-Generators

Recall⁹ that each of the invertible 2-generators arise from mapping cylinders of diffeomorphisms of the underlying surfaces. The action of these generators is simply defined to be the pushforward along the associated diffeomorphisms.

- α and α^{-1}



- ρ , λ , and their inverses



⁹See Remark 44.

- θ and θ^{-1}

(5.24)

- β and β^{-1}

(5.25)

(5.26)

The non-invertible 2-generators

We begin with μ , η , and ϵ^\dagger . We write down the actions first, and then give a brief topological motivation for the chosen definition.

(5.27)

$$(5.28)$$

$$(5.29)$$

Each of μ , η , and ϵ^\dagger represent the bordism implementing the removal of a 2-handle. That is, two disks are deleted and an annulus glued into their place. Since the annulus has nonzero genus, acting in this way on a string-net space may introduce an ambiguity. For example, in the case of ϵ^\dagger , should the \mathbf{Y} strand be moved to the left or to right before removing the 2-handle? In order to fix the ambiguity, we are therefore required to add a cloaking element along the center of the glued annulus.¹⁰

We proceed next to μ^\dagger , η^\dagger , and ϵ . As before, we give the actions first and then provide a brief motivation.

$$(5.30)$$

¹⁰As an additional topological motivation we add that, in Reshetikhin-Turaev (RT) theory, it is known that the cloaking element indicates 2-handle attachment. Of course, this is precisely what the 2-generators themselves do - see Remark 44. One subtle distinction is that, in our case, the simple objects labeling the cloaking element live in \mathcal{A} .

$$\begin{array}{c}
 \text{Cylinder with } f, g, Y, j \\
 \xrightarrow{Z_{SN}^{123}(\mu^\dagger)} \\
 \begin{array}{c}
 \text{Cup } f, Y \\
 \text{Cup } g, Y
 \end{array}
 \end{array}
 \quad \delta_{1,j} \quad (5.31)$$

$$\begin{array}{c}
 \text{Genus-2 surface with } f, g, Y_i \\
 \xrightarrow{Z_{SN}^{123}(\eta^\dagger)} \\
 \begin{array}{c}
 \text{Cylinder } f, Y_i \\
 \text{Cylinder } g, Y_i
 \end{array}
 \end{array}
 \quad \delta_{j,1} \quad (5.32)$$

For each of μ^\dagger , η^\dagger , and ϵ , these 2-morphisms represent the bordism implementing the addition of a 2-handle. That is, an annular region of the surface is excised and disks glued on in its place. Intuitively speaking, when this process acts upon an element of the string-net space, one could say that because the annulus has nonzero genus, it is not always possible to “evacuate” strings safely before the annular region is removed. We interpret this as the trapped strings getting cut - in the definitions, we indicated this via the Kronecker delta.

Finally, for ν and ν^\dagger , the source and target spaces are each isomorphic to \mathbb{C} , so in this case the actions are easier to guess.

$$\square \xrightarrow{Z_{SN}^{123}(\nu)} \frac{1}{\mathcal{D}^2} \text{Sphere} \quad \text{Sphere} \xrightarrow{Z_{SN}^{123}(\nu^\dagger)} \square \quad (5.33)$$

The diagrams on the source and target (for ν or ν^\dagger) represent the trivial string-nets on their respective spaces. The factor $\frac{1}{\mathcal{D}^2}$ appearing above is difficult to motivate from merely the topology represented by ν - it is forced upon us by the adjunction relations.

5.3 Relations

In this section we prove the main result of this chapter, namely, that Z_{SN}^{123} defines an oriented 123-TQFT.

Theorem 71. *The actions of Z_{SN}^{123} on the generating 2-morphisms satisfy the relations of Definition 42, and hence Z_{SN}^{123} defines an oriented 123-TQFT.*

Proof. We check the relations one at a time.

- Monoidal: The monoidal relations are trivially satisfied, and are left as an easy exercise for the reader.
- Adjunction: For the ν - μ adjunction, both of the following composites, as well as their rotations about the x -axis, are clearly equal to the identity.

$$\begin{array}{c}
 \text{Cup with } 1 \text{ and } id \\
 \xrightarrow{Z_{SN}^{123}(\nu)} \frac{1}{\mathcal{D}^2} \left(\text{Cup with } 1 \text{ and } id \cdot \text{Sphere with line} \right) \\
 \xrightarrow{Z_{SN}^{123}(\mu)} \frac{\mathcal{D}^2}{\mathcal{D}^2} \left(\text{Sphere with line} \cdot \text{Cylinder with } 1 \text{ and } id \right) \\
 \text{Cylinder with } 1 \text{ and } id
 \end{array} \quad (5.34)$$

Note that the appearance of the additional \mathcal{D}^2 factor in the second step is owing to the action of μ creating an orange loop, which is able to slide off.

$$\begin{array}{c}
 \text{Cylinder with } 1 \text{ and } id \\
 \xrightarrow{Z_{SN}^{123}(\mu^\dagger)} \left(\text{Cup with } 1 \text{ and } id \cdot \text{Sphere with line} \right) \\
 \xrightarrow{Z_{SN}^{123}(\nu^\dagger)} \text{Cup with } 1 \text{ and } id
 \end{array} \quad (5.35)$$

Similarly, for the η - ϵ adjunction the composite

$$\text{Diagram 1} \xrightarrow{Z_{SN}^{123}(\eta)} \sum_j d_j \text{Diagram 2} \xrightarrow{Z_{SN}^{123}(\epsilon)} \text{Diagram 3} \quad (5.36)$$

equals the identity. Notice that ϵ acts by cutting the loop. The daggered version of the above is given by

$$\text{Diagram 1} \xrightarrow{Z_{SN}^{123}(\epsilon^\dagger)} \sum_j d_j \text{Diagram 2} = \sum_j d_j \text{Diagram 3} \quad (5.37)$$

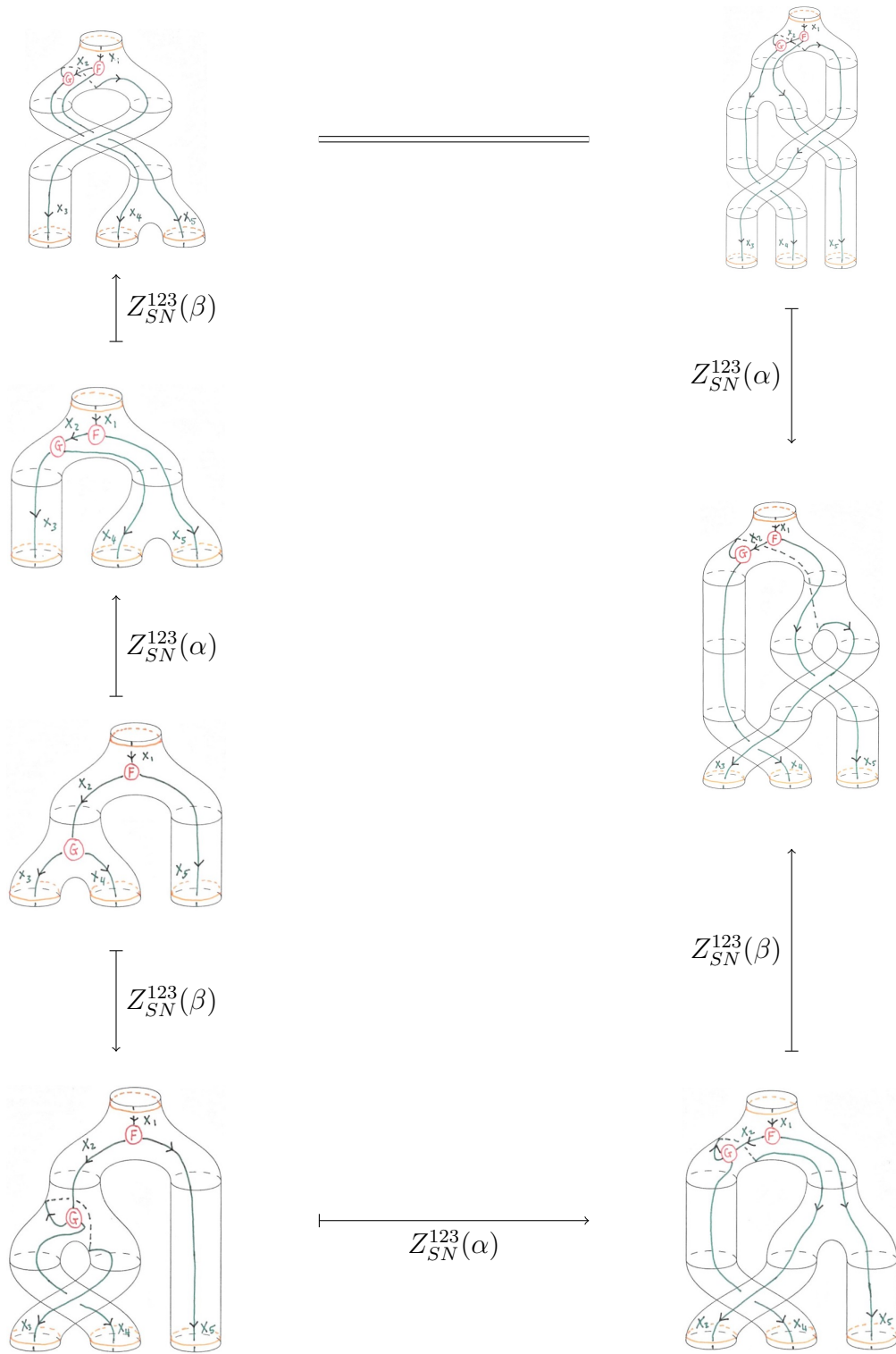
The equality above follows from cloaking. Finally, acting by η^\dagger cuts the loop, so that the composite equals to the identity. The same holds true for versions of the above relations rotated about the x -axis.

- Ribbon: Follows trivially from isotopy.
- Pivotality:

$$\text{Diagram 1} \xrightarrow{Z_{SN}^{123}(\epsilon^\dagger)} \sum_j d_j \text{Diagram 2} \xrightarrow{Z_{SN}^{123}(\mu^\dagger)} \text{Diagram 3} \xrightarrow{Z_{SN}^{123}(\mu)} \text{Diagram 4} \xrightarrow{Z_{SN}^{123}(\epsilon)} \text{Diagram 5} \quad (5.38)$$

This composite clearly equals the identity, and the same is true of its rotation about the z -axis.

- Balanced: The following diagram commutes:



(5.39)

Next we check that the twist is compatible.

$$\begin{array}{ccc}
 \text{Diagram 1} & \xrightarrow{Z_{SN}^{123}(\theta)} & \text{Diagram 2} \\
 \downarrow Z_{SN}^{123}(\beta)^2 & & \parallel \\
 \text{Diagram 3} & \xrightarrow{Z_{SN}^{123}(\theta), Z_{SN}^{123}(\theta)} & \text{Diagram 4}
 \end{array}$$

(5.40)

Note that in the bottom horizontal step we applied a twist to each “leg”, together with the fact that interchanging twice equals the identity. Finally, relation 3.12 is trivial.

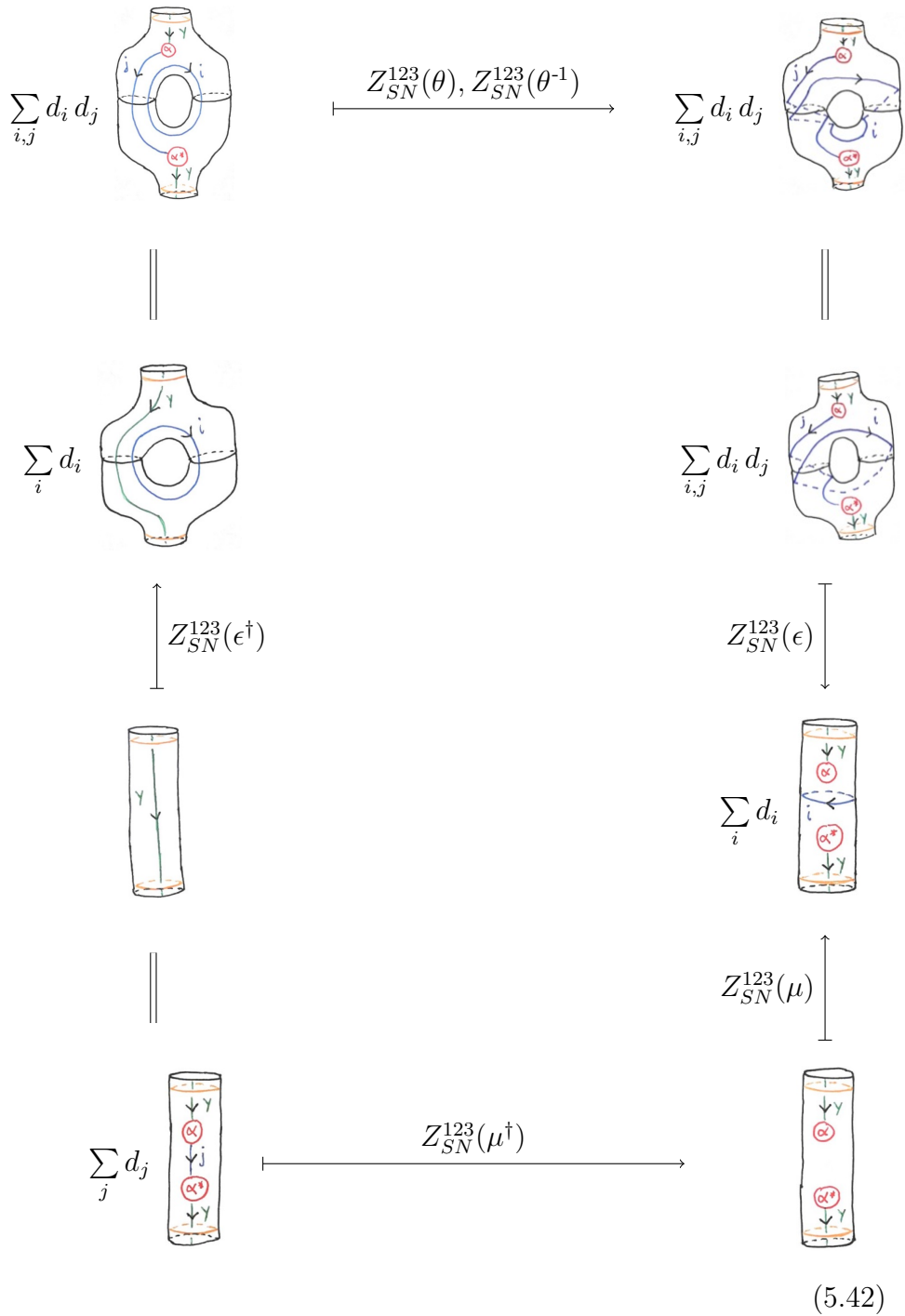
- Rigidity: It is clear that the composite $\phi_l = \epsilon \circ \alpha \circ \eta$ defined in 3.13 is invertible, since the loop created by η is simply cut by ϵ . The remaining rigidity compositions are similar.
- Anomaly-freeness:

$$\text{Diagram 1} \xrightarrow{Z_{SN}^{123}(\epsilon^\dagger)} \sum_i d_i \text{Diagram 2} \xrightarrow{Z_{SN}^{123}(\theta)} \sum_i d_i \text{Diagram 3} \xrightarrow{Z_{SN}^{123}(\epsilon)} \text{Diagram 4}$$

(5.41)

This composite clearly equals the identity.

- Modularity: Clearly, the following diagram commutes.



□

Chapter 6

Extended Turaev-Viro Theory

In this chapter we review in detail the technology Balsam and Kirillov used (see [2]) to formulate Turaev-Viro theory as an extended TQFT.

6.1 Preliminaries

Recall that the generating 1-morphisms (Defined in 3.3) are compact oriented surfaces with boundary. In their paper, Balsam and Kirillov do not define the Turaev-Viro invariant on surfaces with boundary directly, but instead use the equivalent notion of so-called “extended surfaces”, which we define below.

6.1.1 Extended Surfaces

Let $D^2 = [-1, 1] \times [-1, 1]$ denote the standard (PL) disk, and let p_0 be the point $(1, 0)$ on the boundary ∂D^2 .

Definition 72. A *framed embedded disk* in a closed oriented surface N is the image of a homeomorphism

$$\psi : D^2 \rightarrow N \tag{6.1}$$

together with the point $p = \psi(p_0)$.

Definition 73. An *extended surface* N is a closed oriented surface together with a finite collection of disjoint framed embedded disks. We denote the collection of embedded disks by $D(N)$.¹

¹Note that we also permit there to be no embedded disks.

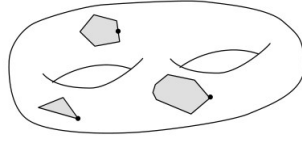


Figure 6.1: An example of an extended surface. The marked points are also shown. This image was taken from [2, pg. 22].

For brevity, we shall omit the word “framed” whenever possible when mentioning embedded disks. It is easy to see that there is a one-to-one correspondence between extended surfaces and surfaces with boundary. Given a surface with boundary, one obtains an extended surface by choosing a parametrization of each boundary circle (which is equivalent, up to homotopy, to choosing a marked point on each boundary circle) and then gluing on copies of the disk. Conversely, given an extended surface, one obtains a surface with boundary simply by deleting the interior of each embedded disk.

Let \mathcal{A} be a spherical fusion category, with $Z(\mathcal{A})$ its Drinfel’d center.

Definition 74. A *colouring* of an extended surface N is a choice of object $\mathbf{Y}_a \in Z(\mathcal{A})$ for each embedded disk $D_a \in D(N)$. A colouring is called *simple* if each \mathbf{Y}_a is simple.

The above definition is motivated by the fact that we are building up to a definition of a Turaev-Viro 123-TQFT. In such a setting, the embedded disks (i.e. the “boundary components”) of Σ are decorated by objects in the category assigned to S^1 . That category is $Z(\mathcal{A})$.

Definition 75. Let N be an extended surface. A PLCW complex Δ is a PLCW decomposition of N if

- Δ is a PLCW decomposition of the underlying closed surface N ,
- the interior of each embedded disk $D_a \in D(N)$ is a 2-cell in Δ , and
- if each marked point $p_a = \psi_a(1, 0)$ is a 0-cell in Δ .

An extended surface together with a choice of PLCW decomposition is called a *extended combinatorial surface*.

We shall write \mathcal{N} for the pair (N, Δ) . We end this section with the following definition.

Definition 76. Let $(\mathcal{N}, \{\mathbf{Y}_a\})$ be a coloured extended combinatorial surface, with PLCW decomposition Δ . We define the *dual surface* of $(\mathcal{N}, \{\mathbf{Y}_a\})$ by $(\overline{\mathcal{N}}, \{\mathbf{Y}_a^*\})$, where $\overline{\mathcal{N}}$ is the same underlying surface (and the same PLCW decomposition) as \mathcal{N} but with opposite orientation, and where $\{\mathbf{Y}_a^*\}$ is the colouring which assigns the dual object of the original colouring to each embedded disk.

6.1.2 The State Space

Let $(\mathcal{N}, \{\mathbf{Y}_a\})$ be a coloured extended combinatorial surface, with Δ its PLCW decomposition. Note that \mathbf{Y}_a need not be simple. Denote by E the set of oriented edges (1-cells) of Δ . Recall that an oriented edge \mathbf{e} is an edge e plus a choice of orientation for e . We denote by $\bar{\mathbf{e}}$ the oriented edge with the same underlying edge e , but with the opposite orientation.

Definition 77. A *labeling* of Δ is a map $l : E \rightarrow \text{Ob}(\mathcal{A})$ which assigns to every oriented edge \mathbf{e} of Δ an object $l(\mathbf{e}) \in \text{Ob}(\mathcal{A})$ such that $l(\bar{\mathbf{e}}) = l(\mathbf{e})^*$. A labeling is called *simple* if for every oriented edge \mathbf{e} , $l(\mathbf{e})$ is a simple object. Finally, two labellings l_1 and l_2 are called equivalent if $l_1(\mathbf{e}) \simeq l_2(\mathbf{e})$ for every $\mathbf{e} \in E$.

For a fixed simple labeling l of \mathcal{N} , we define

$$H_{TV}(\mathcal{N}, \{\mathbf{Y}_a\}, l) := \bigotimes_{\mathbf{C}} H(\mathbf{C}, l) \quad (6.2)$$

where the tensor product runs over all 2-cells of Δ , including the embedded disks, and

$$H(\mathbf{C}, l) = \begin{cases} \langle F(\mathbf{Y}_a), l(\mathbf{e}_1), \dots, l(\mathbf{e}_n) \rangle & \text{if } \mathbf{C} \text{ is the embedded disk } D_a \\ \langle l(\mathbf{e}_1), \dots, l(\mathbf{e}_n) \rangle & \text{if } \mathbf{C} \text{ is an ordinary 2-cell} \end{cases} \quad (6.3)$$

Here F is the forgetful functor $F : Z(\mathcal{A}) \rightarrow \mathcal{A}$, and $\mathbf{e}_1, \dots, \mathbf{e}_n$ are the oriented edges which run counterclockwise around the boundary of \mathbf{C} . We insist that, if \mathbf{C} is one of the embedded disks, then the edges must start at the marked point. If \mathbf{C} is an ordinary 2-cell, the choice of starting point may be chosen arbitrarily. We illustrate this situation with the following diagrams. The diagram on the left shows the embedded disk case, and the diagram on the right shows the case of an ordinary 2-cell. For each case, the space $H(\mathbf{C}, l)$ is also shown.

$$\langle F(\mathbf{Y}_a), l(\mathbf{e}_1), \dots, l(\mathbf{e}_n) \rangle \quad \langle l(\mathbf{e}_1), \dots, l(\mathbf{e}_n) \rangle \quad (6.4)$$

Remark 78. If \mathbf{C} is an ordinary 2-cell, then the space $H(\mathbf{C}, l)$ does not, up to a canonical isomorphism,² depend on the choice of starting point but only on the cyclic order of the boundary edges $l(\mathbf{e}_1), \dots, l(\mathbf{e}_n)$. Therefore, in practical computations, we shall simply choose whichever starting point is most convenient (being careful to be consistent).

Finally, we define the state space to be

$$H_{TV}(\mathcal{N}, \{\mathbf{Y}_a\}) = \bigoplus_l H_{TV}(\mathcal{N}, \{\mathbf{Y}_a\}, l) = \bigoplus_l \bigotimes_{\mathbf{C}} H(\mathbf{C}, l), \quad (6.5)$$

where l ranges over all simple labelings, up to equivalence. If $\mathcal{N} = \emptyset$ we shall, for technical reasons, set $H_{TV}(\emptyset) = \mathbb{C}$. If \mathbf{C} is an oriented 2-cell in Δ , then we have a canonical isomorphism

$$H(\overline{\mathbf{C}}, l) \cong H(\mathbf{C}, l)^*, \quad (6.6)$$

where $\overline{\mathbf{C}}$ is the same underlying 2-cell as \mathbf{C} , but with the opposite orientation. It is easy to see that

$$H(\overline{\mathbf{C}}, l) = \langle X_n^*, \dots, X_1^* \rangle. \quad (6.7)$$

To see that $H(\overline{\mathbf{C}}, l) \cong H(\mathbf{C}, l)^*$, recall that we have a non-degenerate pairing³ between $H(\mathbf{C}, l)$ and $H(\overline{\mathbf{C}}, l)$. It is easy to see that this property applies to all of \mathcal{N} . That is,

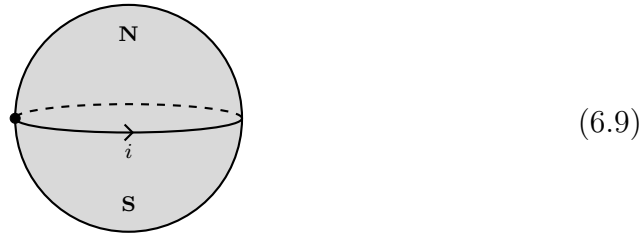
$$H_{TV}(\overline{\mathcal{N}}, \{\mathbf{Y}_a^*\}) \cong H_{TV}(\mathcal{N}, \{\mathbf{Y}_a\})^*. \quad (6.8)$$

In other words, the state space of the dual surface is isomorphic to the dual of the state space of the original surface.

²This is the yanking move isomorphism - see 2.20

³See Equation 2.24.

Example 79. Let Δ denote the PLCW decomposition of S^2 (with its usual orientation) consisting of one 0-cell, one 1-cell, and two 2-cells. The 2-cells are \mathbf{N} and \mathbf{S} , and represent the Northern and Southern hemispheres respectively. Let $\mathcal{S}^2 = (S^2, \Delta)$, and let l be a simple labeling of Δ , assigning the simple object $i \in \mathcal{A}$ to the lone edge.

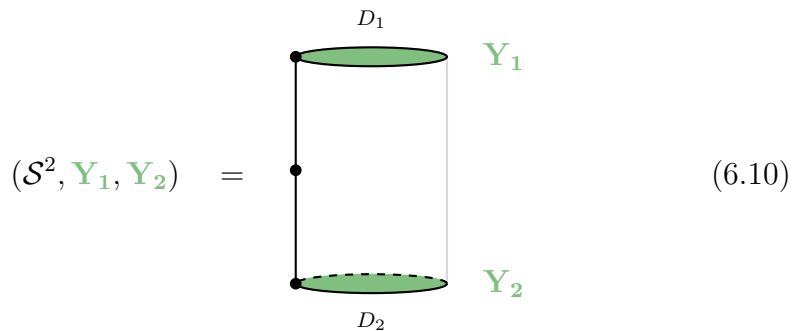


We compute:

$$\begin{aligned} H_{TV}(\mathcal{S}^2) &= \bigoplus_l H(\mathbf{N}, l) \otimes H(\mathbf{S}, l) \\ &= \bigoplus_{i \in \text{Irr}(\mathcal{A})} \langle i \rangle \otimes \langle i^* \rangle \\ &= \langle 1 \rangle \otimes \langle 1^* \rangle \\ &= \mathbb{C}. \end{aligned}$$

Remark 80. Above we made use of the fact that $\langle i \rangle = 0$ unless $i = 1$ for i a simple object. When this happens in future calculations, we shall simply label such edges with 1 from the start.

Example 81. Let S_2^2 denote the 2-sphere with two embedded disks D_1, D_2 , coloured by objects $\mathbf{Y}_1, \mathbf{Y}_2 \in Z(\mathcal{A})$ respectively. Let Δ denote the PLCW decomposition of S_2^2 depicted below and set $\mathcal{S}_2^2 = (S_2^2, \Delta)$.



We compute the state space $H_{TV}(\mathcal{S}_2^2, \mathbf{Y}_1, \mathbf{Y}_2)$. By definition,

$$H_{TV}(\mathcal{S}_2^2, \mathbf{Y}_1, \mathbf{Y}_2) = \bigoplus_l H_{TV}(\mathcal{S}_2^2, \mathbf{Y}_1, \mathbf{Y}_2, l), \quad (6.11)$$

where the sum runs over all simple labelings of \mathcal{S}_2^2 . Let l be the simple labeling shown below:

$$(\mathcal{S}_2^2, \mathbf{Y}_1, \mathbf{Y}_2, l) = \begin{array}{c} \begin{array}{c} U_1 \\ \bullet \text{---} \bullet \\ \uparrow \\ \bullet \\ \downarrow \\ \bullet \\ \downarrow \\ \bullet \\ U_2 \end{array} \begin{array}{c} \mathbf{Y}_1 \\ \mathbf{Y}_2 \end{array} \end{array} \quad (6.12)$$

There are three 2-cells, shown below with their state spaces.

$$\begin{array}{ccc} \begin{array}{c} \mathbf{Y}_1 \\ \bullet \text{---} \bullet \\ U_1 \end{array} & \begin{array}{c} U_1 \\ \bullet \text{---} \bullet \\ \uparrow \quad \uparrow \\ \bullet \quad \bullet \\ \downarrow \quad \downarrow \\ \bullet \quad \bullet \\ U_2 \end{array} & \begin{array}{c} \bullet \text{---} \bullet \\ U_2 \quad \mathbf{Y}_2 \end{array} \\ \langle \mathbf{Y}_1, U_1 \rangle & \langle i_1, U_1^*, i_1^*, i_2, U_2^*, i_2^* \rangle & \langle \mathbf{Y}_2, U_2 \rangle \end{array}$$

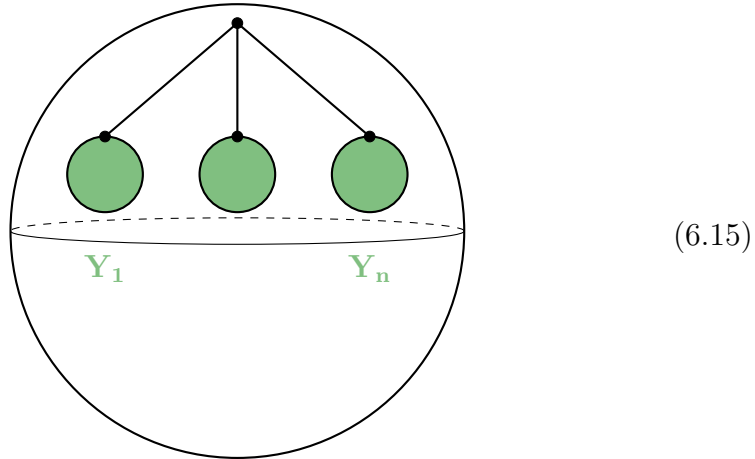
Therefore,

$$H_{TV}(\mathcal{S}_2^2, \mathbf{Y}_1, \mathbf{Y}_2, l) = \langle i_1, U_1^*, i_1^*, i_2, U_2^*, i_2^* \rangle \otimes \langle \mathbf{Y}_1, U_1 \rangle \otimes \langle \mathbf{Y}_2, U_2 \rangle \quad (6.13)$$

and thus

$$H_{TV}(\mathcal{S}_2^2, \mathbf{Y}_1, \mathbf{Y}_2) = \bigoplus_{i_1, i_2, U_1, U_2} \langle i_1, U_1^*, i_1^*, i_2, U_2^*, i_2^* \rangle \otimes \langle \mathbf{Y}_1, U_1 \rangle \otimes \langle \mathbf{Y}_2, U_2 \rangle. \quad (6.14)$$

This calculation can be generalized to S_n^2 (See [2, Example 7.2]), the sphere with n embedded disks. Choose the colouring $\{\mathbf{Y}_a\}$ and PLCW decomposition Δ shown below.



(6.15)

Writing \mathcal{S}_n^2 for (S_n^2, Δ) , we have

$$H_{TV}(\mathcal{S}_n^2, \mathbf{Y}_1, \dots, \mathbf{Y}_n) = \bigoplus_{\substack{i_1, \dots, i_n \\ U_1, \dots, U_n}} \langle i_1, U_1^*, i_1^*, \dots, i_n, U_n^*, i_n^* \rangle \otimes \langle \mathbf{Y}_1, U_1 \rangle \otimes \dots \otimes \langle \mathbf{Y}_n, U_n \rangle \quad (6.16)$$

Though the state space is independent of the choice of simple labeling, it is not yet a topological invariant since it depends on the choice of PLCW decomposition - in particular, it depends on the number of edges.

6.1.3 Extended 3-manifolds

In this section we generalize the notion of an extended combinatorial surface to 3-manifolds.

Definition 82. Let M be a compact PL 3-manifold with boundary. An *open embedded tube* $T \subset M$ is the image of a PL map

$$\varphi : D^2 \times [0, 1] \rightarrow M \quad (6.17)$$

together with the oriented arc $\gamma = \varphi(\{p_0\} \times [0, 1])$ (called the *longitude*). We require that φ satisfy the following conditions:

1. φ must be a homeomorphism onto its image (i.e. a topological embedding).
2. $T \cap \partial M = \varphi(D^2 \times \{0\}) \cup \varphi(D^2 \times \{1\})$.

We call the disks $B_0 = \varphi(D^2 \times \{0\})$ and $B_1 = \varphi(D^2 \times \{1\})$ the bottom and top disks of T respectively.

The longitudes serve to provide a framing for the tubes.

Remark 83. In [2], closed embedded tubes (which are framed embedded tubes which form a loop) are also considered. However, it is not necessary to define them directly in the generators-and-relations approach we use in this thesis. The reader may wish to skip ahead to Chapter 7 and observe that the PLCW decompositions of the generating 2-morphisms only contain open tubes (e.g. 7.17).

Definition 84. An extended 3-manifold M is a PL 3-manifold with boundary, together with a finite collection of disjoint, framed embedded tubes. We denote the set of framed embedded tubes by $T(M)$.

For brevity, we shall usually drop the word “framed” whenever we mention the embedded tubes. Moreover, for our purposes, we shall only ever consider extended 3-manifolds where each embedded tube is open. Hence we make this assumption for the remainder of the thesis.

Definition 85. A *colouring* of an extended 3-manifold is a choice of object $\mathbf{Y}_a \in Z(\mathcal{A})$ for each tube $T_a \in T(M)$. A colouring is called *simple* if each \mathbf{Y}_a is simple.

Definition 86. Let M be an extended 3-manifold. A PLCW complex Δ is a PLCW decomposition of M if

- Δ is a PLCW decomposition of the underlying 3-manifold M ,
- the interior of each open tube $T_a \in T(M)$ is a single 3-cell in Δ ,
- for each open tube $T_a = \varphi_a(D^2 \times [0, 1])$, the interior of the bottom disk $B_0 = \varphi_a(D^2 \times \{0\})$, and the interior of the top disk $B_1 = \varphi_a(D^2 \times \{1\})$ are each single 2-cells in Δ ,
- for each open tube, the marked points on its bottom and top disks, are 0-cells in Δ .

An extended 3-manifold together with a choice of PLCW decomposition is called an *extended combinatorial manifold*. We shall write \mathcal{M} for the pair (M, Δ) .

One may define the notion of a labeling of the edges of Δ analogously to Definition 77. Lastly, note that if \mathcal{M} is a coloured combinatorial 3-manifold, then $\partial\mathcal{M}$ has the structure of a coloured combinatorial surface. Indeed, every open tube T_a gives rise to two embedded disks on $\partial\mathcal{M}$, the bottom disk B_0 and the top disk B_1 . Further, if \mathbf{Y}_a is the colour of T_a , then we declare the colour of B_0 to be \mathbf{Y}_a^* and the colour of B_1 to be \mathbf{Y}_a . We shall usually simply write $\partial\mathcal{M}$ when referring to this surface, leaving the colours of the embedded disks implicit.

6.2 The Invariant

Let $\mathcal{M} = (M, \Delta)$ be a combinatorial 3-manifold and let $\{\mathbf{Y}_a\}$ be a colouring of the open tubes of \mathcal{M} . As we described above, $\partial\mathcal{M}$ may thus be seen as a combinatorial extended surface. In this section we describe a procedure for computing a vector which lives in its state space. Just as the state space is built from the spaces assigned to each oriented 2-cell, the vector we will compute will be built from certain vectors (we shall call them *spherical vectors*) assigned to each oriented 3-cell.

Spherical Vectors

Fix a simple labeling l of Δ , and let \mathbf{F} be an oriented⁴ 3-cell in \mathcal{M} . There are two cases: \mathbf{F} may either be one of the embedded open tubes, or not. Consider first the case where \mathbf{F} is one of the tube cells, with the colour of the tube being $\mathbf{Y} \in Z(\mathcal{A})$, and with γ its longitude.

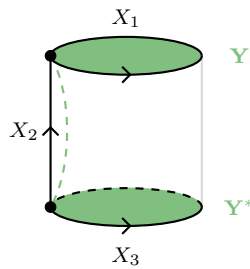


Figure 6.2: An example of a tube 3-cell \mathbf{F} , shown with its labeled PLCW decomposition. The longitude as well as the colours of the top and bottom disks are also indicated.

The boundary $\partial\mathbf{F}$ is a collection of oriented 2-cells⁵ (including the embedded disks)

$$\partial\mathbf{F} = \{\mathbf{C}_\alpha\} \quad (6.18)$$

Since each 3-cell is the image of a characteristic map $\varphi : B^3 \rightarrow \mathbb{R}^N$ (See Definition 32), the collection of 2-cells $\partial\mathbf{F}$ may be pulled back along φ to give a PLCW decomposition of S^2 .⁶ We abuse the notation and write $\partial\mathbf{F}$ for this PLCW decomposition as well.

⁴ \mathbf{F} inherits an orientation from the orientation on M in the obvious way.

⁵See Definition 37.

⁶To see a 2-dimensional version of this idea, consider Example 38. There, the oriented 1-cells $\mathbf{L}_1, \mathbf{L}_2, \overline{\mathbf{L}}_1, \mathbf{L}_3$ which comprise the boundary of the oriented 2-cell \mathbf{C} determine a PLCW decomposition of S^1 - compare with Example 33.

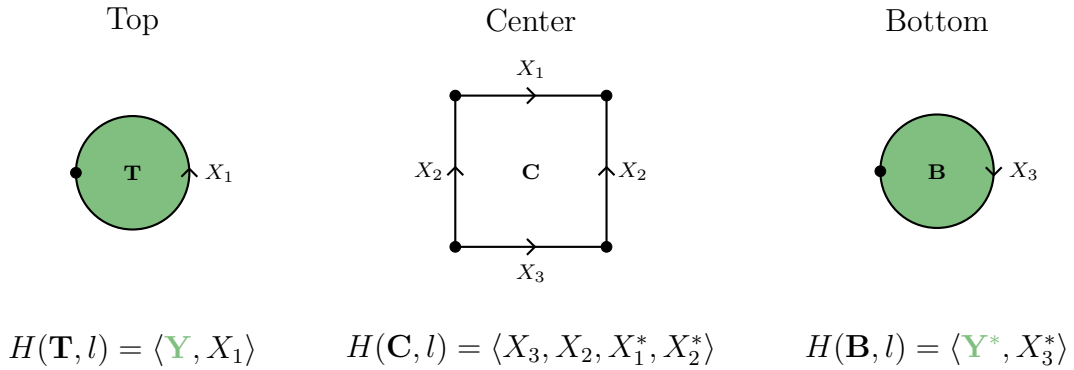


Figure 6.3: The three oriented 2-cells making up $\partial\mathbf{F}$ for the 3-cell in Figure 6.2.

Let Γ be the Poincaré dual graph of the 1-skeleton of $\partial\mathbf{F}$ on $\partial\mathbf{F}$. Using l , we may label the oriented edges of Γ so that the following local relationship holds between the edges of Δ and Γ .



In the figure above, the black line represents an oriented labeled edge in Δ , and the blue line represents the newly labeled oriented edge of Γ . Additionally, we append to Γ short arcs connecting the vertices corresponding to the top and bottom embedded disks to the endpoints of the longitude. Lastly, we also append the longitude itself. The result is an oriented edge connecting the vertices of Γ corresponding to the top and bottom embedded disks. This edge is labeled by the tube colour \mathbf{Y} .

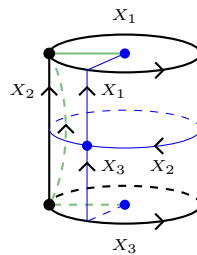


Figure 6.4: The Poincaré dual graph (in blue) of the PLCW decomposition in Figure 6.2. Its oriented edges are labeled according to the rule in 6.19.

Next we remove an arbitrarily selected point (away from the vertices and edges), and then project Γ stereographically onto the plane. Note that this projection is orientation-reversing.

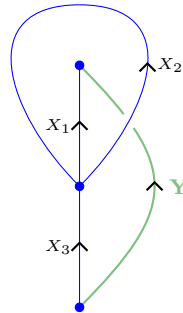


Figure 6.5: This diagram results from removing a point in the lower right of the diagram in Figure 6.4, and then projecting stereographically onto the plane.

We wish to interpret Γ as a tangle diagram (with circular coupons). It remains to label the vertices. Choose for each $\mathbf{C} \in \partial \mathbf{F}$ (including the embedded disks) a vector

$$\varphi_{\mathbf{C}} \in H(\mathbf{C}, l)^* \cong H(\overline{\mathbf{C}}, l). \tag{6.20}$$

We use these vectors to label the vertices.⁷

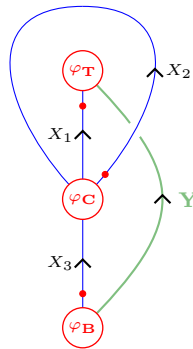


Figure 6.6: The vertices in Figure 6.5 have been labeled by $\varphi_{\mathbf{T}}$, $\varphi_{\mathbf{C}}$, and $\varphi_{\mathbf{B}}$. The result is a tangle diagram in the plane which evaluates to the scalar $S(\mathbf{F}, l)(\varphi_{\mathbf{T}} \otimes \varphi_{\mathbf{C}} \otimes \varphi_{\mathbf{B}})$, where \mathbf{F} is the labeled 3-cell in Figure 6.2.

⁷Recall that each vertex of Γ corresponds to a 2-cell.

Clearly, the tangle diagram formed in this way will simply evaluate to a complex number, and we denote this number by $S(\mathbf{F}, l)(\Phi_{\mathbf{F}})$, where

$$\Phi_{\mathbf{F}} = \bigotimes_{\mathbf{C} \in \partial \mathbf{F}} \varphi_{\mathbf{C}} \in \bigotimes_{\mathbf{C} \in \partial \mathbf{F}} H(\mathbf{C}, l)^* \cong H_{TV}(\partial \mathbf{F}, l)^*. \quad (6.21)$$

In summary, we have described the existence of a map

$$S(\mathbf{F}, l) : H_{TV}(\partial \mathbf{F}, l)^* \rightarrow \mathbb{C}. \quad (6.22)$$

Since $S(\mathbf{F}, l)$ is a functional on the dual space of $H_{TV}(\partial \mathbf{F}, l)$, it corresponds canonically to a vector in $H_{TV}(\partial \mathbf{F}, l)$. We denote this vector by $Z(\mathbf{F}, l)$. It is easily computed that $Z(\mathbf{F}, l)$ is given by

$$Z(\mathbf{F}, l) = S(\mathbf{F}, l) \left(\bigotimes_{\mathbf{C}} \varphi_{\mathbf{C}} \right) \bigotimes_{\mathbf{C}} \varphi_{\mathbf{C}}^* \quad (6.23)$$

In the equation above we are making use of the summation convention described in Remark 20. We call the vectors $Z(\mathbf{F}, l)$ formed this way *spherical vectors*, since they arise from data living on S^2 .

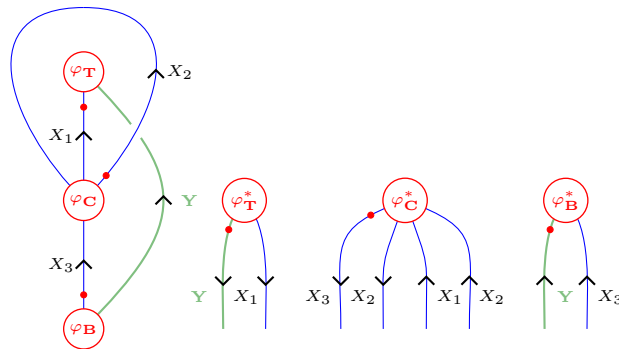


Figure 6.7: The “vector version” $Z(\mathbf{F}, l)$ of the functional in Figure 6.6.

Remark 87. In most practical situations, it is simpler to work with $S(\mathbf{F}, l)$ rather than with $Z(\mathbf{F}, l)$. Since these notions are basically equivalent, we abuse the terminology and refer to $S(\mathbf{F}, l)$ as a spherical vector as well - sometimes we shall call it the “functional form” of the spherical vector.

For the case where \mathbf{F} is an ordinary 3-cell, we proceed in a completely analogous fashion. We still consider $\partial\mathbf{F}$ to be a PLCW decomposition of S^2 .

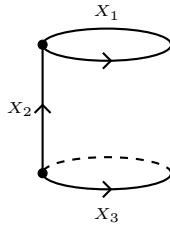


Figure 6.8: An example of an ordinary 3-cell \mathbf{F} . In general 3-cells will have more complicated PLCW decompositions.

We then project its Poincaré dual graph onto the plane, simply ignoring the fact that there is no longitude. Finally, we label the vertices and edges of this graph to obtain a tangle diagram, using the same procedure and notational conventions as before.

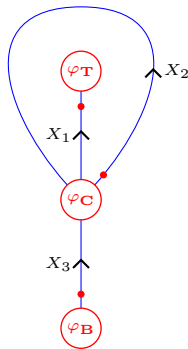


Figure 6.9: The scalar $S(\mathbf{F}, l)(\varphi_{\mathbf{T}} \otimes \varphi_{\mathbf{C}} \otimes \varphi_{\mathbf{B}})$, where \mathbf{F} is the labeled 3-cell in Figure 6.8.

The Invariant

Next we combine the spherical vectors for all the oriented 3-cells in Δ to define the full invariant.

Definition 88 ([2], Defn 8.3). Let $\mathcal{M} = (M, \Delta)$ be an extended combinatorial 3-manifold with boundary, and let $\{\mathbf{Y}_a\}$ be a colouring of \mathcal{M} . Let \mathcal{A} be a spherical fusion category. Then for any simple labeling l of Δ , we define a vector

$$Z_{TV}(\mathcal{M}, \{\mathbf{Y}_a\}, l) \in H_{TV}(\partial\mathcal{M}, l) \quad (6.24)$$

by

$$Z_{TV}(\mathcal{M}, \{\mathbf{Y}_a\}, l) = \text{ev} \left(\bigotimes_{\mathbf{F}} Z(\mathbf{F}, l) \right) \quad (6.25)$$

where

- \mathbf{F} runs over all oriented 3-cells in \mathcal{M} (including the embedded tubes), where the orientation on \mathbf{F} is the one induced from \mathcal{M} , so that

$$\bigotimes_{\mathbf{F}} Z(\mathbf{F}, l) \in \bigotimes_{\mathbf{F}} H_{TV}(\partial\mathbf{F}, l) = H_{TV}(\partial\mathcal{M}, l) \otimes \bigotimes_C H(\mathbf{C}, l) \otimes H(\overline{\mathbf{C}}, l) \quad (6.26)$$

- C runs over all unoriented 2-cells in the interior of \mathcal{M} , and $\mathbf{C}, \overline{\mathbf{C}}$ are the two orientations of such a cell.
- ev is the tensor product over all C of evaluation maps

$$H(\mathbf{C}, l) \otimes H(\overline{\mathbf{C}}, l) = H(\mathbf{C}, l) \otimes H(\mathbf{C}, l)^* \rightarrow \mathbb{C}. \quad (6.27)$$

Finally, we define

$$Z_{TV}(\mathcal{M}, \{\mathbf{Y}_a\}) = \mathcal{D}^{-2v(\mathcal{M})} \sum_l \left(\prod_e d_{l(e)}^{n_e} Z_{TV}(\mathcal{M}, \{\mathbf{Y}_a\}, l) \right) \quad (6.28)$$

where

- the sum is taken over all simple labelings of \mathcal{M}
- e runs over the set of all (unoriented) edges of \mathcal{M}
- \mathcal{D} is the dimension of the category \mathcal{A} , and

$$v(\mathcal{M}) = \text{number of internal vertices of } \mathcal{M} + \frac{1}{2}(\text{number of vertices on } \partial\mathcal{M})$$
- $d_{l(e)}$ is the categorical dimension of $l(e)$ and

$$n_e = \begin{cases} 1, & e \text{ is an internal edge} \\ \frac{1}{2}, & e \in \partial\mathcal{M} \end{cases} \quad (6.29)$$

The functional form of the Invariant

We mentioned before that we frequently use the functional form $S(\mathbf{F}, l)$ for the spherical vectors in our computations instead of $Z(\mathbf{F}, l)$. It is therefore useful to know how to accomplish the evaluation required in Equation 6.24 without needing to change each $S(\mathbf{F}, l)$ to the vector form.

Consider the map

$$\bigotimes_{\mathbf{F}} S(\mathbf{F}, l) : \bigotimes_{\mathbf{F}} H_{TV}(\partial\mathbf{F}, l)^* \rightarrow \mathbb{C}, \quad (6.30)$$

where \mathbf{F} ranges over all oriented 3-cells in \mathcal{M} . Making use of Equation 6.26, we have

$$\begin{aligned} \bigotimes_{\mathbf{F}} H_{TV}(\partial\mathbf{F}, l)^* &= H_{TV}(\partial\mathcal{M}, l)^* \otimes \bigotimes_C H(\mathbf{C}, l)^* \otimes H(\overline{\mathbf{C}}, l)^* \\ &= H_{TV}(\partial\mathcal{M}, l)^* \otimes \bigotimes_C H(\mathbf{C}, l)^* \otimes H(\mathbf{C}, l). \end{aligned}$$

We define a map

$$S_{TV}(\mathcal{M}, \{\mathbf{Y}_a\}, l) : H_{TV}(\partial\mathcal{M}, l)^* \rightarrow \mathbb{C} \quad (6.31)$$

by

$$\Phi \mapsto \bigotimes_{\mathbf{F}} S(\mathbf{F}, l) \left(\Phi \otimes \bigotimes_C \varphi_{\mathbf{C}} \otimes \varphi_{\mathbf{C}}^* \right) \quad (6.32)$$

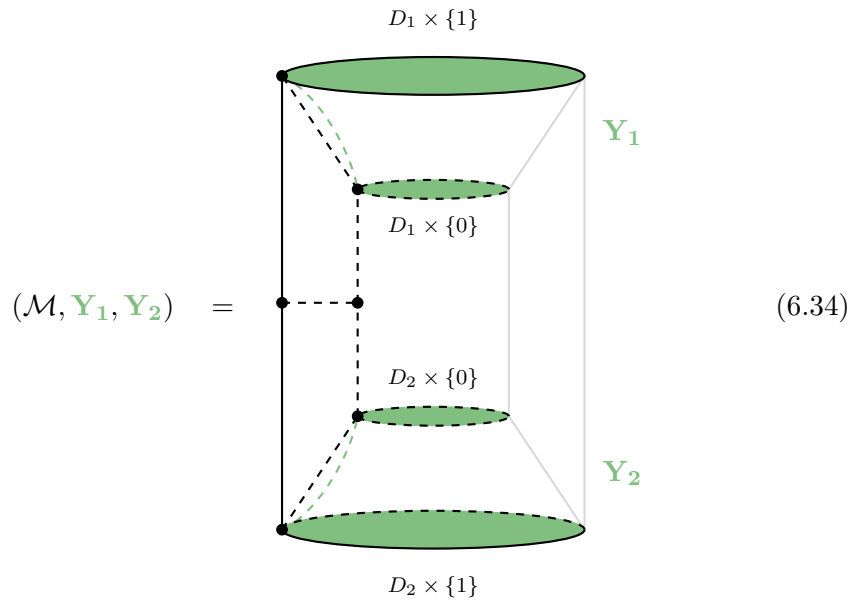
Here we are again making use of the summation convention described in Remark 20. It is easy to see that $S_{TV}(\mathcal{M}, \{\mathbf{Y}_a\}, l)$ is the functional form of $Z_{TV}(\mathcal{M}, \{\mathbf{Y}_a\}, l)$. In other words, the evaluation is performed on the functional version of the spherical vectors by ensuring that dual vector pairs are chosen for the two labels corresponding to an internal 2-cell. Following Equation 6.28, we may also write

$$S_{TV}(\mathcal{M}, \{\mathbf{Y}_a\}) = \mathcal{D}^{-2v(\mathcal{M})} \sum_l \left(\prod_e d_{l(e)}^{n_e} S_{TV}(\mathcal{M}, \{\mathbf{Y}_a\}, l) \right). \quad (6.33)$$

This is the version of the invariant we shall use most frequently in practice.

In the following example, we calculate the invariant of the sphere with two punctures.

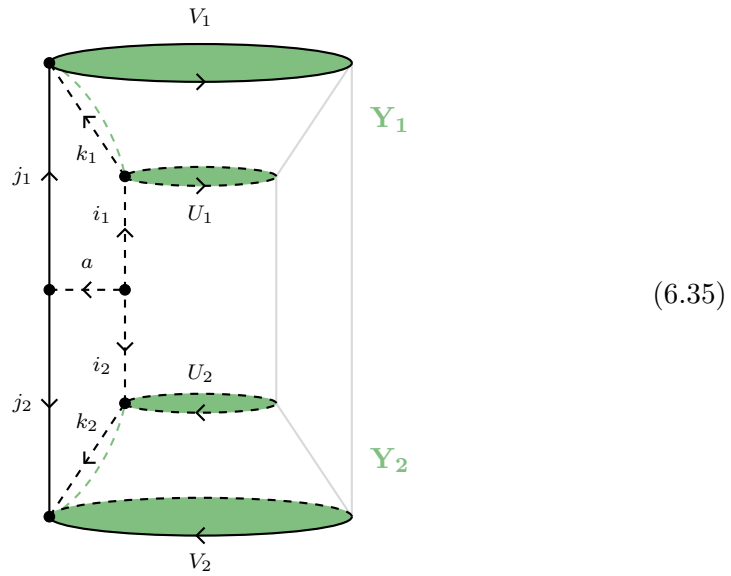
Example 89. Let $\mathcal{S}_2^2 = (S_2^2, \Delta)$ be defined and coloured as in Example 81. Let $M = S_2^2 \times [0, 1]$ and $\mathcal{M} = (M, \Delta \times [0, 1])$, where by $\Delta \times [0, 1]$ we are referring to the natural PLCW decomposition of M coming from taking the cylinder over S_2^2 . It is easy to see that \mathcal{M} is an extended combinatorial 3-manifold with boundary, containing two open tubes $D_1 \times [0, 1]$ and $D_2 \times [0, 1]$, coloured by \mathbf{Y}_1 and \mathbf{Y}_2 respectively. This situation is summarized in the figure below.



It is clear that $\partial\mathcal{M} = \overline{\mathcal{S}_2^2} \amalg \mathcal{S}_2^2$. Therefore, we have

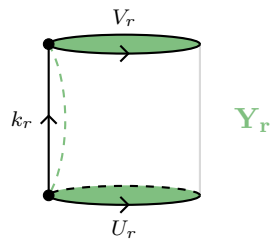
$$\begin{aligned} Z_{TV}(\mathcal{M}, \mathbf{Y}_1, \mathbf{Y}_2) &\in H_{TV}(\overline{\mathcal{S}_2^2}, \mathbf{Y}_1^*, \mathbf{Y}_2^*) \otimes H_{TV}(\mathcal{S}_2^2, \mathbf{Y}_1, \mathbf{Y}_2) \\ &\cong H_{TV}(\mathcal{S}_2^2, \mathbf{Y}_1, \mathbf{Y}_2)^* \otimes H_{TV}(\mathcal{S}_2^2, \mathbf{Y}_1, \mathbf{Y}_2). \end{aligned}$$

We proceed to calculate this invariant. Let l be a simple labeling of \mathcal{M} - See the figure below.



There are three 3-cells in this PLCW decomposition: two open tubes (one at the top and one at the bottom) and a large 3-cell comprising the bulk. We compute the spherical vectors for each of these 3-cells.

- The open tubes \mathbf{T}_r , with $r \in \{1, 2\}$.

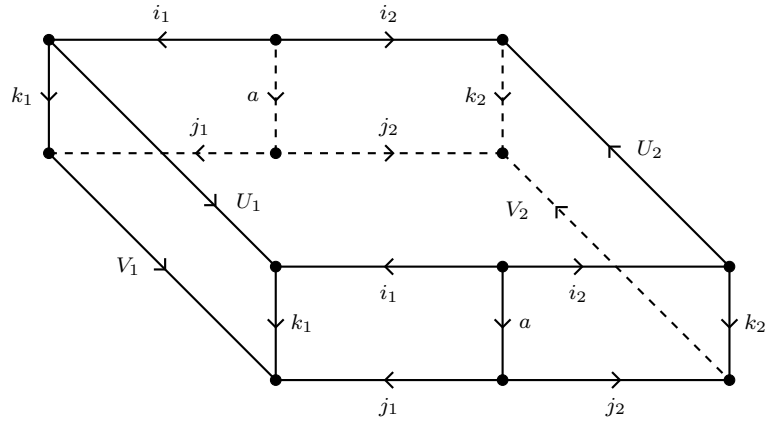


Using a similar procedure to the one leading to Figure 6.6, we see that the spherical vectors $S(\mathbf{T}_1, l)$ and $S(\mathbf{T}_2, l)$ are given by

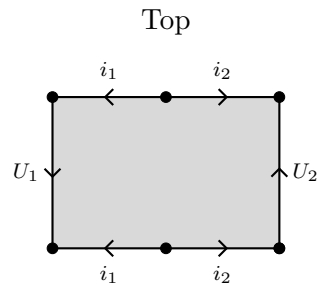
$$S(\mathbf{T}_r, l)(\Phi_r) = \begin{array}{c} \psi_r \\ \uparrow V_r \\ \beta_r \\ \uparrow U_r \\ \varphi_r \end{array} \begin{array}{c} \nearrow k_r \\ \nearrow Y_r \end{array}$$

where $\Phi_r = \varphi_r \otimes \beta_r \otimes \psi_r$.

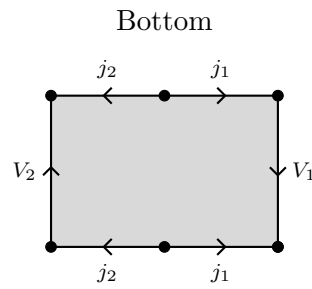
- The cylindrical 3-cell \mathbf{C} .



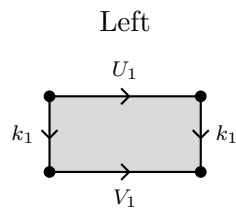
The boundary $\partial\mathbf{C}$ consists of the following oriented 2-cells, shown with their state spaces.



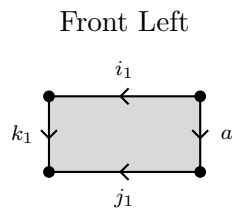
$$\langle i_2, U_2, i_2^*, i_1, U_1, i_1^* \rangle$$



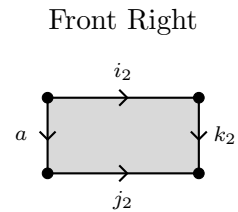
$$\langle j_1, V_1^*, j_1^*, j_2, V_2^*, j_2^* \rangle$$



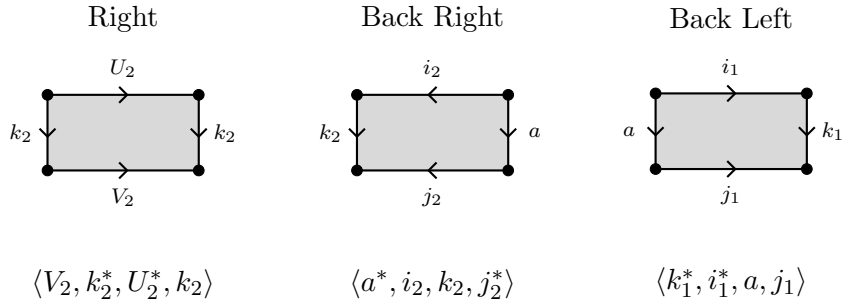
$$\langle k_1, V_1, k_1^*, U_1^* \rangle$$



$$\langle j_1^*, a^*, i_1, k_1 \rangle$$



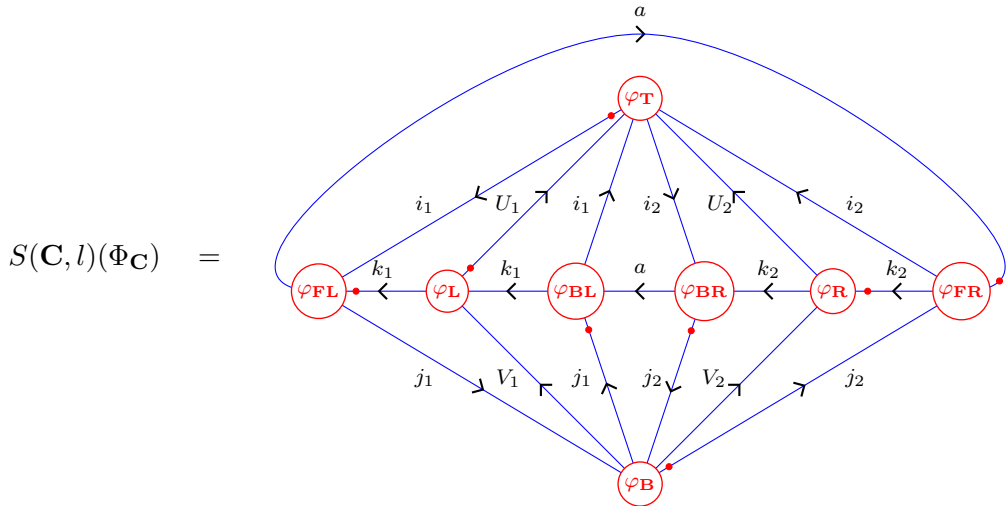
$$\langle j_2, k_2^*, i_2^*, a \rangle$$



Therefore, given a choice of vectors

$$\begin{aligned}
 \varphi_{\mathbf{T}} &\in \langle i_2, U_2, i_2^*, i_1, U_1, i_1^* \rangle^* \cong \langle i_1, U_1^*, i_1^*, i_2, U_2^*, i_2^* \rangle \\
 \varphi_{\mathbf{B}} &\in \langle j_1, V_1^*, j_1^*, j_2, V_2^*, j_2^* \rangle^* \cong \langle j_2, V_2, j_2^*, j_1, V_1, j_1^* \rangle \\
 \varphi_{\mathbf{L}} &\in \langle k_1, V_1, k_1^*, U_1^* \rangle^* \cong \langle U_1, k_1, V_1^*, k_1^* \rangle \\
 \varphi_{\mathbf{FL}} &\in \langle j_1^*, a^*, i_1, k_1 \rangle^* \cong \langle k_1^*, i_1^*, a, j_1 \rangle \\
 \varphi_{\mathbf{FR}} &\in \langle j_2, k_2^*, i_2^*, a \rangle^* \cong \langle a^*, i_2, k_2, j_2^* \rangle \\
 \varphi_{\mathbf{R}} &\in \langle V_2, k_2^*, U_2^*, k_2 \rangle^* \cong \langle k_2^*, U_2, k_2, V_2^* \rangle \\
 \varphi_{\mathbf{BR}} &\in \langle a^*, i_2, k_2, j_2^* \rangle^* \cong \langle j_2, k_2^*, i_2^*, a \rangle \\
 \varphi_{\mathbf{BL}} &\in \langle k_1^*, i_1^*, a, j_1 \rangle^* \cong \langle j_1^*, a^*, i_1, k_1 \rangle
 \end{aligned}$$

we obtain the spherical vector



where $\Phi_{\mathbf{C}} = \varphi_{\mathbf{T}} \otimes \varphi_{\mathbf{B}} \otimes \varphi_{\mathbf{L}} \otimes \varphi_{\mathbf{FL}} \otimes \varphi_{\mathbf{FR}} \otimes \varphi_{\mathbf{R}} \otimes \varphi_{\mathbf{BR}} \otimes \varphi_{\mathbf{BL}}$.

Making use of Equation 6.33, the full invariant $S_{TV}(\mathcal{M}, \mathbf{Y}_1, \mathbf{Y}_2)(\Phi)$ is given by

$$\left(\frac{1}{\mathcal{D}^2}\right)^{\frac{6}{2}} \sum_{\substack{U_1, U_2, V_1, V_2, a \\ i_1, i_2, j_1, j_2, k_1, k_2}} D \cdot \text{ev}(S(\mathbf{T}_1, l)(\Phi_1) \cdot S(\mathbf{T}_2, l)(\Phi_2) \cdot S(\mathbf{C}, l)(\Phi_{\mathbf{C}})) \quad (6.36)$$

where $D = d_{k_1} d_{k_2} d_a \sqrt{d_{U_1}} \sqrt{d_{U_2}} \sqrt{d_{V_1}} \sqrt{d_{V_2}} \sqrt{d_{i_1}} \sqrt{d_{i_2}} \sqrt{d_{j_1}} \sqrt{d_{j_2}}$,

where $\Phi = \varphi_{\mathbf{T}} \otimes \varphi_1 \otimes \varphi_2 \otimes \varphi_{\mathbf{B}} \otimes \psi_1 \otimes \psi_2$, and where the evaluation enforces

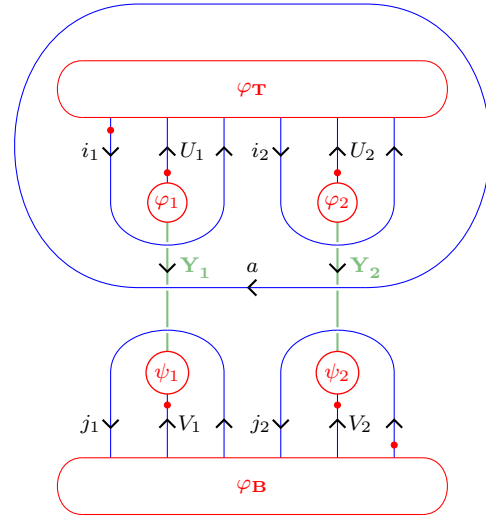
$$\begin{aligned} \varphi_{\mathbf{L}} &= \beta_1^* & \varphi_{\mathbf{FL}} &= \varphi_{\mathbf{BL}}^* \\ \varphi_{\mathbf{R}} &= \beta_2^* & \varphi_{\mathbf{FR}} &= \varphi_{\mathbf{BR}}^* \end{aligned}$$

Performing these changes and then merging $S(\mathbf{T}_1, l)(\Phi_1)$ and $S(\mathbf{T}_2, l)(\Phi_2)$ with $S(\mathbf{C}, l)$ via Lemma 22, Expression 6.36 becomes

$$\left(\frac{1}{\mathcal{D}^2}\right)^3 \sum_{\substack{U_1, U_2, V_1, V_2, a \\ i_1, i_2, j_1, j_2, k_1, k_2}} D$$

Finally, we apply Lemma 21 twice, merging the vertex pairs along the k_1 and k_2 wires. We obtain

$$S_{TV}(\mathcal{M}, \mathbf{Y}_1, \mathbf{Y}_2) = \left(\frac{1}{\mathcal{D}^2}\right)^3 \sum_{\substack{U_1, U_2, V_1, V_2, a \\ i_1, i_2, j_1, j_2}} D'$$



(6.38)

where $D' = d_a \sqrt{d_{U_1}} \sqrt{d_{U_2}} \sqrt{d_{V_1}} \sqrt{d_{V_2}} \sqrt{d_{i_1}} \sqrt{d_{i_2}} \sqrt{d_{j_1}} \sqrt{d_{j_2}}$.

6.3 Properties of the Invariant

It can be shown that the invariant given in Definition 88 satisfies various properties. We shall mention those which will be useful for us, but we shall not prove them here, instead referring the reader to Theorem 8.4 in [2]. Property 4 does not appear in [2] directly (though it is implied) but it is also a generalization of the standard state-sum approach (see p.356. - p.361. in [29]) to the extended TQFT setting.

1 - Independence of Bulk Decomposition

The invariant is independent of the choice of PLCW decomposition on the “bulk” of M . That is, if $\mathcal{M} = (M, \Delta)$ and $\mathcal{M}' = (M, \Delta')$ where Δ and Δ' agree on ∂M , then

$$Z_{TV}(\mathcal{M}, \{\mathbf{Y}_a\}) = Z_{TV}(\mathcal{M}', \{\mathbf{Y}_a\}). \quad (6.39)$$

2 - The Invariant as Cobordism

If \mathcal{M} is a cobordism from \mathcal{N}_{in} to \mathcal{N}_{out} , so that $\partial\mathcal{M} = \overline{\mathcal{N}_{in}} \amalg \mathcal{N}_{out}$, then

$$\begin{aligned} H_{TV}(\overline{\mathcal{N}_{in}}) \otimes H_{TV}(\mathcal{N}_{out}) &\cong H_{TV}(\mathcal{N}_{in})^* \otimes H_{TV}(\mathcal{N}_{out}) \\ &\cong \text{Hom}(H_{TV}(\mathcal{N}_{in}), H_{TV}(\mathcal{N}_{out})). \end{aligned}$$

This implies that we may view $Z_{TV}(\mathcal{M}, \{\mathbf{Y}_a\})$ as a linear map from the state space of the input boundary component to the state space of the output boundary component:

$$Z_{TV}(\mathcal{M}, \{\mathbf{Y}_a\}) : H_{TV}(\mathcal{N}_{in}) \rightarrow H_{TV}(\mathcal{N}_{out}). \quad (6.40)$$

Obviously, it suffices to give this map on basis vectors. Fix a simple labeling l_{in} of \mathcal{N}_{in} and choose $\varphi_{in} \in H_{TV}(\mathcal{N}_{in}, l_{in})$. Then we have

$$Z_{TV}(\mathcal{M}, \{\mathbf{Y}_a\}) : \varphi_{in} \mapsto \mathcal{D}^{-2v(\mathcal{M})} \sum_{l|_{\mathcal{N}_{in}} = l_{in}} \left(\prod_e d_{l(e)}^{n_e} Z_{TV}(\mathcal{M}, \{\mathbf{Y}_a\}, l) \right). \quad (6.41)$$

The sum above runs over all simple labelings of \mathcal{M} which restrict to l_{in} on \mathcal{N}_{in} . Thinking of $Z_{TV}(\mathcal{M}, \{\mathbf{Y}_a\})$ as a linear map will clearly be very useful for us, since we need linear maps to be associated to the generating 2-morphisms of $\mathbf{F}(\mathcal{O})$ to define a generators-and-relations 123-TQFT.

3 - The Invariant Subspace

The state space is not a suitable vector space for Turaev-Viro theory to assign to a coloured extended combinatorial surface - indeed, it is not a topological invariant.⁸ If \mathcal{N} is an extended combinatorial surface whose embedded disks are coloured by $\{\mathbf{Y}_a\}$, then we may consider the cylinder $\mathcal{N} \times [0, 1]$ as a cobordism from \mathcal{N} to itself, and so form the linear map

$$Z_{TV}(\mathcal{N} \times [0, 1], \{\mathbf{Y}_a\}) : H_{TV}(\mathcal{N}, \{\mathbf{Y}_a\}) \rightarrow H_{TV}(\mathcal{N}, \{\mathbf{Y}_a\}). \quad (6.42)$$

It can be shown that this map is idempotent and, making use of it, we define the invariant vector space to be:

$$Z_{TV}(\mathcal{N}, \{\mathbf{Y}_a\}) := \text{im}(Z_{TV}(\mathcal{N} \times [0, 1], \{\mathbf{Y}_a\})). \quad (6.43)$$

This space is functorial in the colours $\{\mathbf{Y}_a\}$ of the embedded disks (see [2, pg. 25]) and does not, up to a canonical isomorphism, depend on the choice of PLCW decomposition of \mathcal{N} . Indeed, if $\mathcal{N}_0 = (N, \Delta_0)$ and $\mathcal{N}_1 = (N, \Delta_1)$, then there exists a PLCW decomposition Δ of $N \times [0, 1]$ which specializes to Δ_0 and Δ_1 on $N \times \{0\}$ and $N \times \{1\}$ respectively. Then, setting $\mathcal{N} \times [0, 1] = (N \times [0, 1], \Delta)$, the map

$$Z_{TV}(\mathcal{N} \times [0, 1], \{\mathbf{Y}_a\}) : Z_{TV}(\mathcal{N}_0, \{\mathbf{Y}_a\}) \rightarrow Z_{TV}(\mathcal{N}_1, \{\mathbf{Y}_a\}) \quad (6.44)$$

is an isomorphism. Recall that the particular choice of PLCW decomposition Δ extending Δ_0 and Δ_1 does not matter. We shall call maps of the above type *cylinder maps*.

4 - Naturality

The space $Z_{TV}(\mathcal{N}, \{\mathbf{Y}_a\})$ is natural with respect to diffeomorphisms of the underlying extended surface N . Indeed, let $f : N \rightarrow N'$ be such a diffeomorphism, and let Δ be a PLCW decomposition of N . Then $f(\Delta)$ will be a PLCW decomposition of N' in the obvious way. Finally, let $\{\mathbf{Y}_a\}$ be a simple colouring of both N and N' (embedded disks which correspond under f receive the same colour). Then we have an isomorphism

$$f_{\#} : Z_{TV}(\mathcal{N}, \{\mathbf{Y}_a\}) \rightarrow Z_{TV}(\mathcal{N}', \{\mathbf{Y}_a\}). \quad (6.45)$$

To see how this map works, note that each oriented 2-cell \mathbf{C} in Δ corresponds to an oriented 2-cell $f(\mathbf{C})$ in $f(\Delta)$. Further, any simple labeling l of Δ is immediately also a simple labeling of $f(\Delta)$. Therefore, the vector spaces $H(\mathbf{C}, l)$ and $H(f(\mathbf{C}), l)$ are identical. The isomorphism $f_{\#}$ follows.

⁸For example, it depends on the number of edges in the chosen PLCW decomposition.

Example 90. Let $\mathcal{M} = \mathcal{S}_2^2 \times [0, 1]$ be defined as in Example 89. We calculated the invariant $S_{TV}(\mathcal{M}, \{\mathbf{Y}_1, \mathbf{Y}_2\})$ in Equation 6.38. We now wish to view this invariant as a linear map. Recall the state space of \mathcal{S}_2^2 :

$$H_{TV}(\mathcal{S}_2^2, \mathbf{Y}_1, \mathbf{Y}_2) = \bigoplus_{i_1, i_2, U_1, U_2} \langle i_1, U_1^*, i_1^*, i_2, U_2^*, i_2^* \rangle \otimes \langle \mathbf{Y}_1, U_1 \rangle \otimes \langle \mathbf{Y}_2, U_2 \rangle, \quad (6.46)$$

where i_1, i_2, U_1, U_2 range over the simple objects of \mathcal{A} . It suffices to show the map on a basis vector. Therefore, choose

$$\varphi_{\mathbf{T}} \otimes \varphi_1 \otimes \varphi_2 \in \langle i_1, U_1^*, i_1^*, i_2, U_2^*, i_2^* \rangle \otimes \langle U_1, \mathbf{Y}_1 \rangle \otimes \langle U_2, \mathbf{Y}_2 \rangle. \quad (6.47)$$

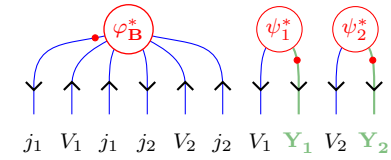
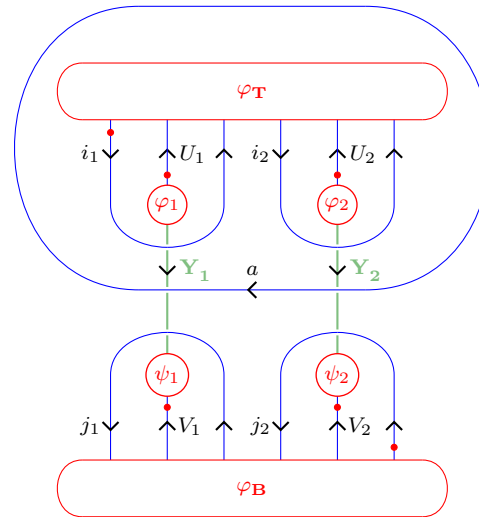
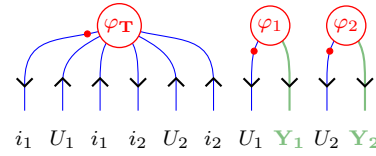
With this choice, the desired linear map

$$Z_{TV}(\mathcal{M}; \{\mathbf{Y}_1, \mathbf{Y}_2\}) : H_{TV}(\mathcal{S}_2^2; \{\mathbf{Y}_1, \mathbf{Y}_2\}) \longrightarrow H_{TV}(\mathcal{S}_2^2; \{\mathbf{Y}_1, \mathbf{Y}_2\}) \quad (6.48)$$

is given by

94

$$\xrightarrow{Z_{TV}(\mathcal{M};\{\mathbf{Y}_1, \mathbf{Y}_2\})} \frac{\sqrt{d_{i_1}}\sqrt{d_{i_2}}\sqrt{d_{U_1}}\sqrt{d_{U_2}}}{\mathcal{D}^2} \sum_{\substack{V_1, V_2, a \\ j_1, j_2}} \tilde{D}$$



where $\tilde{D} = d_a \sqrt{d_{V_1}} \sqrt{d_{V_2}} \sqrt{d_{j_1}} \sqrt{d_{j_2}}$.

(6.49)

Applying the Fusion lemma one more time, we obtain

$$\begin{array}{c}
 \begin{array}{c}
 \textcircled{\varphi_T} \\
 \swarrow \quad \downarrow \quad \searrow \\
 i_1 \quad U_1 \quad i_1 \quad i_2 \quad U_2 \quad i_2 \\
 \uparrow \quad \downarrow \quad \uparrow \quad \downarrow \quad \uparrow \quad \downarrow \\
 \textcircled{\varphi_1} \quad \textcircled{\varphi_2} \\
 \downarrow \quad \downarrow \\
 U_1 \quad Y_1 \quad U_2 \quad Y_2
 \end{array}
 \xrightarrow{Z_{TV}(\mathcal{M};\{Y_1, Y_2\})}
 \frac{\sqrt{d_{i_1}}\sqrt{d_{i_2}}\sqrt{d_{U_1}}\sqrt{d_{U_2}}}{\mathcal{D}^2}
 \sum_{\substack{V_1, V_2, a \\ j_1, j_2}} \tilde{D}
 \end{array}
 \begin{array}{c}
 \begin{array}{c}
 \textcircled{\varphi_T} \\
 \swarrow \quad \downarrow \quad \searrow \\
 i_1 \quad U_1 \quad i_2 \quad U_2 \\
 \uparrow \quad \downarrow \quad \uparrow \quad \downarrow \\
 \textcircled{\varphi_1} \quad \textcircled{\varphi_2} \\
 \downarrow \quad \downarrow \\
 Y_1 \quad a \quad Y_2 \\
 \downarrow \quad \downarrow \\
 \textcircled{\psi_1} \quad \textcircled{\psi_2} \\
 \downarrow \quad \downarrow \\
 j_1 \quad V_1 \quad j_2 \quad V_2
 \end{array}
 \quad
 \begin{array}{c}
 \textcircled{\psi_1^*} \quad \textcircled{\psi_2^*} \\
 \downarrow \quad \downarrow \\
 V_1 \quad Y_1 \quad V_2 \quad Y_2
 \end{array}
 \end{array}
 \tag{6.50}$$

6.4 TV = String-Nets

In this section we give Kirillov's result that the Turaev-Viro and string-net spaces are isomorphic. We end by showing how this works with the example of the 2-punctured sphere.

Let N be a compact oriented surface whose boundary components are indexed by a finite set A . For each $a \in A$, choose a parametrization

$$\psi_a : S^1 \rightarrow \partial N_a. \quad (6.51)$$

Then we can form the closed oriented surface \widehat{N} by gluing a copy of the disk D onto each boundary component. We denote by D_a the image of the disk which was glued onto the component ∂N_a . Let $p_a = \psi_a(1, 0)$ and let v_a denote the incoming tangent direction which connects p_a to the center of D_a - see the figure below.

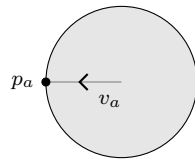


Figure 6.10: The gray shaded area represents D_a .

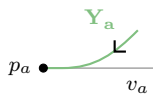
It is easy to see that the collection $(\widehat{N}, \{p_a\}, \{v_a\})$ determines an extended surface, in the sense of Definition 73.

Definition 91. Let $(\widehat{N}, \{p_a\}, \{v_a\})$ be as described above, and choose an object $\mathbf{Y}_a \in Z(\mathcal{A})$ for each $a \in A$. Then we define the vector space

$$H^{string}(\widehat{N}, \{p_a\}, \{v_a\}, \{\mathbf{Y}_a\}) = \text{VGraph}'(\widehat{N}, \{p_a\}, \{v_a\}, \{\mathbf{Y}_a\}) / \text{Null}'(\widehat{N})$$

where

- $\text{VGraph}'(\widehat{N}, \{p_a\}, \{v_a\}, \{\mathbf{Y}_a\})$ is the vector space of all formal finite linear combinations of labeled graphs on \widehat{N} , such that each labeled graph has an unlabeled, one-valent vertex at each point p_a , with the corresponding edge coming in from the direction v_a , and labeled by the object $F(\mathbf{Y}_a)$.



- $\text{Null}'(\widehat{N})$ is a subspace of local relations, spanned by the same local relations as those in Definition 56 (coming from embedded disks $D \subset \widehat{N}$ not containing the points p_a) together with the following additional relation in a neighbourhood of each marked point p_a .

$$\left(\text{blue wavy line} \right) \text{---} \bullet \text{---} \text{green line} = \bullet \text{---} \text{green line} \text{---} \left(\text{blue wavy line} \right) \quad (6.52)$$

The following theorem shows the space defined above is isomorphic to the string-net space in Definition 64.

Theorem 92. [18, Thm 7.2.] *Let N and \widehat{N} be as above, and let $\{\mathbf{Y}_a\}$ be a collection of objects in $Z(\mathcal{A})$, one for each boundary component of N . Then there is a canonical isomorphism*

$$T : H^{string}(\widehat{N}, \{p_a\}, \{v_a\}, \{\mathbf{Y}_a\}) \xrightarrow{\cong} H^{string}(N, \{\psi_a\}, \{\mathbf{Y}_a\}). \quad (6.53)$$

Using 6.53, it is possible to write down “alternate versions” of the actions of the 2-generators. For example, the action of μ when written in the language of Definition 91 looks as follows:

$$\left(\text{cup-shaped surface with } p_1, p_2, Y_1, Y_2, F, G \right) \xrightarrow{\widehat{Z}_{SN}^{123}(\mu)} \left(\text{cylinder-shaped surface with } p_1, p_2, Y_1, Y_2, F, G \right) \quad (6.54)$$

Remark 93. Notice that we write $\widehat{Z}_{SN}^{123}(\mu)$ instead of $Z_{SN}^{123}(\mu)$ to avoid confusion.

Obviously, similar calculations can be done for each of the other 2-generators; these are left as a simple exercise for the reader. The reason for introducing an alternative definition for the string-net space is to facilitate a connection between Turaev-Viro theory and string-nets (recall that the Turaev-Viro theory formulated in the preceding section pertains to *extended surfaces*, not surfaces with boundary). This connection is given by the following theorem.

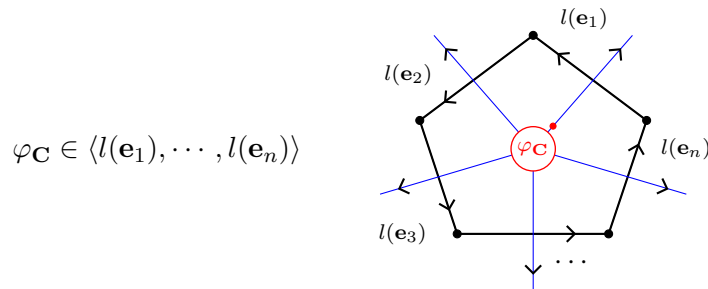
Theorem 94. [18, Thm 7.3.] *Let N and \widehat{N} be as above, let Δ be a PLCW decomposition⁹ of \widehat{N} , and let $\{\mathbf{Y}_a\}$ be a collection of objects in $Z(\mathcal{A})$, one for each boundary component of N . Let $\widehat{N} = (\widehat{N}, \Delta)$. Then there is a canonical isomorphism*

$$\pi_\Delta : Z_{TV}(\widehat{N}, \{\mathbf{Y}_a\}) \rightarrow H^{string}(\widehat{N}, \{p_a\}, \{v_a\}, \{\mathbf{Y}_a\}). \quad (6.55)$$

Proof. We shall merely describe π_Δ (on basis vectors), referring the reader to [18] for the proof that it is an isomorphism. Fix a simple labeling l of Δ , and let

$$\bigotimes_{\mathbf{C}} \varphi_{\mathbf{C}} \in H_{TV}(\widehat{N}, \{\mathbf{Y}_a\}, l) \subset H_{TV}(\widehat{N}, \{\mathbf{Y}_a\}),$$

where the product runs over all oriented 2-cells \mathbf{C} in Δ , including the embedded disks. Let Γ_Δ denote the Poincaré dual of Δ . Now the simple labeling l immediately gives a simple labeling of the edges of Γ_Δ , and the vector $\varphi_{\mathbf{C}}$ defines a labeling of the vertex of Γ_Δ corresponding to \mathbf{C} , as shown in the figure below.



Finally, we define

$$\bigotimes_{\mathbf{C}} \varphi_{\mathbf{C}} \xrightarrow{\pi_\Delta} \left(\frac{1}{D^2} \right)^{\frac{|\Delta_0|}{2}} \prod_e d_{l(e)}^{\frac{1}{2}} \Gamma_\Delta. \quad (6.56)$$

Here the product ranges over all unoriented edges of Δ and $|\Delta_0|$ is the number of 0-cells in Δ . □

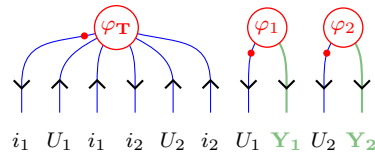
⁹Recall from Definition 75 that the marked points p_a are required to be 0-cells in Δ .

In the following example, we demonstrate a concrete example of the map π_Δ for the case of the 2-punctured sphere. The simplifications which follow are typical

Example 95. Let the 2-punctured sphere \mathcal{S}_2^2 be defined and labeled as in Example 81. Choose a basis vector (as in Example 90)

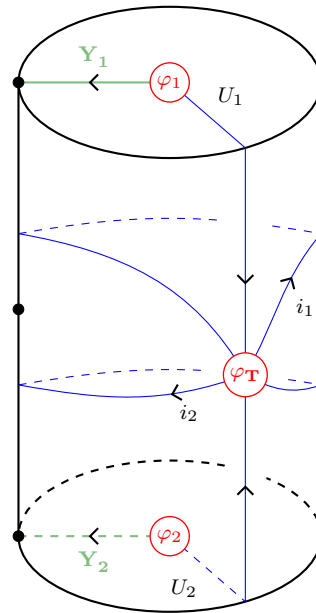
$$\varphi_{\mathbf{T}} \otimes \varphi_1 \otimes \varphi_2 \in \langle i_1, U_1^*, i_1^*, i_2, U_2^*, i_2^* \rangle \otimes \langle U_1, \mathbf{Y}_1 \rangle \otimes \langle U_2, \mathbf{Y}_2 \rangle.$$

Obviously, it suffices to give π_Δ on the basis vector above.

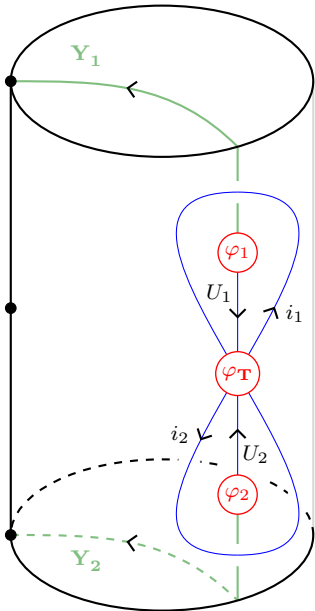


π_Δ

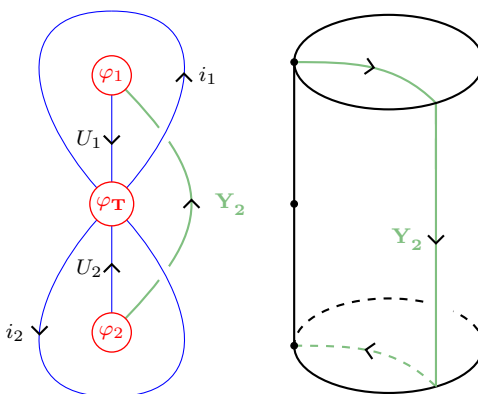
$$\left(\frac{1}{\mathcal{D}^2}\right)^{\frac{3}{2}} \sqrt{d_{i_1}} \sqrt{d_{i_2}} \sqrt{d_{U_1}} \sqrt{d_{U_2}}$$



Making use of isotopy and Relation 6.52, which allows us to move the loops labeled by i_1 and i_2 past the marked points, we may simplify the preceding output vector to obtain

$$\left(\frac{1}{\mathcal{D}^2}\right)^{\frac{3}{2}} \sqrt{d_{i_1}} \sqrt{d_{i_2}} \sqrt{d_{U_1}} \sqrt{d_{U_2}}$$


Making use of Theorem 92 and Corollary 67, we may simplify the output even further:

$$\left(\frac{1}{\mathcal{D}^2}\right)^{\frac{3}{2}} \frac{\delta_{Y_1^*, Y_2}}{d_{Y_2}} \sqrt{d_{i_1}} \sqrt{d_{i_2}} \sqrt{d_{U_1}} \sqrt{d_{U_2}}$$


Chapter 7

The Turaev-Viro 123-TQFT

In this chapter we use Corollary 47 to define a generators-and-relations oriented 123-TQFT based on the extended Turaev-Viro theory given in Chapter 6. We take as input a fixed spherical fusion category \mathcal{A} , and denote our yet to be defined 123-TQFT by Z_{TV}^{123} . The bulk of the chapter consists of computing the actions of each of the generating 2-morphisms. After this, we prove that the relations are satisfied by comparing the Turaev-Viro and string-net actions. A consequence of this is that the Turaev-Viro and string-net 123-TQFTs will be equivalent.

7.1 Generators

Firstly, we need a $\mathbf{Vect}_{\mathbb{C}}$ -enriched category to be assigned to S^1 , and we define this to be $Z(\mathcal{A})$.

$$\circlearrowleft \xrightarrow{Z_{TV}^{123}} Z(\mathcal{A}). \quad (7.1)$$

Note that this assignment is the same as in the string-net case - see Equation 5.13.

Next we define the vector spaces assigned to the 1-generators. First, note that for each 1-generator, every boundary circle automatically comes equipped with a parametrization.¹ This implies that we may close up all the boundary components by gluing in embedded disks, thus obtaining an extended surface in the sense of Definition 73.

Remark 96. If σ is a 1-generator, we shall usually abuse the notation and also write σ for the extended surface formed from the procedure in the preceding

¹This is due to the fact that they are “standard surfaces”. For brevity, we shall suppress this fact in our notation.

paragraph. We shall be careful to make sure that the precise meaning is clear from the context.

Finally, we define the spaces assigned to the 1-generators as follows:

$$\begin{aligned} Z_{TV}^{123}(\ominus)^{\mathbf{Y}} &:= Z_{TV}(\ominus, \Delta, \mathbf{Y}^*), \\ Z_{TV}^{123}(\odot)_{\mathbf{Y}} &:= Z_{TV}(\odot, \Delta, \mathbf{Y}). \\ Z_{TV}^{123}(\mathcal{A})_{\mathbf{Y}_2 \boxtimes \mathbf{Y}_3}^{\mathbf{Y}_1} &:= Z_{TV}(\mathcal{A}, \Delta, \{\mathbf{Y}_1^*, \mathbf{Y}_2, \mathbf{Y}_3\}), \\ Z_{TV}^{123}(\mathcal{B})_{\mathbf{Y}_3}^{\mathbf{Y}_1 \boxtimes \mathbf{Y}_2} &:= Z_{TV}(\mathcal{B}, \Delta, \{\mathbf{Y}_1^*, \mathbf{Y}_2^*, \mathbf{Y}_3\}), \end{aligned}$$

Once more, by the space $Z_{TV}^{123}(\ominus)^{\mathbf{Y}}$ we mean the following:

- The standard parametrization of the lone boundary circle has been used, by which an embedded disk was glued on. This makes \ominus into an extended surface.
- The embedded disk is then coloured by the object $\mathbf{Y}^* \in Z(\mathcal{A})$.
- Some PLCW decomposition Δ of \ominus is chosen.
- Finally, the Turaev-Viro invariant subspace of this coloured extended combinatorial surface is computed, as described in Chapter 6.

An analogous description holds for the spaces associated to the remaining three 1-generators. We note that, from property 6.3, the spaces defined above are functorial in the boundary labels. Next we recall that, via the cylinder maps (see 6.44), these spaces do not depend on the choice of PLCW decomposition.

In fact, one could go further and remove the appearance of a PLCW decomposition altogether using the following standard² technique: For a coloured extended surface $(N, \{\mathbf{Y}_a\})$, define a space $Z_{TV}(N, \{\mathbf{Y}_a\})$ whose elements are families of vectors, $\{v_\Delta \in Z_{TV}(N, \Delta, \{\mathbf{Y}_a\})\}_\Delta$, where Δ ranges over all PLCW decompositions of N . Two vectors v_Δ and $v_{\Delta'}$ are in the same family if and only if the relevant cylinder map sends v_Δ to $v_{\Delta'}$. It follows that a family is uniquely determined by a single member v_Δ . In categorical terms, $Z_{TV}(N, \{\mathbf{Y}_a\})$ is a colimit over a certain diagram.³ Since one must always choose a particular PLCW decomposition in order to do practical computations (such as those done in this chapter)

²See Chapter 7, Section 3.3 in [29] for an example.

³Let $P(N)$ denote the indiscrete groupoid with objects the collection of all PLCW decompositions of N , and such that there is a unique formal morphism between any pair of objects. Let $D_N : P(N) \rightarrow \mathbf{Vect}$ be the diagram which sends Δ to $Z_{TV}((N, \Delta), \{\mathbf{Y}_a\})$, and which sends $\Delta \rightarrow \Delta'$ to the relevant cylinder map. Then $Z_{TV}(N, \{\mathbf{Y}_a\})$ is the colimit over D_N .

we shall content ourselves with dealing only with the spaces $Z_{TV}(N, \Delta, \{\mathbf{Y}_a\})$ and avoid talking about the above “colimit space” directly.

Next we investigate the space which Z_{TV}^{123} assigns to a *composite* of the generating 1-morphisms. The discussion here mirrors the one in Section 5.2.

Let Σ be a composite of the generating 1-morphisms, with m top boundary circles and n bottom boundary circles, labeled by $\mathbf{X}_1, \dots, \mathbf{X}_m$ and $\mathbf{Y}_1, \dots, \mathbf{Y}_n$ respectively. Then, by Definition 2.38, we have

$$Z_{TV}^{123}(\Sigma)_{\mathbf{Y}_1 \boxtimes \dots \boxtimes \mathbf{Y}_n}^{\mathbf{X}_1 \boxtimes \dots \boxtimes \mathbf{X}_m} = \bigoplus_L \bigotimes_{\sigma} Z_{TV}^{123}(\sigma) / \sim \quad (7.2)$$

where the tensor product ranges over all 1-generators σ appearing in the decomposition of Σ , and the direct sum ranges over all possible labellings (with objects in $Z(\mathcal{A})$) of the internal boundary circles. Each generating profunctor $Z_{TV}^{123}(\sigma)$ is computed using the boundary conditions induced from L and the given boundary conditions on the top and bottom circles.

Theorem 97. *Let Σ be a composite of the generating 1-morphisms of $\mathbf{F}(\mathcal{O})$, and let the top- and bottom boundary circles of Σ be labeled by $\mathbf{X}_1, \dots, \mathbf{X}_m$ and $\mathbf{Y}_1, \dots, \mathbf{Y}_n$ respectively. Let Δ be a PLCW decomposition of Σ .⁴ Then we have a natural isomorphism*

$$Z_{TV}^{123}(\Sigma)_{\mathbf{Y}_1 \boxtimes \dots \boxtimes \mathbf{Y}_n}^{\mathbf{X}_1 \boxtimes \dots \boxtimes \mathbf{X}_m} \cong Z_{TV}(\Sigma, \Delta, \{\mathbf{X}_1^*, \dots, \mathbf{X}_m^*, \mathbf{Y}_1, \dots, \mathbf{Y}_n\}) \quad (7.3)$$

Proof. The statement here is equivalent to the gluing axiom for extended surfaces, and we refer the reader to [2, Thm 8.4] for the proof. \square

Next we define the actions of the generating 2-morphisms. We shall divide the discussion up between the invertible- and the non-invertible generators.

The Invertible 2-Generators

Recall⁵ that each of the invertible 2-generators represent mapping cylinders of diffeomorphisms of the underlying surfaces. Let $N_s \xrightarrow{\kappa} N_t$ be any invertible 2-generator and let Δ_s be any PLCW decomposition of Σ . Then setting $\Delta_t = \kappa(\Delta_s)$, we define $Z_{TV}^{123}(\kappa)$ to be the pushforward⁶

$$Z_{TV}^{123}(N_s, \Delta_s) \xrightarrow{\kappa\#} Z_{TV}^{123}(N_t, \Delta_t). \quad (7.4)$$

⁴We are abusing the notation here in the same way as in Remark 96, writing Σ for the algebraic composite of the generators, as well as the underlying extended surface which can be formed by gluing all the generators together along the internal boundary circles, and gluing on embedded disks on the top and bottom external boundary circles.

⁵See Remark 44.

⁶See 6.45.

Note that we are abusing the notation somewhat by writing κ for both the 2-morphism as well as the diffeomorphism whose mapping cylinder it represents.

The Non-Invertible 2-Generators

Let $N_s \xrightarrow{\kappa} N_t$ be a non-invertible generating 2-morphism in $\mathbf{F}(\mathcal{O})$. Recall that in order to define the spaces which Z_{TV}^{123} assigned to the 1-generators, we thought of the 1-generators as extended surfaces rather than surfaces with boundary. This means that the action of κ will be witnessed by an extended 3-manifold with boundary, which we denote by M_κ . In other words, we have

$$\partial M_\kappa = \overline{N_s} \amalg N_t \quad (7.5)$$

so that we can think of M_κ as a 3-dimensional cobordism from N_s to N_t . Note first that the embedded disks on $\overline{N_s}$ and N_t occur in corresponding pairs⁷. For each such pair there will be a corresponding open tube in M_κ going from $\overline{N_s}$ to N_t (so that the embedded disk on $\overline{N_s}$ is the “bottom” disk of the tube, and the one on N_t the “top” disk - see Definition 82). It follows immediately that any labeling of the boundary circles induces a labeling of the corresponding open tubes.

Finally, we may describe the procedure for computing the action of κ . Given simple objects⁸ $\{\mathbf{X}_1, \dots, \mathbf{X}_m\}$ and $\{\mathbf{Y}_1, \dots, \mathbf{Y}_n\}$ labeling the top and bottom boundary circles respectively of N_s (and N_t), we do the following:

- (1) Colour the open tubes in M_κ in correspondence with the colours of the pairs of embedded disks, as explained above.
- (2) Choose any PLCW decomposition Δ of M_κ and let Δ_s and Δ_t denote the restriction of Δ to N_s and N_t respectively. This gives combinatorial extended surfaces $\mathcal{N}_s = (N_s, \Delta_s)$, $\mathcal{N}_t = (N_t, \Delta_t)$ and a combinatorial extended 3-manifold with boundary $\mathcal{M}_\kappa = (M_\kappa, \Delta)$.
- (3) Using the technology described in Chapter 6, compute the invariant $Z_{TV}(\mathcal{M}_\kappa, \{\mathbf{X}_1^*, \dots, \mathbf{X}_m^*, \mathbf{Y}_1, \dots, \mathbf{Y}_n\})$.
- (4) Making use of Property 6.3 to interpret the invariant as a linear map

$$Z_{TV}(\mathcal{N}_s, \{\mathbf{X}_1^*, \dots, \mathbf{X}_m^*, \mathbf{Y}_1, \dots, \mathbf{Y}_n\}) \rightarrow Z_{TV}(\mathcal{N}_t, \{\mathbf{X}_1^*, \dots, \mathbf{X}_m^*, \mathbf{Y}_1, \dots, \mathbf{Y}_n\}),$$

$$\text{we define } Z_{TV}^{123}(\kappa) = Z_{TV}(\mathcal{M}_\kappa, \{\mathbf{X}_1^*, \dots, \mathbf{X}_m^*, \mathbf{Y}_1, \dots, \mathbf{Y}_n\}).$$

⁷Every external boundary circle in N_s has a corresponding partner on N_t , otherwise κ would not be a valid 2-morphism.

⁸Recall that it is sufficient to consider such labelings - see [9, Lemma 5.3].

Remark 98. In order to avoid unnecessary duals in our formulas we shall colour the open tubes in \mathcal{M}_κ simply by $\mathbf{Y}_1, \dots, \mathbf{Y}_n$.

Now since $\partial M_\kappa = \overline{N}_s \amalg N_t = \overline{N}_s \amalg \overline{N}_t$, we may also interpret the invariant as a linear map

$$Z_{TV}(\overline{N}_t, \{\mathbf{X}_1, \dots, \mathbf{X}_m, \mathbf{Y}_1^*, \dots, \mathbf{Y}_n^*\}) \rightarrow Z_{TV}(\overline{N}_s, \{\mathbf{X}_1, \dots, \mathbf{X}_m, \mathbf{Y}_1^*, \dots, \mathbf{Y}_n^*\}), \tag{7.6}$$

Finally, since κ^\dagger represents the time-reversed bordism of κ , we have $M_{\kappa^\dagger} = \overline{M}_\kappa$, and hence the action of κ^\dagger can be computed from 7.6. This saves a great deal of time, as we only have to compute the invariant for M_κ - see 7.27 for a concrete example.

Remark 99. Since ν and ν^\dagger don't have boundary circles, the calculation of the invariant and associated linear maps are particularly simple, and so we perform all the calculations in full detail. For the remaining generators the calculations are somewhat repetitive, and so we show only a selection of them to illustrate the technique. The omitted calculations are done similarly.

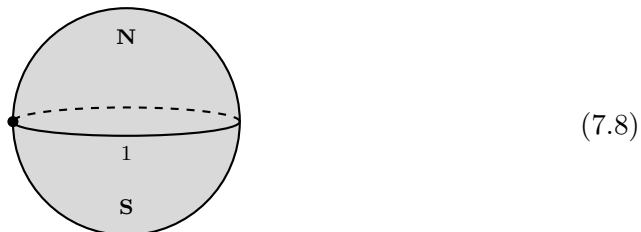
7.1.1 Nu and its dagger.

Recall that ν and ν^\dagger are defined by

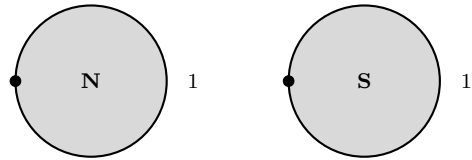
$$\square \begin{matrix} \xrightarrow{\nu} \\ \xleftarrow{\nu^\dagger} \end{matrix} \textcircled{\hspace{1cm}} \tag{7.7}$$

Recall further that $Z_{TV}(\emptyset) \cong H^{string}(\emptyset) \cong \mathbb{C}$, elements simply being scalar multiples of the empty string-net. Similarly, $Z_{TV}(S^2) \cong H^{string}(S^2) \cong \mathbb{C}$, with elements being scalar multiples of the empty string-net on S^2 . We next compute the desired linear maps.

The underlying 3-manifold M_ν with boundary which witnesses ν is simply the closed 3-dimensional disk. It has a standard PLCW decomposition, we call it Δ , consisting of one 0-cell, one 1-cell, two 2-cells \mathbf{N} and \mathbf{S} (representing the Northern- and Southern hemispheres respectively), and one 3-cell \mathbf{F} . There are no embedded disks. There is a unique non-zero simple labeling, assigning 1 to the lone edge.



We compute the spherical vector $Z(\mathbf{F}, l)$. Obviously $\partial\mathbf{F}$ simply consists of \mathbf{N} and \mathbf{S} . They are shown below with their state spaces.



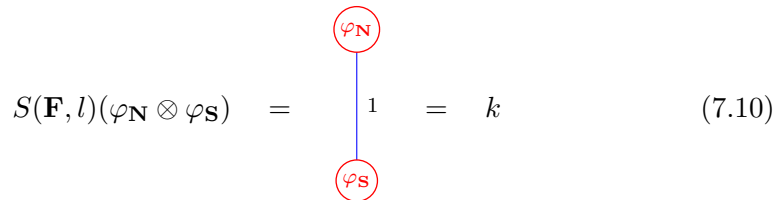
$$(7.9)$$

$$H(\mathbf{N}, l) = \langle 1 \rangle \quad H(\mathbf{S}, l) = \langle 1 \rangle$$

Therefore, given a choice of vectors

$$\begin{aligned} \varphi_{\mathbf{N}} &\in H(\mathbf{N}, l)^* = \langle 1 \rangle, \\ \varphi_{\mathbf{S}} &\in H(\mathbf{S}, l)^* = \langle 1 \rangle, \end{aligned}$$

we obtain the spherical vector



$$S(\mathbf{F}, l)(\varphi_{\mathbf{N}} \otimes \varphi_{\mathbf{S}}) = \text{diagram} = k \quad (7.10)$$

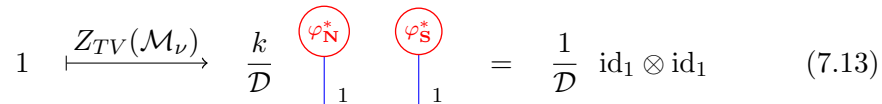
for some scalar k . The invariant is therefore given by

$$S_{TV}(\mathcal{M}_\nu)(\varphi_{\mathbf{N}} \otimes \varphi_{\mathbf{S}}) = \frac{k}{\mathcal{D}} \quad (7.11)$$

Next we turn this invariant into a linear map. Consider ν first. It arises as a cobordism from \emptyset to S^2 . We therefore obtain a map

$$Z_{TV}(\mathcal{M}_\nu) : H_{TV}(\emptyset) \rightarrow H_{TV}(S^2, \Delta) \quad (7.12)$$

given by



$$1 \xrightarrow{Z_{TV}(\mathcal{M}_\nu)} \frac{k}{\mathcal{D}} \text{diagram} = \frac{1}{\mathcal{D}} \text{id}_1 \otimes \text{id}_1 \quad (7.13)$$

For ν^\dagger , which arises as a cobordism from S^2 to \emptyset , we have the map

$$Z_{TV}(\mathcal{M}_{\nu^\dagger}) : H_{TV}(S^2, \Delta) \rightarrow H_{TV}(\emptyset) \quad (7.14)$$

given by

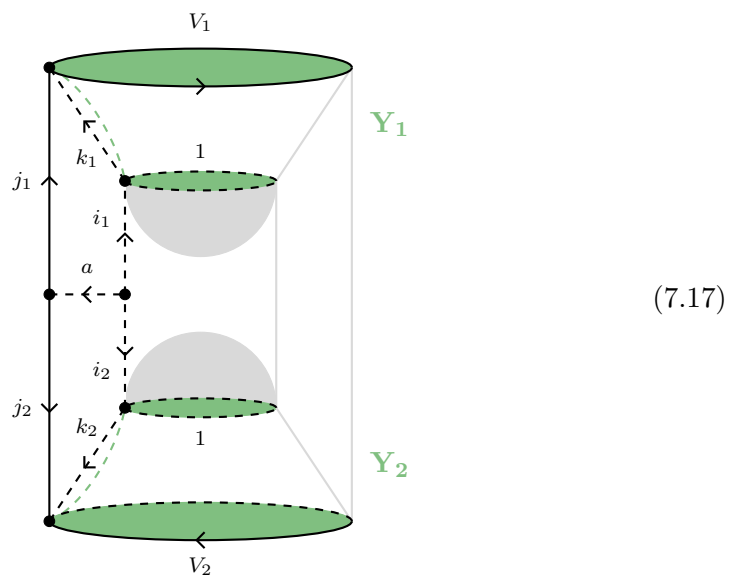
$$\text{id}_1 \otimes \text{id}_1 \xrightarrow{Z_{TV}(\mathcal{M}_{\nu^\dagger})} \frac{1}{\mathcal{D}}. \quad (7.15)$$

7.1.2 Mu and its dagger.

Recall that μ and μ^\dagger are defined by

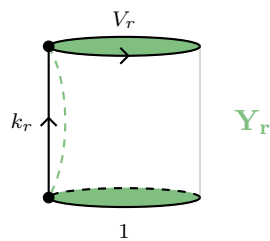
$$\begin{array}{ccc}
 \text{cup} & \xrightarrow{\mu} & \text{tube} \\
 \text{cup}^\dagger & \xleftarrow{\mu^\dagger} & \text{tube}
 \end{array}
 \tag{7.16}$$

Consider the following PLCW decomposition of M_μ , called Δ , shown with a simple labeling l . The two open tubes are coloured by simple objects $\mathbf{Y}_1, \mathbf{Y}_2 \in Z(\mathcal{A})$, as shown. The longitudes of the open tubes are shown as dashed green arcs.



Note that the edges of the bottom disks of the embedded tubes are labeled by 1 since they also form the boundary of the gray shaded 2-cells. There are four 3-cells in Δ . We compute the spherical vector for each one in turn.

- The open tubes \mathbf{T}_r , with $r \in \{1, 2\}$:



As usual the spherical vectors $S(\mathbf{T}_1, l)$ and $S(\mathbf{T}_2, l)$ are given by

$$S(\mathbf{T}_r, l)(\Phi_r) = \begin{array}{c} \text{---} \psi_r \text{---} \\ \uparrow V_r \\ \text{---} \beta_r \text{---} \\ \uparrow 1 \\ \text{---} \varphi_r \text{---} \end{array} \begin{array}{c} \text{---} k_r \text{---} \\ \uparrow Y_r \\ \text{---} \end{array}$$

where $\Phi_r = \varphi_r \otimes \beta_r \otimes \psi_r$.

- The middle 3-cell \mathbf{M}

$$(7.18)$$

The boundary $\partial\mathbf{M}$ consists of three oriented 2-cells, shown with their state spaces.

$$\langle 1 \rangle \quad \langle i_2^*, i_1, 1, i_1^*, i_2, 1 \rangle \quad \langle 1 \rangle$$

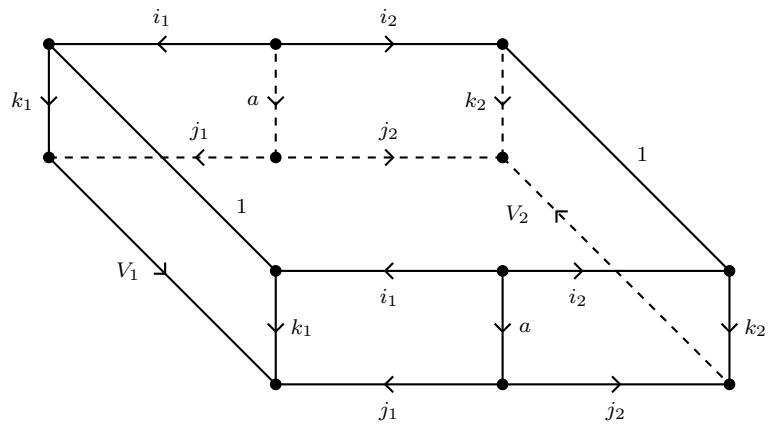
Therefore, given a choice of vectors

$$\begin{aligned} \text{id} &\in \langle 1 \rangle^* \cong \langle 1 \rangle, \\ \omega &\in \langle i_2^*, i_1, 1, i_1^*, i_2, 1 \rangle^* \cong \langle 1, i_2^*, i_1, 1, i_1^*, i_2 \rangle, \\ \text{id} &\in \langle 1 \rangle^* \cong \langle 1 \rangle, \end{aligned}$$

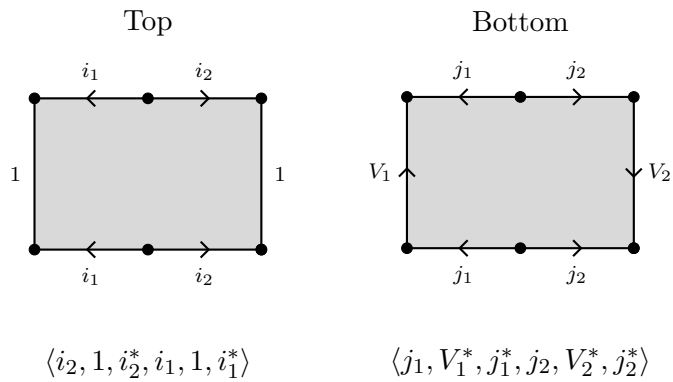
and letting $\Phi_{\mathbf{M}} = \text{id}_1 \otimes \omega \otimes \text{id}_1$, we obtain the spherical vector

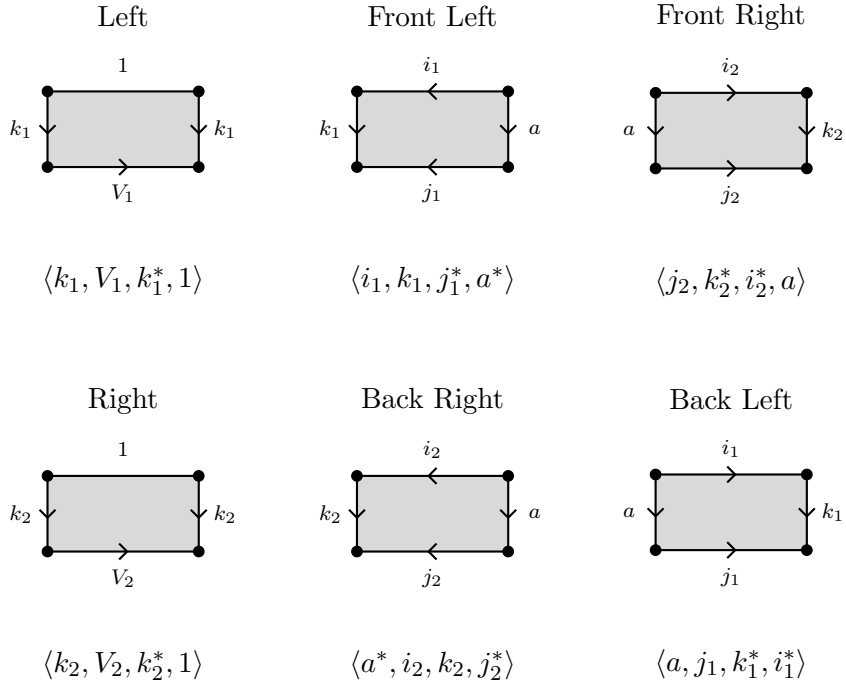
$$S(\mathbf{M}, l)(\Phi_{\mathbf{M}}) = \text{Diagram} \quad (7.19)$$

- The cylindrical 3-cell \mathbf{C}



The boundary $\partial\mathbf{C}$ consists of the following oriented 2-cells, shown with their state spaces.



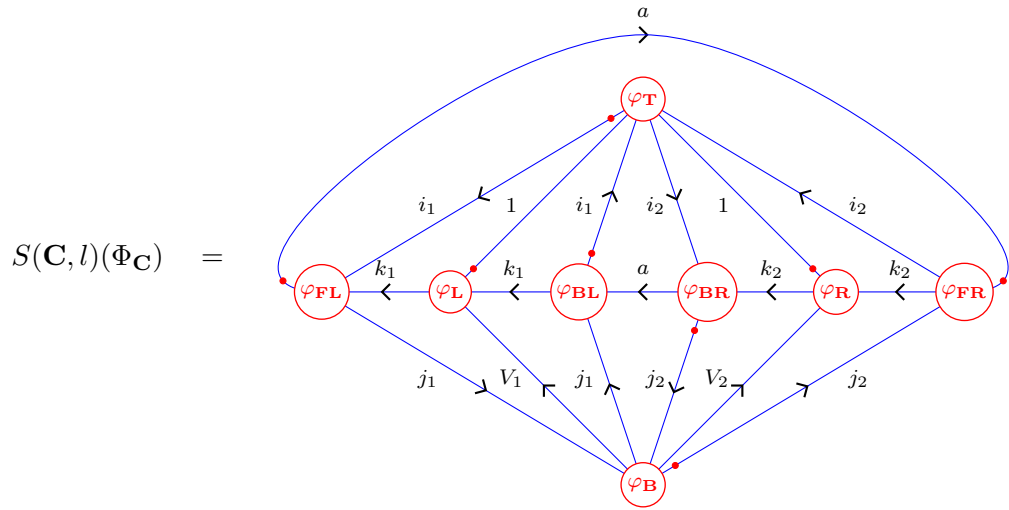


Therefore, given a choice a vectors

$$\begin{aligned}
 \varphi_{\mathbf{T}} &\in \langle i_2, 1, i_2^*, i_1, 1, i_1^* \rangle^* \cong \langle i_1, 1, i_1^*, i_2, 1, i_2^* \rangle, \\
 \varphi_{\mathbf{B}} &\in \langle j_1, V_1^*, j_1^*, j_2, V_2^*, j_2^* \rangle^* \cong \langle j_2, V_2, j_2^*, j_1, V_1, j_1^* \rangle, \\
 \varphi_{\mathbf{L}} &\in \langle k_1, V_1, k_1^*, 1 \rangle^* \cong \langle 1, k_1, V_1^*, k_1^* \rangle, \\
 \varphi_{\mathbf{FL}} &\in \langle i_1, k_1, j_1^*, a^* \rangle^* \cong \langle a, j_1, k_1^*, i_1^* \rangle, \\
 \varphi_{\mathbf{FR}} &\in \langle j_2, k_2^*, i_2^*, a \rangle^* \cong \langle a^*, i_2, k_2, j_2^* \rangle, \\
 \varphi_{\mathbf{R}} &\in \langle k_2, V_2, k_2^*, 1 \rangle^* \cong \langle 1, k_2, V_2^*, k_2^* \rangle, \\
 \varphi_{\mathbf{BR}} &\in \langle a^*, i_2, k_2, j_2^* \rangle^* \cong \langle j_2, k_2^*, i_2^*, a \rangle, \\
 \varphi_{\mathbf{BL}} &\in \langle a, j_1, k_1^*, i_1^* \rangle^* \cong \langle i_1, k_1, j_1^*, a^* \rangle,
 \end{aligned}$$

and letting $\Phi_{\mathbf{C}} = \varphi_{\mathbf{T}} \otimes \varphi_{\mathbf{B}} \otimes \varphi_{\mathbf{L}} \otimes \varphi_{\mathbf{FL}} \otimes \varphi_{\mathbf{FR}} \otimes \varphi_{\mathbf{R}} \otimes \varphi_{\mathbf{BR}} \otimes \varphi_{\mathbf{BL}}$, we obtain

the spherical vector



Making use of Equation 6.31, the full invariant $S_{TV}(\mathcal{M}_\mu, \{\mathbf{Y}_1, \mathbf{Y}_2\})(\Phi)$ is given by

$$\left(\frac{1}{\mathcal{D}^2}\right)^{1+\frac{5}{2}} \sum_l D \operatorname{ev}(S(\mathbf{T}_1, l)(\Phi_1) \cdot S(\mathbf{T}_2, l)(\Phi_2) \cdot S(\mathbf{M}, l)(\Phi_{\mathbf{M}}) \cdot S(\mathbf{C}, l)(\Phi_{\mathbf{C}})). \quad (7.20)$$

where the sum runs over all simple labelings l of Δ , where

$$D = d_{i_1} d_{i_2} d_{k_1} d_{k_2} d_a \sqrt{d_{V_1}} \sqrt{d_{V_2}} \sqrt{d_{j_1}} \sqrt{d_{j_2}},$$

where

$$\Phi = \operatorname{id}_1 \otimes \psi_1 \otimes \operatorname{id}_1 \otimes \psi_2 \otimes \varphi_2 \otimes \varphi_1 \otimes \varphi_{\mathbf{B}},$$

and where the evaluation enforces

$$\begin{aligned} \varphi_{\mathbf{L}} &= \beta_1^* & \varphi_{\mathbf{T}} &= \omega^* & \varphi_{\mathbf{FL}} &= \varphi_{\mathbf{BL}}^* \\ \varphi_{\mathbf{R}} &= \beta_2^* & & & \varphi_{\mathbf{FR}} &= \varphi_{\mathbf{BR}}^* \end{aligned}$$

Finally, we make use of Lemma 21 and Lemma 22, obtaining

$$S_{TV}(\mathcal{M}_\mu, \{\mathbf{Y}_1, \mathbf{Y}_2\})(\Phi) = \left(\frac{1}{\mathcal{D}^2}\right)^{\frac{7}{2}} \sum_{\substack{V_1, V_2, a \\ i_1, i_2, j_1, j_2}} \tilde{D}$$

where $\tilde{D} = d_{i_1} d_{i_2} d_a \sqrt{d_{V_1}} \sqrt{d_{V_2}} \sqrt{d_{j_1}} \sqrt{d_{j_2}}$.

It remains to compute the linear map version of $S_{TV}(\mathcal{M}_\mu, \{\mathbf{Y}_1, \mathbf{Y}_2\})$. As usual, it suffices to define the map on basis vectors. We obtain

113

$$\xrightarrow{Z_{TV}(\mathcal{M}_\mu, \{\mathbf{Y}_1, \mathbf{Y}_2\})} \left(\frac{1}{\mathcal{D}^2}\right)^{\frac{7}{2}} \sum_{\substack{V_1, V_2, a \\ i_1, i_2, j_1, j_2}} \tilde{D}$$

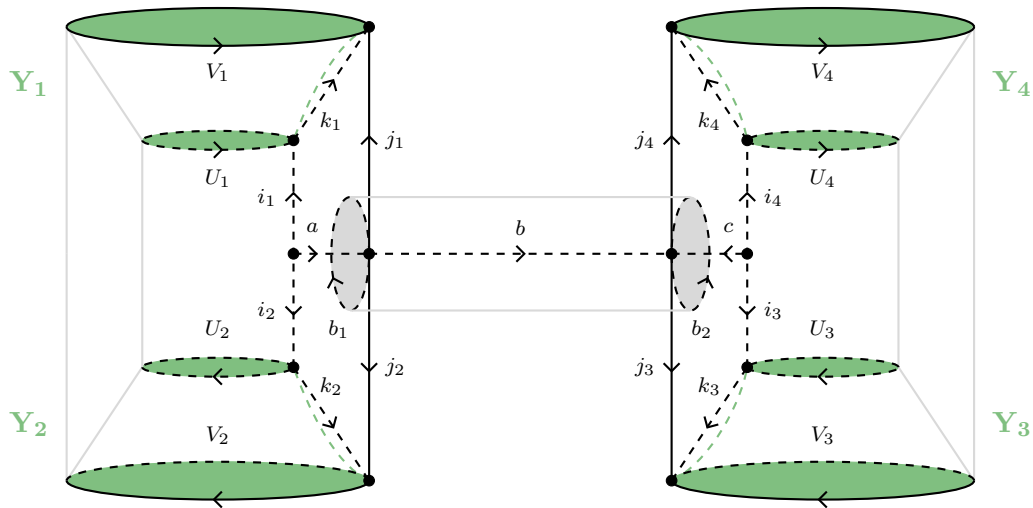
(7.21)

7.1.3 Eta and its dagger.

Recall that η and η^\dagger are defined by

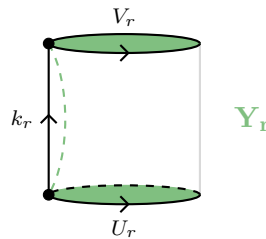
$$\begin{array}{ccc}
 \text{cylinder} & \xrightarrow{\eta} & \text{pair of pants} \\
 \text{cylinder} & \xleftarrow{\eta^\dagger} & \text{pair of pants}
 \end{array}
 \tag{7.23}$$

Consider the following PLCW decomposition of η . There are four tube cells, coloured by simple objects $\mathbf{Y}_1, \dots, \mathbf{Y}_4$ in $Z(\mathcal{A})$ as shown. The longitudes of the tubes are indicated by the dashed green lines.



Apart from the four tube cells, there are three 3-cells: two cylindrically shaped 3-cells (one for each “tower”), and a “bridge” 3-cell. We compute the spherical vector for each 3-cell below.

- The open tubes \mathbf{T}_r , with $r \in \{1, \dots, 4\}$:



As usual the spherical vectors are given by

$$S(\mathbf{T}_r, l)(\Phi_r) = \begin{array}{c} \text{---} k_r \text{---} \\ \uparrow \\ \psi_r \\ \uparrow V_r \\ \beta_r \\ \uparrow U_r \\ \varphi_r \end{array}$$

where $\Phi_r = \varphi_r \otimes \beta_r \otimes \psi_r$.

- The bridge 3-cell \mathbf{B}

$$(7.24)$$

The boundary $\partial\mathbf{B}$ consists of three oriented 2-cells, pictured below together with their state spaces.

$$\langle b_1 \rangle = \delta_{1, b_1} \langle 1 \rangle \qquad \langle b, b_2, b^*, b_1^* \rangle \qquad \langle b_2 \rangle = \delta_{1, b_2} \langle 1 \rangle$$

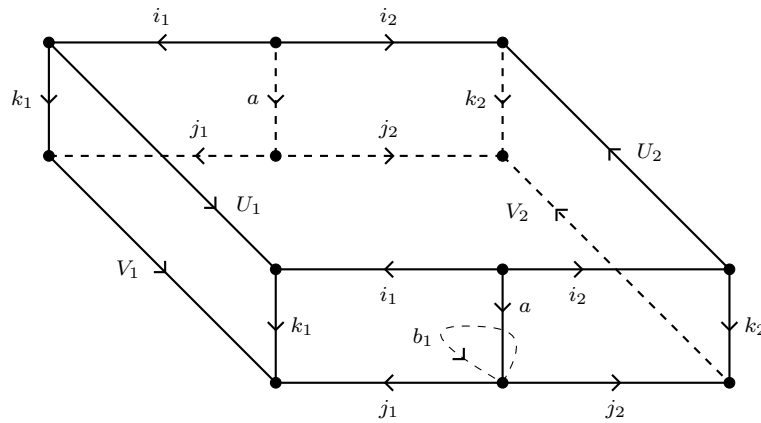
Therefore, given a choice of vectors

$$\begin{aligned} \gamma_{\mathbf{L}} &\in \delta_{1, b_1} \langle 1 \rangle^* \cong \delta_{1, b_1} \langle 1 \rangle, \\ \gamma &\in \langle b, b_2, b^*, b_1^* \rangle^* \cong \langle b_1, b, b_2^*, b^* \rangle, \\ \gamma_{\mathbf{R}} &\in \delta_{1, b_2} \langle 1 \rangle^* \cong \delta_{1, b_2} \langle 1 \rangle, \end{aligned}$$

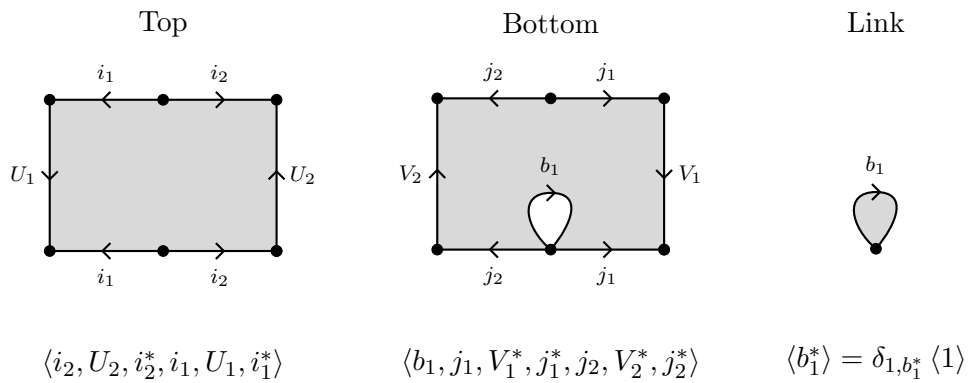
and letting $\Phi_{\mathbf{B}} = \gamma_{\mathbf{L}} \otimes \gamma \otimes \gamma_{\mathbf{R}}$, we obtain the spherical vector

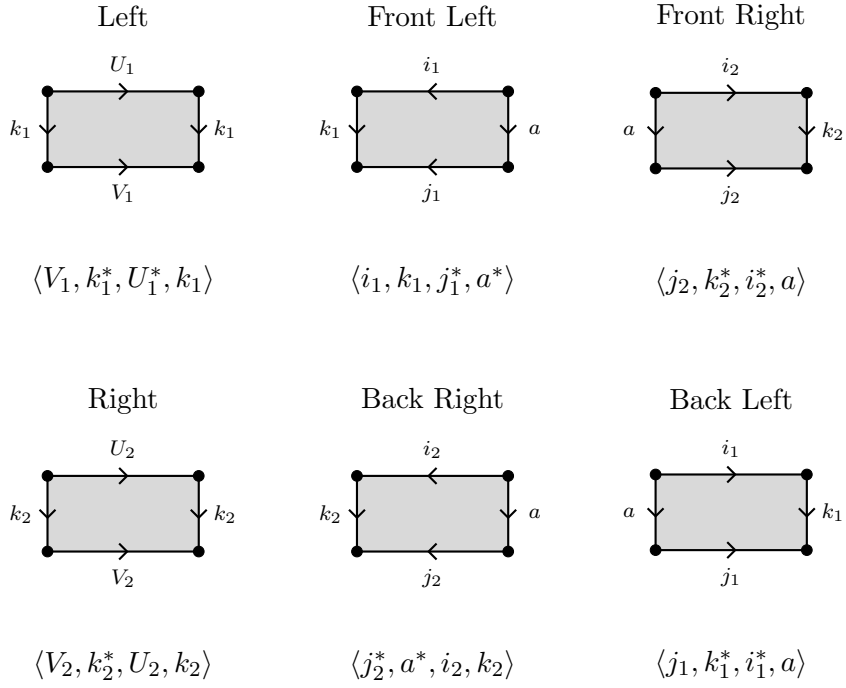
$$S(\mathbf{B}, l)(\Phi_{\mathbf{B}}) = \delta_{1,b_1} \delta_{1,b_2} \quad \begin{array}{c} \textcircled{\gamma_{\mathbf{L}}} \text{---} 1 \text{---} \textcircled{\gamma} \text{---} 1 \text{---} \textcircled{\gamma_{\mathbf{R}}} \\ \text{---} b \end{array}$$

- The left cylindrical 3-cell \mathbf{L}



The boundary $\partial\mathbf{L}$ consists of the following oriented 2-cells, shown with their state spaces.

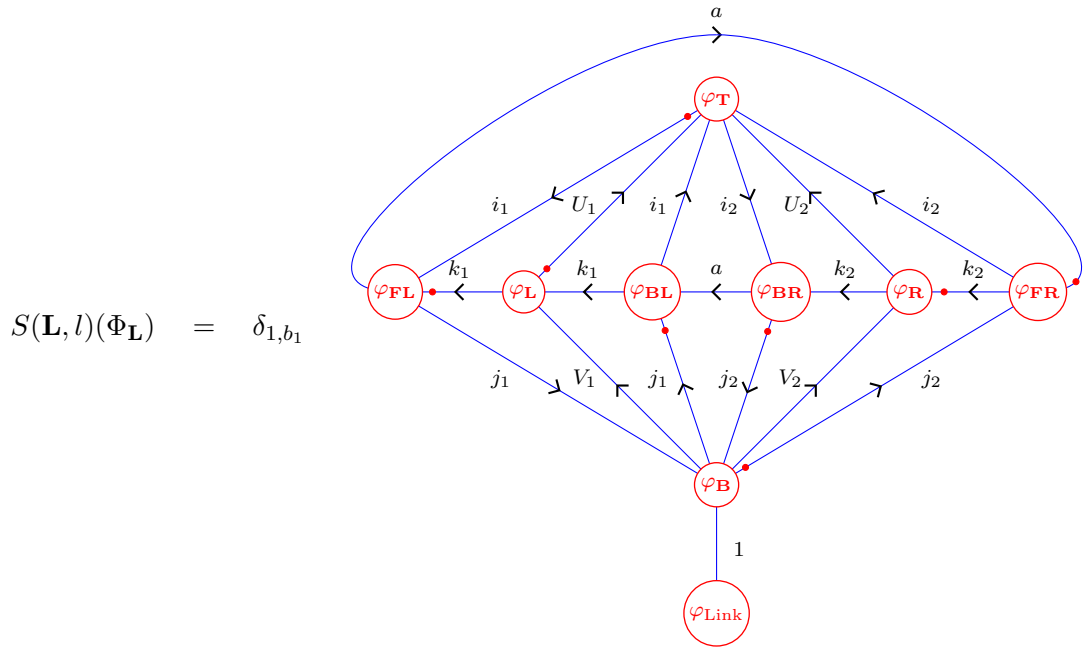




Therefore, given a choice of vectors

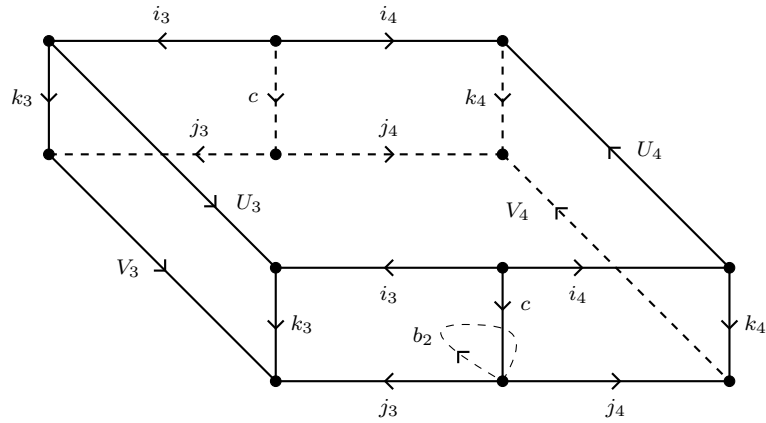
$$\begin{aligned}
 \varphi_{\mathbf{T}} &\in \langle i_2, U_2, i_2^*, i_1, U_1, i_1^* \rangle^* \cong \langle i_1, U_1^*, i_1^*, i_2, U_2^*, i_2^* \rangle, \\
 \varphi_{\mathbf{B}} &\in \langle b_1, j_1, V_1^*, j_1^*, j_2, V_2^*, j_2^* \rangle^* \cong \langle j_2, V_2, j_2^*, j_1, V_1, j_1^*, b_1^* \rangle, \\
 \varphi_{\mathbf{Link}} &\in \delta_{1,b_1} \langle 1 \rangle^* \cong \delta_{1,b_1} \langle 1 \rangle, \\
 \varphi_{\mathbf{L}} &\in \langle V_1, k_1^*, U_1^*, k_1 \rangle^* \cong \langle k_1^*, U_1, k_1, V_1^* \rangle, \\
 \varphi_{\mathbf{FL}} &\in \langle i_1, k_1, j_1^*, a^* \rangle^* \cong \langle a, j_1, k_1^*, i_1^* \rangle, \\
 \varphi_{\mathbf{FR}} &\in \langle j_2, k_2^*, i_2^*, a \rangle^* \cong \langle a^*, i_2, k_2, j_2^* \rangle, \\
 \varphi_{\mathbf{R}} &\in \langle V_2, k_2^*, U_2, k_2 \rangle^* \cong \langle k_2^*, U_2^*, k_2, V_2^* \rangle, \\
 \varphi_{\mathbf{BR}} &\in \langle j_2^*, a^*, i_2, k_2 \rangle^* \cong \langle k_2^*, i_2^*, a, j_2 \rangle, \\
 \varphi_{\mathbf{BL}} &\in \langle j_1, k_1^*, i_1^*, a \rangle^* \cong \langle a^*, i_1, k_1, j_1^* \rangle,
 \end{aligned}$$

we obtain the spherical vector



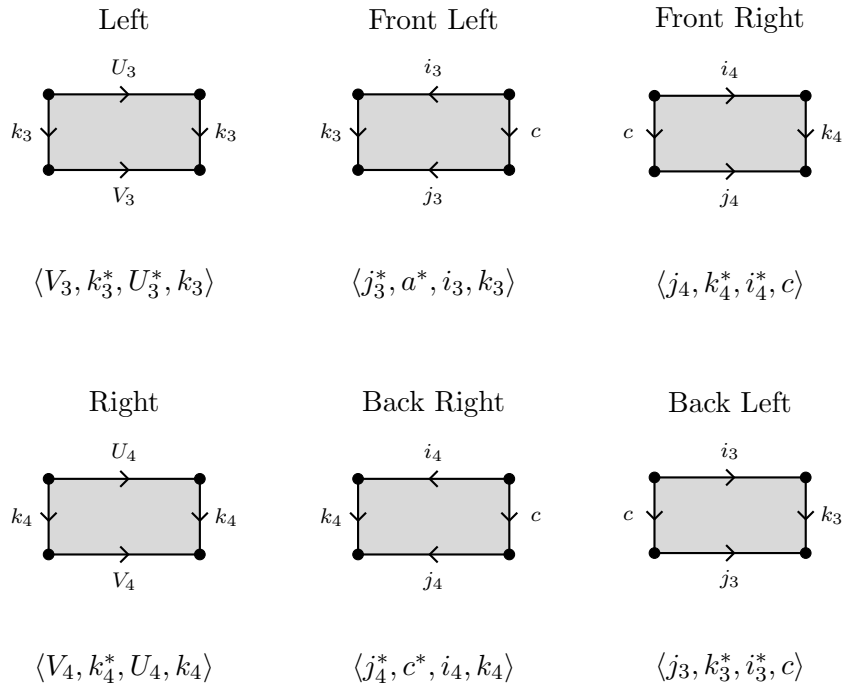
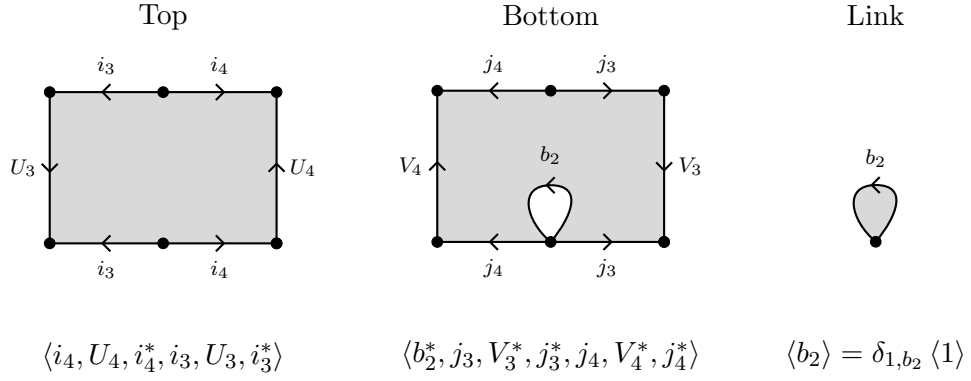
where $\Phi_{\mathbf{L}} = \varphi_{\mathbf{FL}} \otimes \varphi_{\mathbf{L}} \otimes \varphi_{\mathbf{BL}} \otimes \varphi_{\mathbf{BR}} \otimes \varphi_{\mathbf{R}} \otimes \varphi_{\mathbf{FR}} \otimes \varphi_{\mathbf{T}} \otimes \varphi_{\mathbf{B}} \otimes \varphi_{\mathbf{Link}}$.

- The right cylindrical 3-cell \mathbf{R}



The boundary $\partial \mathbf{R}$ consists of the following oriented 2-cells, shown with their

state spaces.

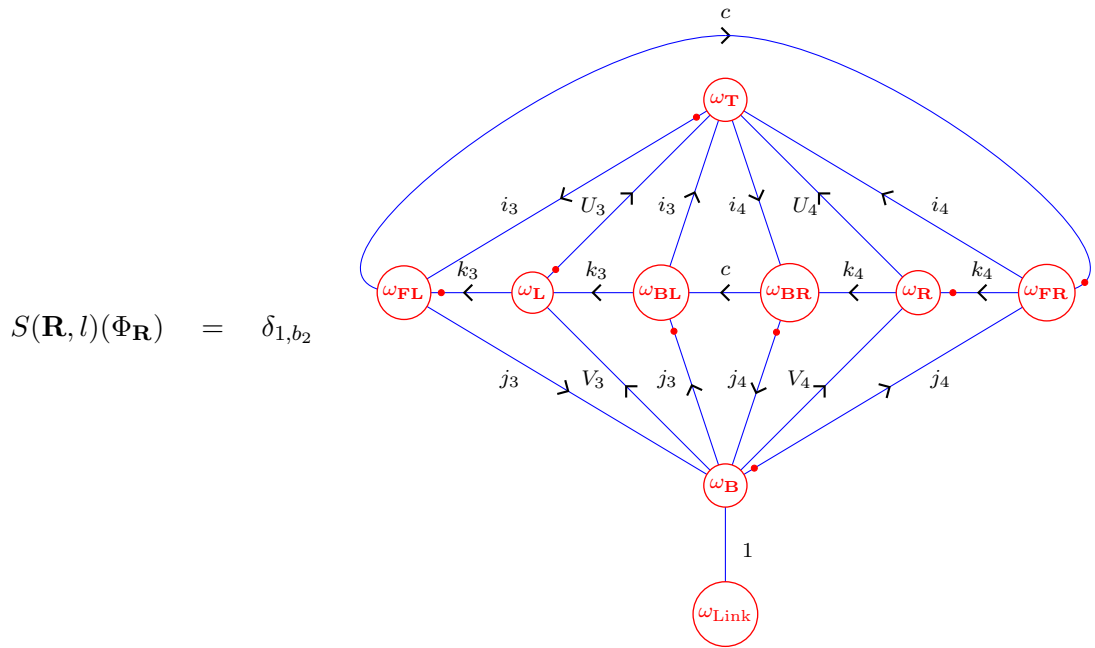


Therefore, given a choice of vectors

$$\begin{aligned}
 \omega_{\mathbf{T}} &\in \langle i_4, U_4, i_4^*, i_3, U_3, i_3^* \rangle^* \cong \langle i_3, U_3^*, i_3^*, i_4, U_4^*, i_4^* \rangle, \\
 \omega_{\mathbf{B}} &\in \langle b_2^*, j_3, V_3^*, j_3^*, j_4, V_4^*, j_4^* \rangle^* \cong \langle j_4, V_4, j_4^*, j_3, V_3, j_3^*, b_2 \rangle, \\
 \omega_{\text{Link}} &\in \langle 1 \rangle^* \cong \langle 1 \rangle, \\
 \omega_{\mathbf{L}} &\in \langle V_3, k_3^*, U_3^*, k_3 \rangle^* \cong \langle k_3^*, U_3, k_3, V_3^* \rangle, \\
 \omega_{\mathbf{FL}} &\in \langle j_3^*, c^*, i_3, k_3 \rangle^* \cong \langle k_3^*, i_3^*, c, j_3 \rangle, \\
 \omega_{\mathbf{FR}} &\in \langle j_4, k_4^*, i_4^*, c \rangle^* \cong \langle c^*, i_4, k_4, j_4^* \rangle,
 \end{aligned}$$

$$\begin{aligned}\omega_{\mathbf{R}} &\in \langle V_4, k_4^*, U_4, k_4 \rangle^* \cong \langle k_4^*, U_4^*, k_4, V_4^* \rangle, \\ \omega_{\mathbf{BR}} &\in \langle j_4^*, c^*, i_4, k_4 \rangle^* \cong \langle k_4^*, i_4^*, c, j_4 \rangle, \\ \omega_{\mathbf{BL}} &\in \langle j_3, k_3^*, i_3^*, c \rangle^* \cong \langle c^*, i_3, k_3, j_3^* \rangle,\end{aligned}$$

we obtain the spherical vector



where $\Phi_{\mathbf{R}} = \omega_{\mathbf{FL}} \otimes \omega_{\mathbf{L}} \otimes \omega_{\mathbf{BL}} \otimes \omega_{\mathbf{BR}} \otimes \omega_{\mathbf{R}} \otimes \omega_{\mathbf{FR}} \otimes \omega_{\mathbf{T}} \otimes \omega_{\mathbf{B}} \otimes \omega_{\mathbf{Link}}$.

Making use of Equation 6.33, the full invariant $S_{TV}(\mathcal{M}_\eta; \{\mathbf{Y}_1, \mathbf{Y}_2, \mathbf{Y}_3, \mathbf{Y}_4\})(\Phi)$ is given by

$$\left(\frac{1}{\mathcal{D}^2}\right)^{\frac{12}{2}} \sum_l D \cdot \text{ev} \left(\prod_{r=1}^4 S(\mathbf{T}_r, l)(\Phi_r) \cdot S(\mathbf{B}, l)(\Phi_{\mathbf{B}}) \cdot S(\mathbf{L}, l)(\Phi_{\mathbf{L}}) \cdot S(\mathbf{R}, l)(\Phi_{\mathbf{R}}) \right)$$

where the sum runs over all simple labelings l of Δ , where

$$D = \delta_{1,b_1} \delta_{1,b_2} d_a d_c \sqrt{d_b} \prod_{r=1}^4 d_{k_r} \sqrt{d_{U_r}} \sqrt{d_{V_r}} \sqrt{d_{i_r}} \sqrt{d_{j_r}},$$

where

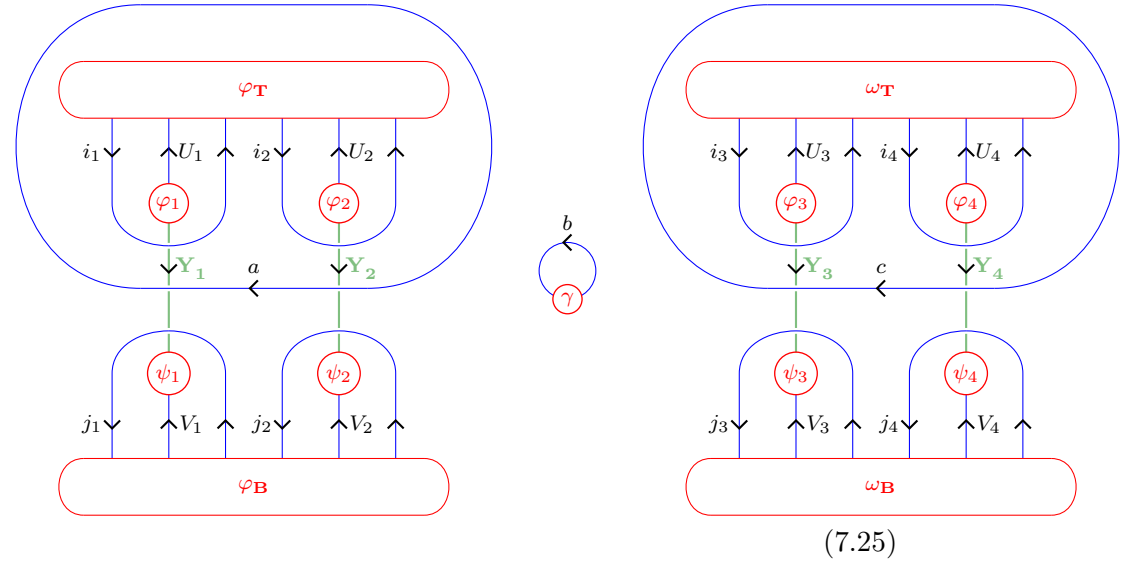
$$\Phi = \gamma \otimes \bigotimes_{r=1}^4 (\varphi_r \otimes \psi_r) \otimes \varphi_{\mathbf{T}} \otimes \varphi_{\mathbf{B}} \otimes \omega_{\mathbf{T}} \otimes \omega_{\mathbf{B}},$$

and where the evaluation enforces

$$\begin{array}{lllll} \beta_1 = \varphi_{\mathbf{L}}^* & \beta_3 = \omega_{\mathbf{L}}^* & \gamma_{\mathbf{L}} = \varphi_{\text{Link}}^* & \varphi_{\mathbf{FL}} = \varphi_{\mathbf{BL}}^* & \omega_{\mathbf{FL}} = \omega_{\mathbf{BL}}^* \\ \beta_2 = \varphi_{\mathbf{R}}^* & \beta_4 = \omega_{\mathbf{R}}^* & \gamma_{\mathbf{R}} = \omega_{\text{Link}}^* & \varphi_{\mathbf{FR}} = \varphi_{\mathbf{BR}}^* & \omega_{\mathbf{FR}} = \omega_{\mathbf{BR}}^* \end{array}$$

In diagrammatic form, we have the following:

$$S_{TV}(\mathcal{M}_\eta; \{\mathbf{Y}_1, \mathbf{Y}_2, \mathbf{Y}_3, \mathbf{Y}_4\})(\Phi) = \left(\frac{1}{\mathcal{D}^2}\right)^6 \sum \tilde{D}$$

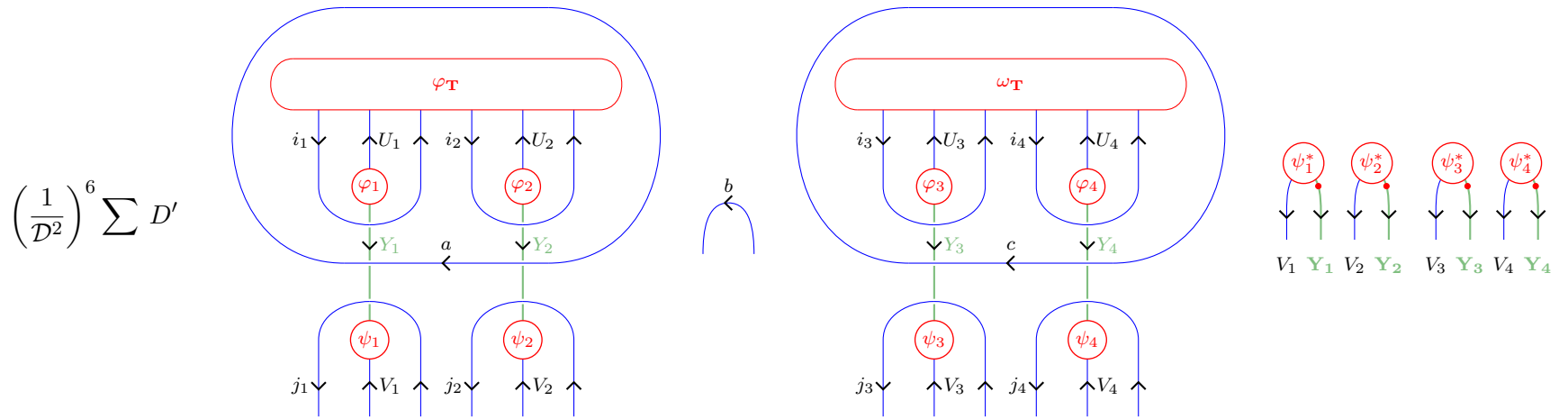
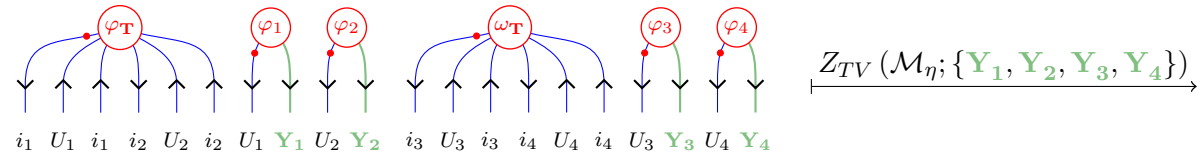


where the sum runs over all simple edge labelings

$$U_1, U_2, U_3, U_4, V_1, V_2, V_3, V_4, i_1, i_2, i_3, i_4, j_1, j_2, j_3, j_4, a, b, b_1, b_2, c,$$

and where

$$\tilde{D} = \delta_{1,b_1} \delta_{1,b_2} d_a d_c \sqrt{d_b} \prod_{r=1}^4 \sqrt{d_{U_r}} \sqrt{d_{V_r}} \sqrt{d_{i_r}} \sqrt{d_{j_r}}.$$



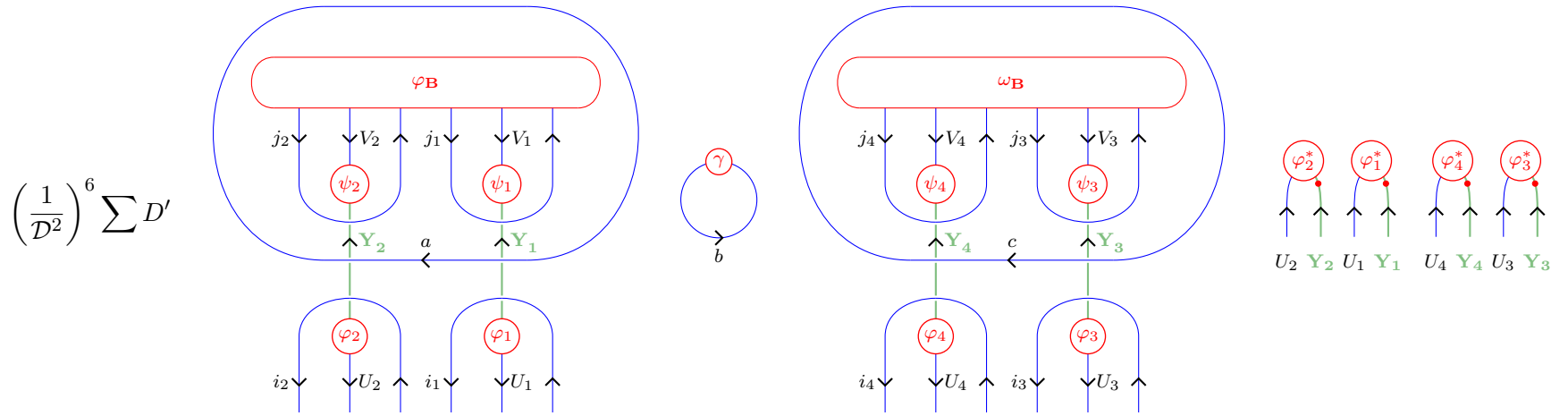
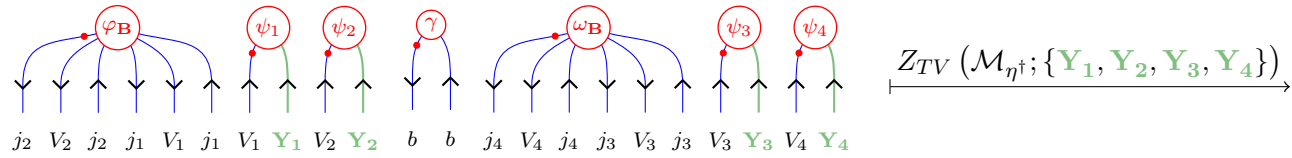
(7.26)

where the sum runs over all simple edge labelings

$$V_1, V_2, V_3, V_4, j_1, j_2, j_3, j_4, a, b, b_1, b_2, c,$$

and where

$$D' = \delta_{1,b_1} \delta_{1,b_2} d_a d_c \sqrt{d_b} \prod_{r=1}^4 \sqrt{d_{V_r}} \sqrt{d_{j_r}}.$$



(7.27)

where the sum runs over all simple edge labelings

$$U_1, U_2, U_3, U_4, i_1, i_2, i_3, i_4, a, c, b_1, b_2$$

and where

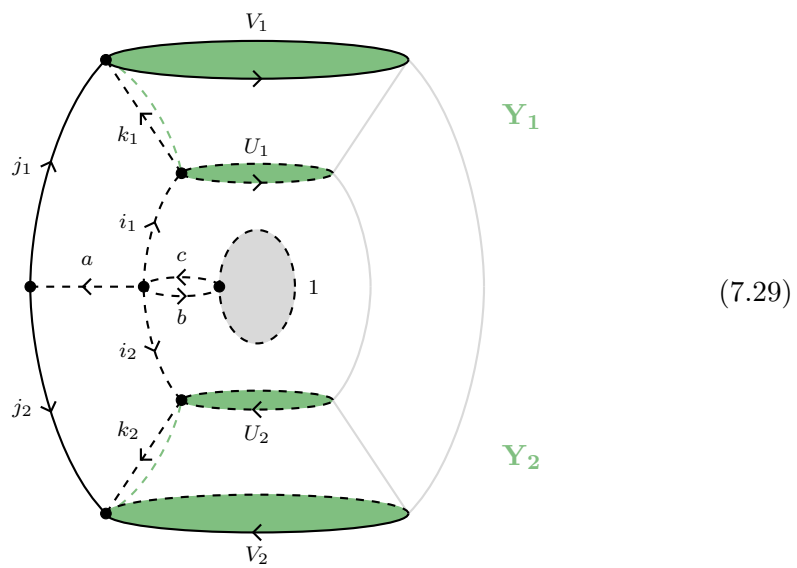
$$D' = \delta_{1,b_1} \delta_{1,b_2} d_a d_c \prod_{r=1}^4 \sqrt{d_{U_r}} \sqrt{d_{i_r}}.$$

7.1.4 Epsilon and its dagger

Recall that ϵ and ϵ^\dagger are defined by

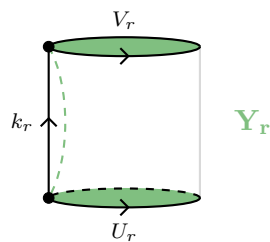
$$\begin{array}{ccc}
 \text{[Diagram of a sphere with a hole]} & \begin{array}{c} \xrightarrow{\epsilon} \\ \xleftarrow{\epsilon^\dagger} \end{array} & \text{[Diagram of a tube]} \\
 & & (7.28)
 \end{array}$$

Consider the following PLCW decomposition, called Δ , of M_ϵ , shown with a simple labeling l . There are two tube cells, coloured by simple objects \mathbf{Y}_1 and \mathbf{Y}_2 in $Z(\mathcal{A})$.



There are three 3-cells in this PLCW decomposition - the two open tubes and a big central 3-cell.

- The open tubes \mathbf{T}_r , with $r \in \{1, 2\}$:

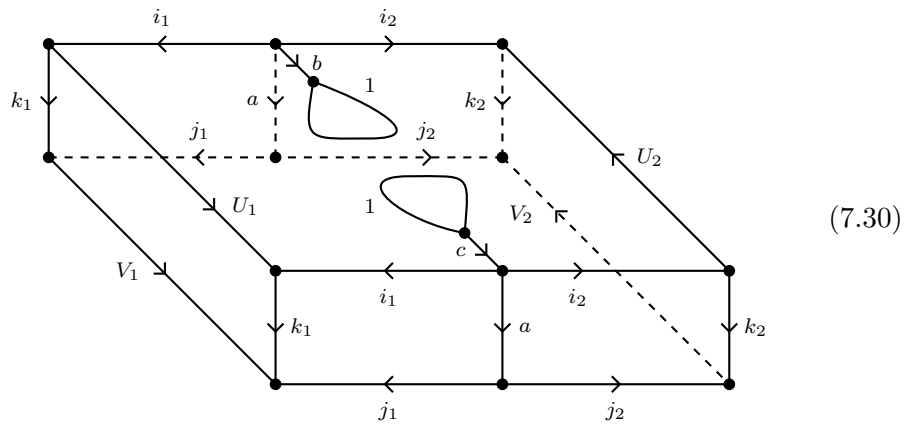


As usual the spherical vectors $S(\mathbf{T}_1, l)$ and $S(\mathbf{T}_2, l)$ are given by

$$S(\mathbf{T}_r, l)(\Phi_r) =$$

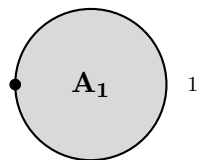
where $\Phi_r = \varphi_r \otimes \beta_r \otimes \psi_r$.

- The central 3-cell \mathbf{C} :



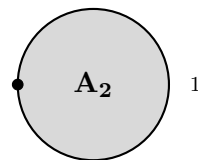
The boundary $\partial\mathbf{C}$ consists of the following oriented 2-cells, shown with their state spaces.

Front Axis Link

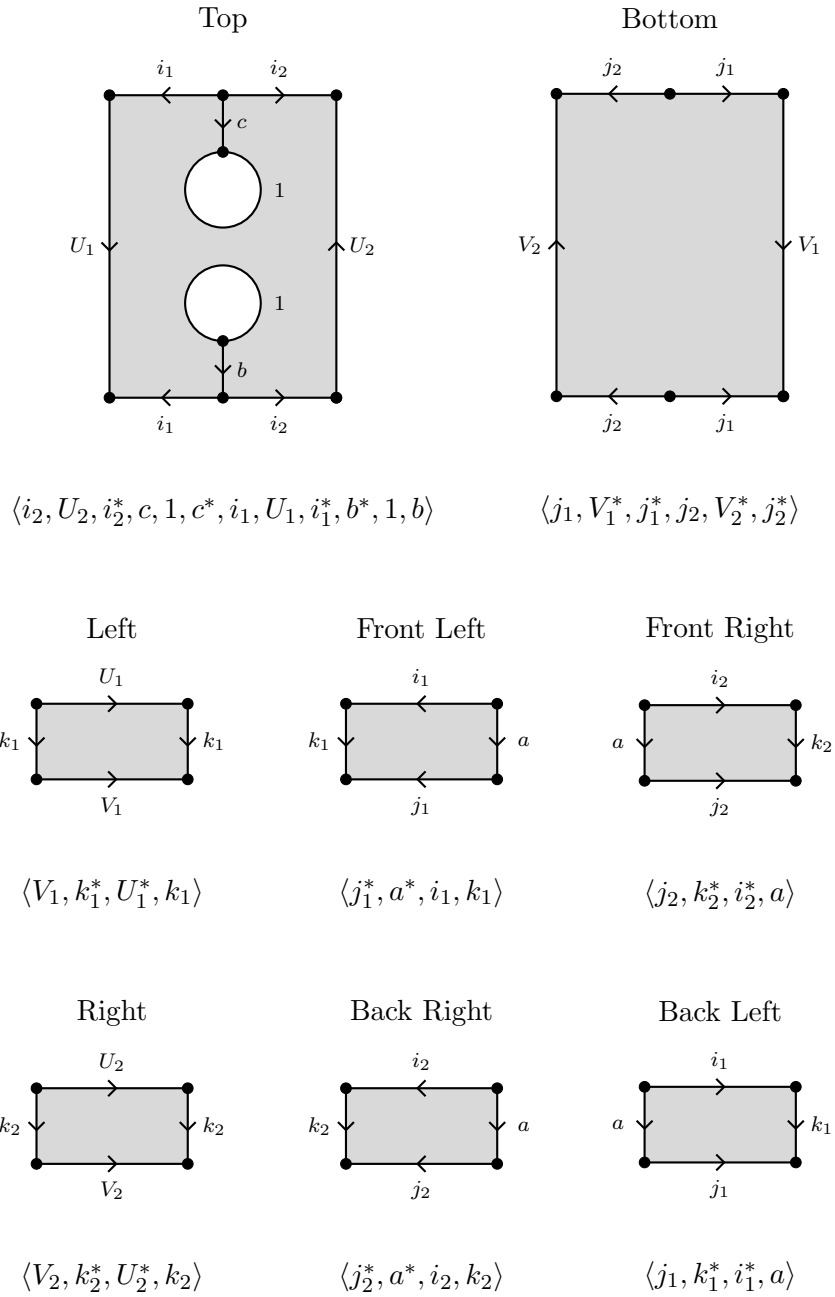


$\langle 1 \rangle$

Back Axis Link



$\langle 1 \rangle$



Therefore, given a choice of vectors

$$\varphi_{\mathbf{A}_1} \in \langle 1 \rangle^* = \langle 1 \rangle = \mathbb{C},$$

$$\varphi_{\mathbf{A}_2} \in \langle 1 \rangle^* = \langle 1 \rangle = \mathbb{C},$$

$$\begin{aligned}
 \varphi_{\mathbf{T}} &\in \langle i_2, U_2, i_2^*, c, 1, c^*, i_1, U_1, i_1^*, b^*, 1, b \rangle^* = \langle b^*, 1, b, i_1, U_1^*, i_1^*, c, 1, c^*, i_2, U_2^*, i_2^* \rangle, \\
 \varphi_{\mathbf{B}} &\in \langle j_1, V_1^*, j_1^*, j_2, V_2^*, j_2^* \rangle^* = \langle j_2, V_2, j_2^*, j_1, V_1, j_1^* \rangle, \\
 \varphi_{\mathbf{L}} &\in \langle V_1, k_1^*, U_1^*, k_1 \rangle^* = \langle k_1^*, U_1, k_1, V_1^* \rangle, \\
 \varphi_{\mathbf{FL}} &\in \langle j_1^*, a^*, i_1, k_1 \rangle^* = \langle k_1^*, i_1^*, a, j_1 \rangle, \\
 \varphi_{\mathbf{FR}} &\in \langle j_2, k_2^*, i_2^*, a \rangle^* = \langle a^*, i_2, k_2, j_2^* \rangle, \\
 \varphi_{\mathbf{R}} &\in \langle V_2, k_2^*, U_2^*, k_2 \rangle^* = \langle k_2^*, U_2, k_2, V_2^* \rangle, \\
 \varphi_{\mathbf{BR}} &\in \langle j_2^*, a^*, i_2, k_2 \rangle^* = \langle k_2^*, i_2^*, a, j_2 \rangle, \\
 \varphi_{\mathbf{BL}} &\in \langle j_1, k_1^*, i_1^*, a \rangle^* = \langle a^*, i_1, k_1, j_1^* \rangle,
 \end{aligned}$$

we obtain the following spherical vector

$$S(\mathbf{C}, l)(\Phi_{\mathbf{C}}) =$$

(7.31)

where $\Phi_{\mathbf{C}} = \varphi_{\mathbf{A}_1} \otimes \varphi_{\mathbf{A}_2} \otimes \varphi_{\mathbf{FL}} \otimes \varphi_{\mathbf{L}} \otimes \varphi_{\mathbf{BL}} \otimes \varphi_{\mathbf{BR}} \otimes \varphi_{\mathbf{R}} \otimes \varphi_{\mathbf{FR}} \otimes \varphi_{\mathbf{T}} \otimes \varphi_{\mathbf{B}}$.

Making use of Equation 6.33, the full invariant $S_{TV}(\mathcal{M}_\epsilon, \{\mathbf{Y}_1, \mathbf{Y}_2\})(\Phi)$ is given by

$$\left(\frac{1}{\mathcal{D}^2}\right)^{\frac{7}{2}} \sum_{\substack{V_1, V_2, U_1, U_2, k_1, k_2 \\ i_1, i_2, j_1, j_2, a, b, c}} D \cdot \text{ev}(S(\mathbf{T}_1, l)(\Phi_1) \otimes S(\mathbf{T}_2, l)(\Phi_2) \otimes S(\mathbf{C}, l)(\Phi_{\mathbf{C}})), \quad (7.32)$$

where

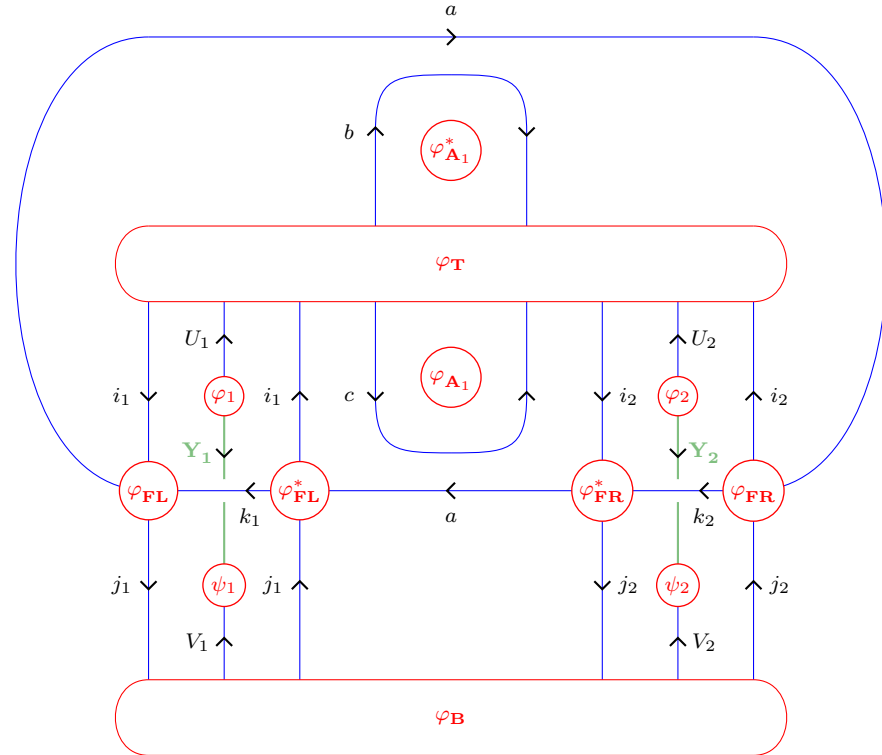
$$D = d_a d_{k_1} d_{k_2} \sqrt{d_{i_1}} \sqrt{d_{i_2}} \sqrt{d_{j_1}} \sqrt{d_{j_2}} \sqrt{d_{U_1}} \sqrt{d_{U_2}} \sqrt{d_{V_1}} \sqrt{d_{V_2}} \sqrt{d_b} \sqrt{d_c},$$

and where the evaluation enforces

$$\begin{aligned} \beta_1 &= \varphi_{\mathbf{L}}^* & \varphi_{\mathbf{A}_1}^* &= \varphi_{\mathbf{A}_2} & \varphi_{\mathbf{FL}} &= \varphi_{\mathbf{BL}}^* \\ \beta_2 &= \varphi_{\mathbf{R}}^* & & & \varphi_{\mathbf{FR}} &= \varphi_{\mathbf{BR}}^* \end{aligned}$$

If we perform these changes we may merge the diagrams for $S(\mathbf{T}_1, l)$ and $S(\mathbf{T}_2, l)$ into $S(\mathbf{C}, l)$ via the Fusion lemma [22]. Doing so yields the following:

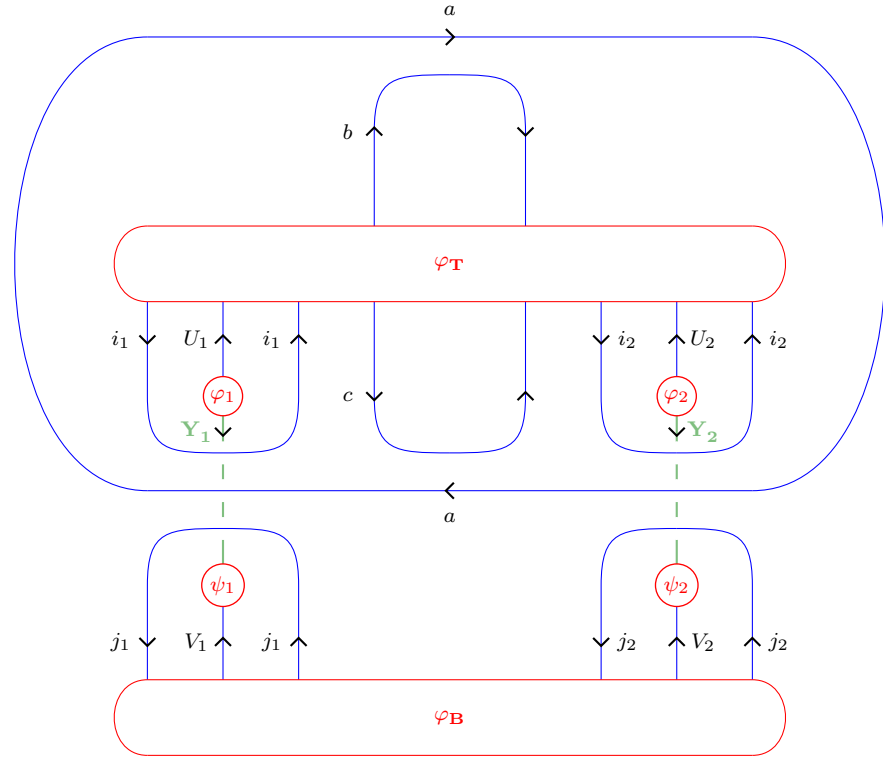
$$S_{TV}(\mathcal{M}_\epsilon, \{\mathbf{Y}_1, \mathbf{Y}_2\})(\Phi) = \left(\frac{1}{\mathcal{D}^2}\right)^{\frac{7}{2}} \sum_{\substack{V_1, V_2, U_1, U_2, k_1, k_2 \\ i_1, i_2, j_1, j_2, a, b, c}} D$$



(7.33)

The vertices labeled φ_{A_1} and $\varphi_{A_1}^*$ will cancel, since they are simply reciprocal scalars. Finally, applying Lemma 21 along the edges labeled by k_1 and k_2 yields

$$S_{TV}(\mathcal{M}_\epsilon, \{\mathbf{Y}_1, \mathbf{Y}_2\})(\Phi) = \left(\frac{1}{\mathcal{D}^2}\right)^{\frac{7}{2}} \sum_{\substack{V_1, V_2, U_1, U_2 \\ i_1, i_2, j_1, j_2, a, b, c}} \tilde{D}$$



(7.34)

where

$$\tilde{D} = d_a \sqrt{d_{i_1}} \sqrt{d_{i_2}} \sqrt{d_{j_1}} \sqrt{d_{j_2}} \sqrt{d_{U_1}} \sqrt{d_{U_2}} \sqrt{d_{V_1}} \sqrt{d_{V_2}} \sqrt{d_b} \sqrt{d_c}.$$

7.2 Relations

Having defined the actions of each of the generating 2-morphisms, it remains to check that all of the relations are satisfied. It would be incredibly cumbersome to check the relations directly using the Turaev-Viro actions as they currently stand, as the formulas are rather messy and technical. Instead, our strategy shall be to compare the Turaev-Viro actions with the string-net actions from Section 5.2.

Theorem 100. *Let $N_s \xrightarrow{\kappa} N_t$ be any generating 2-morphism in $\mathbf{F}(\mathcal{O})$, and let Δ_s and Δ_t be PLCW decompositions of N_s and N_t respectively. Then (for any permissible labeling of the boundary circles) the following diagram commutes:*

$$\begin{array}{ccc}
 Z_{TV}^{123}(\mathcal{N}_s) & \xrightarrow{Z_{TV}^{123}(\kappa)} & Z_{TV}^{123}(\mathcal{N}_t) \\
 \pi_{\Delta_s} \downarrow & & \downarrow \pi_{\Delta_t} \\
 Z_{SN}^{123}(N_s) & \xrightarrow{Z_{SN}^{123}(\kappa)} & Z_{SN}^{123}(N_t)
 \end{array} \tag{7.35}$$

Before we prove this theorem, we note its consequences. The first of these is that Z_{TV}^{123} defines a generators-and-relations 123-TQFT.

Corollary 101. *Under Z_{TV}^{123} the actions of the generating 2-morphisms satisfy the required relations, and hence Z_{TV}^{123} defines an oriented 123-TQFT.*

Theorem 102. *We have an equivalence of oriented 123-TQFTs*

$$Z_{SN}^{123} \simeq Z_{TV}^{123}. \tag{7.36}$$

Proof. This follows immediately from Theorem 100, Theorem 94, and Definition 49. \square

Proof of Theorem 100. For each of the invertible 2-generators commutativity follows trivially since the horizontal maps are, in both cases, simply the pushforward along the diffeomorphism associated to κ . For the non-invertible generators, because the calculations are fairly repetitive, we shall only write the commuting square for μ in full detail. The calculations for the remaining generators follow exactly the same pattern.

Applying π_{Δ_s} to the source vector in Equation 7.22, we obtain the following:

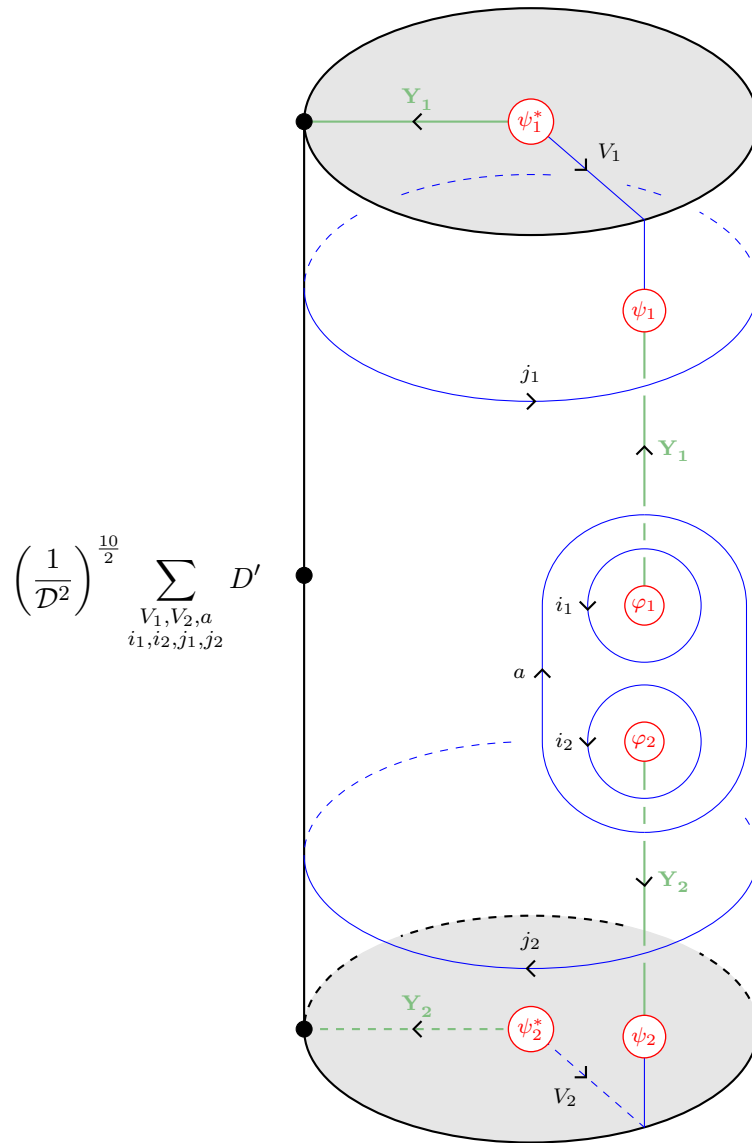
$$\begin{matrix} \text{id} & \varphi_1 & \text{id} & \varphi_2 \\ | & | & | & | \\ 1 & 1 & 1 & 1 \\ \downarrow & \downarrow & \downarrow & \downarrow \\ & Y_1 & & Y_2 \end{matrix} \xrightarrow{\pi_{\Delta}} \frac{1}{\mathcal{D}^2} \begin{matrix} \varphi_1 \\ \downarrow \\ Y_1 \\ \varphi_2 \\ \downarrow \\ Y_2 \end{matrix} \quad (7.37)$$

On the the other hand, the target vector in Equation 7.22 is given by

$$\left(\frac{1}{\mathcal{D}^2}\right)^{\frac{7}{2}} \sum_{\substack{V_1, V_2, a \\ i_1, i_2, j_1, j_2}} \tilde{D} \begin{matrix} \text{id} & \text{id} \\ | & | \\ i_1 \downarrow & i_2 \downarrow \\ 1 & 1 \\ | & | \\ \varphi_1 & \varphi_2 \\ | & | \\ Y_1 & Y_2 \\ \leftarrow a \\ \psi_1 & \psi_2 \\ | & | \\ j_1 \downarrow & j_2 \downarrow \\ V_1 & V_2 \end{matrix} \quad \begin{matrix} \psi_1^* & \psi_2^* \\ | & | \\ V_1 & V_2 \\ | & | \\ Y_1 & Y_2 \end{matrix}$$

where $\tilde{D} = d_{i_1} d_{i_2} d_a \sqrt{d_{V_1}} \sqrt{d_{V_2}} \sqrt{d_{j_1}} \sqrt{d_{j_2}}$.

Applying π_{Δ_t} to the above yields the following:



$$\left(\frac{1}{D^2}\right)^{\frac{10}{2}} \sum_{\substack{V_1, V_2, a \\ i_1, i_2, j_1, j_2}} D'$$

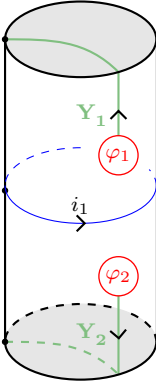
where $D' = d_{i_1} d_{i_2} d_a d_{V_1} d_{V_2} d_{j_1} d_{j_2}$.

Next we perform several moves in sequence:

- (1) Apply the Resolution Lemma along the edges labeled V_1 and V_2 .
- (2) Using Relation 6.52, slide the loops labeled j_1 and j_2 off of the surface.
- (3) Slide the loop labeled a off of the surface.
- (4) Slide the loop labeled i_2 off of the surface. This is possible due to Relation 6.52, as well as the cloaking provided by the i_1 loop.

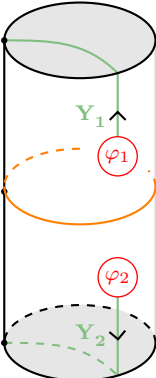
- (5) Slide the i_1 loop past the top marked point so that it eventually goes around the “waist” of the cylinder.

The result of doing these moves is the following:

$$\left(\frac{1}{\mathcal{D}^2}\right)^5 \sum_{\substack{a, i_1, i_2 \\ j_1, j_2}} d_{i_1} d_a^2 d_{j_1}^2 d_{j_2}^2 d_{i_2}^2$$


The diagram shows a cylinder with a green path starting from the top, going down, around the back, and up to the bottom. A blue loop labeled i_1 is shown around the middle of the cylinder. Two red circles labeled φ_1 and φ_2 are positioned on the cylinder's surface. Green arrows labeled Y_1 and Y_2 point upwards and downwards respectively.

It is easy to see that this simplifies to the following:

$$\frac{1}{\mathcal{D}^2}$$


The diagram shows a cylinder with a dashed green path starting from the top, going down, around the back, and up to the bottom. An orange loop is shown around the middle of the cylinder. Two red circles labeled φ_1 and φ_2 are positioned on the cylinder's surface. Green arrows labeled Y_1 and Y_2 point upwards and downwards respectively.

The commutativity of the square now follows immediately from Equation 6.54. □

Bibliography

- [1] B. Bakalov and A.A. Kirillov. *Lectures on Tensor Categories and Modular Functors*. Translations of Mathematical Monographs. American Mathematical Soc., 2001. [3](#), [2.1.2](#), [6](#)
- [2] Benjamin Balsam and Alexander Kirillov, Jr. Turaev-Viro Invariants as an Extended TQFT. <http://arxiv.org/abs/1004.1533>, 2010. [1](#), [2.1.3](#), [26](#), [27](#), [2.3](#), [2.3](#), [34](#), [2.1](#), [2.2](#), [2.3](#), [36](#), [5.1](#), [6](#), [6.1](#), [6.1.2](#), [83](#), [88](#), [6.3](#), [6.3](#), [7.1](#)
- [3] John W. Barrett and Bruce W. Westbury. Invariants of piecewise-linear 3-manifolds. *Transactions of the American Mathematical Society*, 348(10), 1996. [13](#), [7](#)
- [4] John W Barrett and Bruce W Westbury. Spherical categories. *Advances in Mathematics*, 143(2):357–375, 1999. [12](#)
- [5] Bruce Bartlett. Fusion categories via string diagrams. *Communications in Contemporary Mathematics*, 18(05):1550080, 2016. [5](#)
- [6] Bruce Bartlett, Chris Douglas, Chris Schommer-Pries, and Jamie Vicary. A finite presentation of the 3-dimensional bordism bicategory. In preparation. [1](#), [3](#), [3](#)
- [7] Bruce Bartlett, Chris Douglas, Chris Schommer-Pries, and Jamie Vicary. Modular categories as representations of modular structures. In preparation. [1](#), [3](#)
- [8] Bruce Bartlett, Chris Douglas, Chris Schommer-Pries, and Jamie Vicary. Extended 3-dimensional bordism as the theory of modular objects. <http://arxiv.org/abs/1411.0945>, 2014. [1](#), [3](#), [3](#), [42](#), [43](#), [1](#)
- [9] Bruce Bartlett, Chris Douglas, Chris Schommer-Pries, and Jamie Vicary. Modular categories as representations of the 3-dimensional bordism 2-category. <http://arxiv.org/abs/1509.06811>, 2015. [1](#), [3](#), [3](#), [45](#), [3](#), [5.2](#), [8](#)
- [10] Pierre Deligne. Catégories tannakiennes. *The Grothendieck Festschrift*, pages 111–195, 2007. [11](#)

- [11] Vladimir Drinfeld, Shlomo Gelaki, Dmitri Nikshych, and Victor Ostrik. On braided fusion categories i. *Selecta Mathematica*, 16(1):1–119, 2010. [2.1.1](#)
- [12] Pavel Etingof, Dmitri Nikshych, and Viktor Ostrik. On fusion categories. *Annals of Mathematics*, pages 581–642, 2005. [2.1.1](#)
- [13] André Joyal and Ross Street. Planar diagrams and tensor algebra. *Draft available at <http://www.math.mq.edu.au/~street/PlanarDiags.pdf>*, 585:658, 1988. [2.1.2](#)
- [14] André Joyal and Ross Street. The geometry of tensor calculus, i. *Advances in Mathematics*, 88(1):55–112, 1991. [2.1.2](#)
- [15] André Joyal and Ross Street. The geometry of tensor calculus ii. *Draft available at <http://www.math.mq.edu.au/~street/GTCII.pdf>*, 585, 1991. [2.1.2](#)
- [16] Max Kelly. *Basic concepts of enriched category theory*, volume 64. CUP Archive, 1982. [3](#)
- [17] Alexander Kirillov, Jr. On Piecewise Linear Cell Decompositions. <http://arxiv.org/abs/1009.4227>, 2011. [2.3](#), [12](#), [32](#), [2.3](#), [39](#)
- [18] Alexander Kirillov, Jr. String-net model of Turaev-Viro Invariants. <http://arxiv.org/abs/1106.6033>, 2011. [1.1](#), [1.1](#), [4](#), [54](#), [58](#), [60](#), [61](#), [5.1](#), [92](#), [94](#), [6.4](#)
- [19] Alexei Kitaev. Fault-tolerant quantum computation by anyons. *Annals of physics*, 303:2–30, 2003. [4](#)
- [20] Tom Leinster. Basic bicategories. *arXiv preprint math.CT/9810017*, 589, 1998. [2.2](#)
- [21] Michael Levin and Xiao-Gang Wen. String-net condensation: A physical mechanism for topological phases. *Physics Review B*, 7, 2005. [1.1](#), [4](#)
- [22] Jacob Lurie et al. On the classification of topological field theories. *Current developments in mathematics*, 2008:129–280, 2009. [1](#)
- [23] Saunders Mac Lane. *Categories for the working mathematician*, volume 5. Springer Science & Business Media, 2013. [2.1](#), [6](#), [8](#), [2.1.1](#), [18](#)
- [24] Michael Müger. From subfactors to categories and topology ii: The quantum double of tensor categories and subfactors. *Journal of Pure and Applied Algebra*, 180(1):159–219, 2003. [2.1.3](#), [2.1.3](#)
- [25] Roger Penrose. Applications of negative dimensional tensors. *Combinatorial mathematics and its applications*, 221244, 1971. [2.1.2](#)

- [26] Colin Patrick Rourke and Brian Joseph Sanderson. *Introduction to piecewise-linear topology*. Springer-Verlag, 1982. 2.3
- [27] Chris Schommer-Pries. The Classification of Two-Dimensional Extended Topological Field Theories. <http://arxiv.org/abs/1112.1000>, 2011. 30, 41, 3, 46, 2
- [28] Peter Selinger. A survey of graphical languages for monoidal categories. In *New structures for physics*, pages 289–355. Springer, 2010. 2.1.2
- [29] V.G. Turaev. *Quantum Invariants of Knots and 3-Manifolds*. De Gruyter Studies in Mathematics. De Gruyter, 2010. 3, 2.1.2, 6.3, 2
- [30] Vladimir G Turaev and Oleg Ya Viro. State sum invariants of 3-manifolds and quantum 6j-symbols. *Topology*, 31(4):865–902, 1992. 1
- [31] Zhenghan Wang. *Topological quantum computation*. Number 112. American Mathematical Soc., 2010. 7